MULTIFREQUENCY EDDY CURRENT INSPECTION FOR CRACKS UNDER FASTENERS

BATTELLE'S COLUMBUS LABORATORIES
505 KING AVENUE
COLUMBUS, OHIO 43201

DECEMBER 1976

FINAL REPORT DECEMBER 1975–OCTOBER 1976

Approved for public release; distribution unlimited.

AIR FORCE MATERIALS LABORATORY
AIR FORCE WRIGHT AERONAUTICAL LABORATORIES
AIR FORCE SYSTEMS COMMAND
WRIGHT-PATTERSON AIR FORCE BASE, OHIO 45433

NOTICE

When Government drawings, specifications, or other data are used for any purpose other than in connection with a definitely related Government procurement operation, the United States Government thereby incurs no responsibility nor any obligation whatsoever; and the fact that the government may have formulated, furnished, or in any way supplied the said drawings, specifications, or other data, is not to be regarded by implication or otherwise as in any manner licensing the holder or any other person or corporation, or conveying any rights or permission to manufacture, use, or sell any patented invention that may in any way be related thereto.

For the Commander

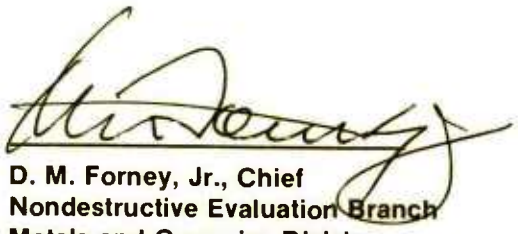

D. M. Forney, Jr., Chief
Nondestructive Evaluation Branch
Metals and Ceramics Division

Copies of this report should not be returned unless return is required by security considerations, contractual obligations, or notice on a specific document.

AIR FORCE - 31 MAY 77 - 425

UNCLASSIFIED

SECURITY CLASSIFICATION OF THIS PAGE *(When Data Entered)*

REPORT DOCUMENTATION PAGE		READ INSTRUCTIONS BEFORE COMPLETING FORM
1. REPORT NUMBER AFML-TR-76-209	2. GOVT ACCESSION NO.	3. RECIPIENT'S CATALOG NUMBER
4. TITLE *(and Subtitle)* MULTIFREQUENCY EDDY CURRENT INSPECTION FOR CRACKS UNDER FASTENERS		5. TYPE OF REPORT & PERIOD COVERED Final Report Dec., 1975 to Oct., 1976 6. PERFORMING ORG. REPORT NUMBER
7. AUTHOR(s) J. H. Flora, H. T. Gruber, R.E. Thomas, and R. P. Meister		8. CONTRACT OR GRANT NUMBER(s) F33615-76-C-5062
9. PERFORMING ORGANIZATION NAME AND ADDRESS Battelle Columbus Laboratories 505 King Avenue Columbus, Ohio 43201		10. PROGRAM ELEMENT, PROJECT, TASK AREA & WORK UNIT NUMBERS Project No. 735109
11. CONTROLLING OFFICE NAME AND ADDRESS Air Force Materials Laboratory Air Force Systems Command Wright Patterson Air Force Base, Ohio		12. REPORT DATE December 15, 1976 13. NUMBER OF PAGES 125
14. MONITORING AGENCY NAME & ADDRESS *(if different from Controlling Office)*		15. SECURITY CLASS. *(of this report)* Unclassified 15a. DECLASSIFICATION/DOWNGRADING SCHEDULE

16. DISTRIBUTION STATEMENT *(of this Report)*

Approved for public release, distribution unlimited.

17. DISTRIBUTION STATEMENT *(of the abstract entered in Block 20, if different from Report)*

18. SUPPLEMENTARY NOTES

19. KEY WORDS *(Continue on reverse side if necessary and identify by block number)*

Nondestructive Evaluation, Eddy Current, Fasteners

20. ABSTRACT *(Continue on reverse side if necessary and identify by block number)*

This report describes the first phase of a two-phase program for the development of multiple frequency eddy-current, MFEC, inspection for cracks under installed fasteners.

The experimental evaluation was conducted on two typical wing splice joint configurations used in the C5-A aircraft consisting of two aluminum layers each 3/16 to 1/4 inches thick. Notches simulating cracks were machined in a

DD FORM 1 JAN 73 1473 EDITION OF 1 NOV 65 IS OBSOLETE

UNCLASSIFIED

SECURITY CLASSIFICATION OF THIS PAGE *(When Data Entered)*

radial direction extending from the fastener hole and the faying surface between sheets. A digital eddy-current system designed around a PDP-11/40 minicomputer was utilized for the experimental evaluations. The digital system was programmed to generate the signal wave-forms that excite the test coil and perform the function of phase-sensitive detection of response signals that are received from the test coil. Special test coils were designed to induce eddy currents in the aluminum alloy that lies beneath the head of the fasteners.

A series of measurements were taken on the wing-splice samples at various frequencies, excitation levels, and phase settings. These data were analyzed using the Automatic Interaction Detector, AID, computer code to indicate initial capabilities of crack detection, and to compare the various operating parameters such as excitation frequency and test coil design. At the present stage of development, the AID analysis indicates that in the second layer of the samples evaluated, cracks as small as 0.3 inch can be detected under titanium fasteners with a probability of 0.81 with a 95 percent confidence interval of 0.41 to 0.98. Cracks as small as 0.4 inch can be detected under titanium fasteners with a probability of nearly one with a 95 percent confidence interval of 0.63 to 1.0 using the digital eddy-current system.

The AID analysis indicates that cracks 0.1 inch and greater near steel fasteners in the samples evaluated can be detected with a probability approach 1.0 with a 95 percent confidence interval of 0.99 to 1.0. Based on the data taken during this program, reliable detection of these crack sizes would not be possible using a single frequency eddy-current system.

FOREWORD

This report describes the Digital Multifrequency Eddy Current System developed at Battelle's Columbus Laboratories and its application using a statistically based learning-application approach to detection of cracks under installed fasteners in a typical aircraft structure. The program was conducted in the Fabrication and Quality Assurance Section. Mr. R. P. Meister served as Program Manager. The program was performed under the technical direction of Mr. J. H. Flora as Principal Investigator. Mr. H. T. Gruber was responsible for the computer programming and statistical analysis was directed by Dr. R. E. Thomas. Recognition is given to Mr. J. R. Fox for sample preparation and data acquisition and to Mr. R. W. Cote for assistance in statistical analysis. The Air Force Project Monitor was Mr. Richard R. Rowand, AFML/LLP, assisted by Dr. J. A. Moyzis.

TABLE OF CONTENTS

LIST OF ILLUSTRATIONS

LIST OF ILLUSTRATIONS (CONTINUED)

LIST OF ILLUSTRATIONS (CONTINUED)

LIST OF TABLES

SECTION I
SUMMARY

This report describes the first phase of a two-phase program for the development of multiple frequency eddy-current, MFEC, inspection for cracks under installed fasteners. Phase I was directed toward the evaluation and demonstration of MFEC using actual wing-splice samples and laboratory instrumentation to detect cracks under titanium and steel fasteners. A prototype MFEC system for field inspection of aircraft is to be constructed during Phase II.

Evolving from this Phase I investigation is a digital eddy-current system that provides a stable acquisition of eddy-current response signals, more reliable detection of cracks and a versatile automatic control of the inspection process. Frequency and amplitude stability of the digital eddy-current system is better than 0.1 percent and phase sensitive detection is stable within 0.05 percent. Operating parameters such as excitation frequencies, phase references and classification algorithms are easily selected for the test conditions at hand with a minimum change in hardware.

At the present stage of development, the AID analysis indicates that in the second layer of the samples evaluated, cracks as small as 0.3 inch can be detected under titanium fasteners with a probability of 0.81 with a 95 percent confidence interval of 0.41 to 0.98. Cracks as small as 0.4 inch can be detected under titanium with a probability of nearly 1.0 with a 95 percent confidence interval of 0.63 to 1.0 using the digital eddy-current system.

The AID analysis indicates that cracks 0.1 inch and greater near steel fasteners in the samples evaluated can be detected with a probability approaching 1.0 with a 95 percent confidence interval of 0.99 to 1.0. The probabilities of detection for cracks is based on the AID analysis rather than on experimental evaluations of implemented models derived from AID. Therefore, it is believed that the probabilities provided by the AID analysis represent the maximum

reliability which can be obtained with a digital MFEC system. However, based on the data taken during this program, reliable detection of these crack sizes would not be possible using a single frequency eddy-current system.

The experimental evaluation was conducted on two typical wing splice joint configurations used in the C5-A aircraft consisting of two aluminum layers each 3/16 to 1/4 inches thick. Fasteners and sealant were removed and notches simulating cracks were machined in a radial direction extending from the fastener hole and the faying surface between sheets. The samples were then assembled with intentional variable spacing between the spliced plates. Typical variables such as fastener-to-edge distance, fastener alignment, fastener protrusion and variation in fastener material were observed in the wing-splice samples provided by the Air Force. Preliminary investigations indicate that more subtle effects such as the existence of filings in the sealant and slight variation in fastener fit did not affect the eddy-current test.

Special test coils were designed to induce eddy currents in the aluminum alloy that lies beneath the head of the fasteners. Emphasis was placed on providing sufficient penetration and sensitivity to detect cracks in the second layer. The coils were designed for temperature and mechanical stability and to facilitate a consistent, precise initialization of the instrumentation on the standard reference fasteners. The coils were installed in a protective housing to facilitate alignment and positioning over the center of the fasteners and to provide electrical shielding from extraneous electromagnetic radiation.

A digital eddy-current system designed around a PDP-11/40 minicomputer was utilized for the experimental evaluations. The digital system was programmed to generate the signal waveforms that excite the test coil and perform the function of phase-sensitive detection of response signals that are received from the test coil. A significant advantage of the digital eddy-current system is its highly stable eddy-current operation at relatively low frequencies required for detection of cracks under fasteners.

The digital eddy-current system also facilitates a number of additional inspection functions. The minicomputer was programmed to perform automatic initial balance and to filter the data samples taken on each fastener. System operational parameters such as frequencies, phase settings, test coil excitation, and amplitude are easily selectable by computer instruction. Finally, the minicomputer was programmed for implementation of the decision functions and to display output data for the inspection of both steel and titanium fasteners.

A series of measurements were taken on the wing-splice samples at various frequencies, excitation levels, and phase settings. These data were analyzed using the Automatic Interaction Detector, AID, computer code to indicate initial capabilities of crack detection, and to compare the various operating parameters such as excitation frequency and test coil design. Linear discriminant analysis was performed on the data using variables derived from the AID analysis.

The most effective decision process resulting from these investigations involves the implementation of the decision tree derived from AID analysis. Using this approach, the MFEC inspection requires steps which can be executed in rapid succession by the minicomputer as follows:

(1) Acquisition of MFEC data

(2) Nonlinear transformation of measurements

(3) Application of transformed measurements to the decision algorithm

(4) Display of results indicating the existence or nonexistence of a crack.

SECTION II
INTRODUCTION

Fatigue cracks propagating from fastener holes in multilayered, fastened members is a problem common to many aircraft structures. Stress levels in interior structural layers of a mechanically fastened joint can equal or exceed the stress levels in the exterior layer. Therefore, there is a high probability that primary crack initiation and growth can occur in interior layers. These cracks usually initiate at the faying surface between joined plates and propagate in a radial direction from the fastener hole.

A nondestructive test that can detect cracks in interior layers is highly desirable because removal of fasteners for inspection is extremely costly. Fastener nuts are not readily accessible and fastener bolts are difficult to remove without damaging the hole. Holes usually have to be resized and finished after the fasteners are removed. Substantial savings in the costs of unnecessarily removing fasteners can be realized if a fastener hole can be inspected with the fastener in place. Since aircraft such as the C-5A can have hundreds of critical fastener holes that require inspection, the savings provided by a reliable inspection technique is considerable.

Inspection by X-rays is difficult and costly. Radiography lacks sensitivity and definition in many cases where structures are complex. Ultrasonic techniques are essentially limited to the exterior layer only and, therefore, provide less than adequate inspection.

The C-5A SPO funded Lockheed-Georgia to contact those organizations knowledgeable about nondestructive techniques that might be used for detecting cracks under fasteners in multilayered aluminum structures. The MFEC technqiue developed by Battelle-Columbus appeared to have the greatest potential for success. Under a C-5A SPO funded Contract (No. F33657-73-C-0281), it was found that with MFEC we had the potential of detecting 0.125-inch

radial length cracks 0.4 inch below the surface with fasteners installed. Since this potential detection capability could satisfy many inspection requirement on aircraft structures, such as B-52, KC-135, and F-5, as well as the C-5A, successful development of the MFEC technique offered promise of tremendous cost savings warranting continuing the development of the technique under Air Force sponsorship.

The MFEC technique, like other eddy-current techniques, offers several capabilities that are desirable for inspection for cracks under fasteners. In general, the eddy-current techniques are fast and require no coupling media between test coil and inspection piece. However, standard commercial eddy-current devices do not appear to be good candidates for detecting cracks under fasteners, because (1) the cracks are subsurface and eddy-current testing is penetration limited, and (2) the eddy-current signal response is highly influenced by variables associated with the fastener and sheet material.

MFEC involves the simultaneous energization of the eddy-current test coil with a number of sinusoidal current waveforms, each having a different frequency. The test-coil response signals associated with each frequency are then filtered, detected, and recombined to provide a composite signal that is a measure of the variable of interest, in this case, the crack under the fastener. The responses of the eddy-current test coil to the different variables changes with a change in the excitation current frequency. It is possible to take advantage of these changes in response at different frequencies to sort out the responses produced by the variables of interest from the response of all the other variables. In this way, the variable of interest produces a maximized response, while the response of the unwanted variables is minimized; the composite signal is influenced to a minimum extent by minor variations in fastener fit, metallurgical variations in the fastener or aluminum sheet, joint geometry variation, and test-coil position with respect to the fastener center.

At the conclusion of the preliminary studies carried out under Contract F-33657-73-C-0281, Battelle proposed a program to develop a prototype MFEC system for detecting cracks under fasteners in layered aircraft structures. This program consisted of two phases. Phase 1 was to be directed at optimizing the techniques and procedures required to detect simulated cracks (machined notches) in fastener holes, at least 0.1 inch in radial length in the second layer of an equithickness two layer joint 0.4 inches thick. Phase 2 was to be directed at design, construction, and evaluation of the prototype MFEC inspection system defined by Phase 1.

In December, 1975, the Air Force authorized the start of the work in Phase 1. Specific objectives were to:

- Develop improved test coils
- Develop improved signal generation and balancing techniques
- Optimize data analysis procedures for evaluating MFEC output.

This report describes the work carried out and results obtained in this development.

SECTION III
EXPERIMENTAL INVESTIGATION

Laboratory experiments which preceded the present investigation indicated that eddy-current coils can be used to detect cracks which extend from fastener holes with the fasteners in place. Preliminary analysis also indicated that MFEC techniques could be employed to reduce the effects of unwanted variables such as probe liftoff and test coil position with respect to the fastener center. Realizing that several other nuisance variables including center-to-edge distance, space between spliced plates, fastener protrusion and fastener fit would be significant in field application of the MFEC technique, it has been the purpose of this present phase of study to develop and evaluate the MFEC techniques that will detect sublayer cracks in actual wing splice samples.

Wing splice samples were selected and prepared to exhibit typical variations in geometrical and electrical conditions which can adversely affect the eddy-current signal. Since relatively low frequencies are required to provide penetration within the subsurface plate layers and since signal responses to small cracks in these layers are quite small, digital eddy-current techniques have been developed to provide maximum stability and sensitivity. Test coil design has also been an important factor in providing eddy-current penetration, sensitivity and stability.

Since project goals have been directed toward the detection of as small a crack as possible, trainable decision functions have been developed using a statistical analysis tool called AID, automatic interaction detector. The following sections describe these techniques and the results of the experimental evaluation using the digital MFEC instrumentation.

1. MULTIPLE FREQUENCY EDDY-CURRENT CONCEPT

When an alternating current flows in a coil which is placed near the surface of an electrical conducting material, a magnetic field penetrates the material. Since the magnitude of the field changes with time, eddy currents are induced within the material. These eddy currents are affected by the geometry of the material, its conductivity, magnetic permeability, etc. Eddy currents are also affected by the presence or absence of cracks such as those which occur around the fastener holes.

The eddy currents in the material in turn produce a magnetic field of their own which tend to oppose the original magnetic field. These counter magnetic fields induce a voltage in the original driving coil or in separate pickup coils. The complex impedance change in the driving coil or the complex voltage that appears at the terminals of the pickup coil reflect the presence or the absence of the cracks that the system is looking for. On the other hand, this complex voltage also reflects changes in all of the other variables in the material.

Multifrequency eddy-current signals can be processed by a variety of methods to predict the presence of defects or estimate change in material variables in the presence of unwanted signals caused by nuisance variables. For the most part, MFEC analysis has involved the derivation of algebraic formulas using methods such as regression analysis to estimate crack depth or the other variables of interest. In contrast, the present application of inspection for cracks under fasteners places emphasis on detection of as small a crack as possible. There has been relatively little interest in estimating crack length since the presence of any crack would call for fastener removal and specified maintenance procedures.

The concept of MFEC inspection for cracks under fasteners has been one of development of classification algorithms which are easily implemented on digital equipment such as minicomputers. This has involved the use of statistical analysis tools such as

linear discriminant analysis (LDA) and automatic interaction detector (AID) to determine and evaluate trainable decision algorithms. Other innovations have been the development of digital eddy-current techniques which are discussed in the following section.

2. DIGITAL MFEC

Digital eddy-current instrumentation was developed for this project to provide several advantages over conventional analog circuitry that is normally used in eddy-current systems. Based on the use of the PDP 11/40 minicomputer, the digital technique offers broad flexibility in implementing the functions essential to MFEC inspection of a variety of fastener sizes, geometries, and plate thicknesses. Operating parameters such as excitation frequencies, phase references and classification algorithms are easily selected for the test conditions at hand with a minimum change in hardware. The digital system also provides greater precision and stability in MFEC data acquisition as well as simplification in control of the MFEC inspection process. From computer specifications, frequency accuracy and amplitude stability is better than 0.01 percent and phase-sensitive detection has been measured to be stable within 0.05 percent.

Details of the digital eddy-current system which was designed, assembled, and programmed for the laboratory investigation are described in Appendix A. In brief, the PDP 11/40 minicomputer used in conjunction with test coil interface circuitry is programmed to perform the following functions.

(1) Generate sinusoidal excitation currents at a number of frequencies with selectable amplitudes.

(2) Generate sinusoidal balance reference voltages to provide initial output null when the test coil is placed on a standard reference fastener.

(3) Detect amplified test coil signals by sampling the off-null voltage at precise intervals to provide stable in-phase and quadrature measurements of test coil response signals.

(4) Use sample voltages to automatically adjust the balance reference voltage to obtain an output null voltage within ±10 millivolts.

(5) Acquire an average of a series of in-phase and quadrature samples for a number of excitation frequencies and store the values for additional signal processing.

(6) Apply the average coil response measurements to transformation functions and decision algorithms.

(7) Display the results of the MFEC signal processing indicating the probability of a crack occurring under the fastener in question.

The minicomputer based eddy-current system offers additional capabilities for field inspection which were not incorporated in the laboratory system. For example, the digital system can be used to perform automatic centering of the test coil over the fastener. The computer can also be programmed to perform calibration of the eddy-current equipment and to make minor adjustments in the classification algorithms. The adjustment would be required when test coils are changed or when new conditions, i.e., fastener type and plate thickness, are encountered.

The digital eddy-current system when integrated with a sensitive, stable test coil will provide maximum basic sensitivity to cracks under fasteners with a minimum effect from variables such as ambient temperatures which can cause long-term drift. This is necessary to provide the maximum potential for successful application of the MFEC techniques.

3. TEST COIL DESIGN

All factors including test coil design which affect test coil sensitivity have been significant in the investigation. Preliminary experiments indicated that the sensitivity to subsurface cracks is relatively small compared to the sensitivity to other variables.

Relatively low sensitivity to these cracks is attributed to the thickness of the top plate material which serves to shield the alternating magnetic flux that is generated by the test coil. Consequently, the test coil was designed to provide adequate penetration while limiting sensitivity to variations in nuisance variables such as center-to-edge distance and test coil liftoff. Other factors affecting sensitivity were test coil impedance, ambient temperature variations and power dissipation.

Preliminary evaluation of the coil design involved investigation of three basic geometries: the cup coil, the straddle coil, and the side coil. The cup coil configuration was selected for extensive MFEC analysis since it exhibited superior sensitivity to cracks in the secondary plate layers. Also, the cup core coil did not require rotation about the fastener center to accommodate complete inspection and was less sensitive to variations in the center-to-edge distance in comparison to the other coil designs. The straddle coil and side coil designs are described in Appendix B.

As illustrated in Figure 1, the cup core coil induces eddy currents to flow around the fastener in both the top and bottom plates. Since the plate layers are nonferromagnetic, the gap between the plates has relatively little effect on the eddy-current flow. The magnitude of the induced currents at a given distance beneath the surface is primarily a function of diameter of the coil, the core material, the frequency of excitation, and the fastener material.

Two cup core coils of different diameters were designed and constructed for the experimental evaluation. Figure 2 shows the final configuration of the cup core coil probes. The core of each coil was ground to dimension from a ferrite cup core used for construction of transformers and inductors. The ferrite was selected for its low temperature coefficient in the anticipated operating temperature range. The center hole of the cup core was filled with additional ferrite material to provide increased concentrations of the magnetic field in the center of the core and, therefore, increased concen-

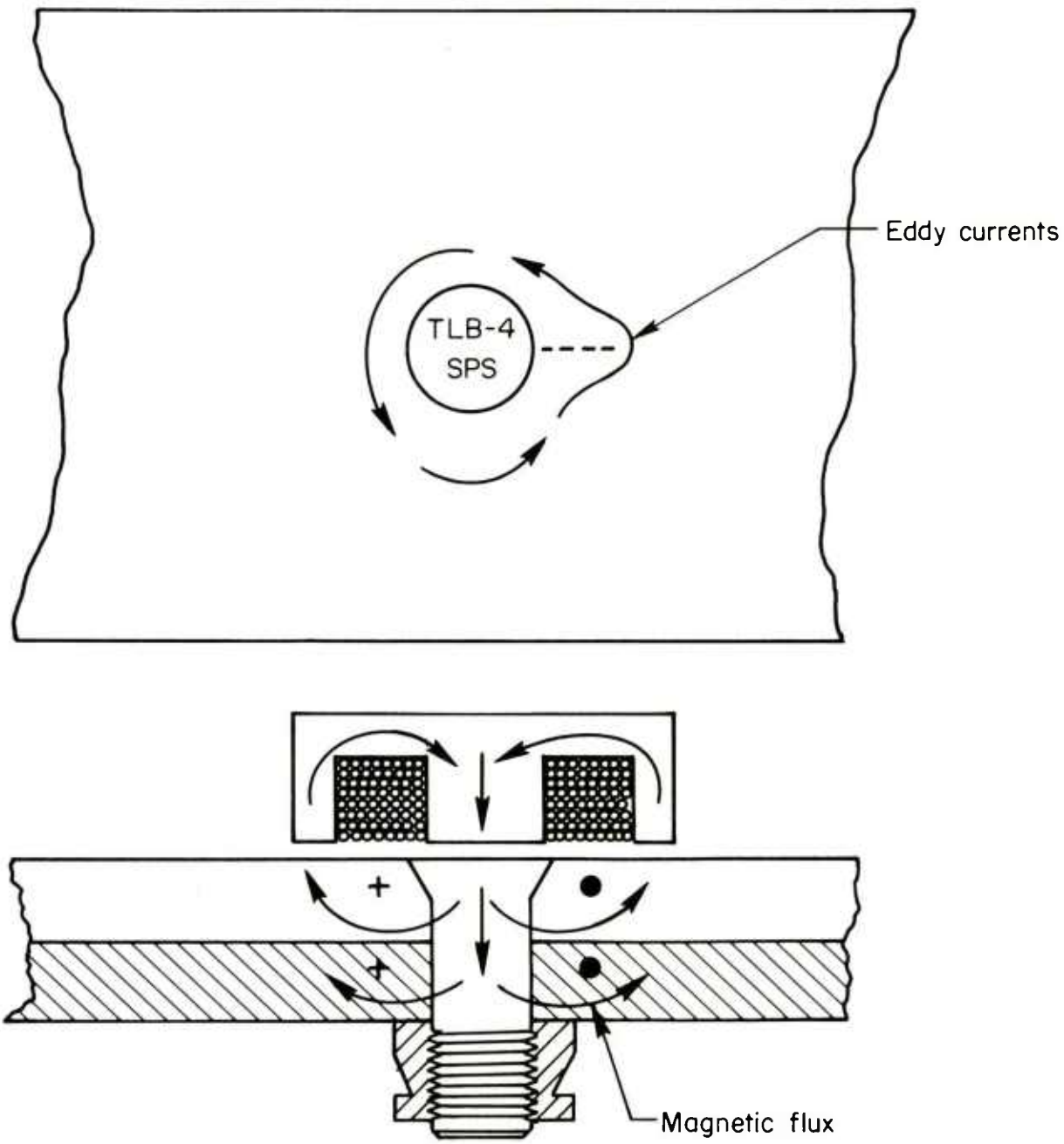

FIGURE 1. CUP CORE COIL ELECTROMAGNETICALLY COUPLED TO WING-SPLICE AND FASTENER

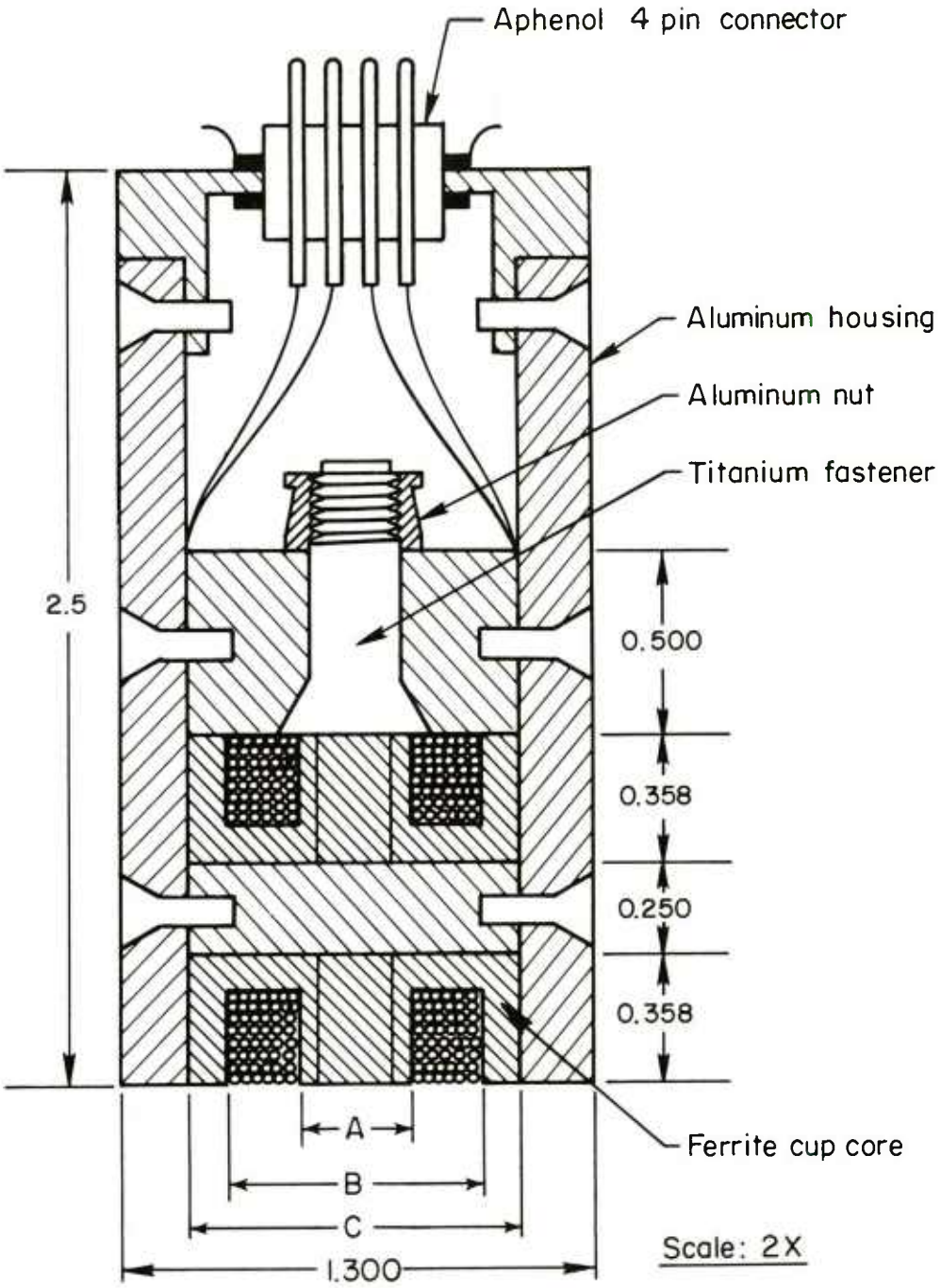

Coil	Dimensions, inches A	B	C	Number of Turns in Coil	Coil Wire Size
1	0.300	0.700	0.900	530	36 AWG
2	0.364	0.850	1.091	358	33 AWG

FIGURE 2. CONFIGURATION OF CUP CORE EDDY-CURRENT PROBE FOR DETECTION OF CRACKS AROUND INSTALLED FASTENERS

tration of eddy currents near the fastener shank where the cracks initiate. The test coils were bifilar wound on thin plastic coil forms to provide a maximum number of turns with a nominal electrical resistance in the coil windings. One of the bifilar wound coils serves as the driver coil and the second as the pickup coil. This configuration minimizes temperature drift when incorporated with a suitable electronic interface network.

Two of the bifilar wound coils were inserted in an aluminum housing and connected so that the pickup coils are in series opposition. The coil at the open end of the housing serves as the sensor coil when the probe is placed on the fastener head. The internal coil acts as a reference coil when the pickup coil is connected in series opposition. In this configuration, a near zero voltage is measured at the output terminals when the coil is placed on a standard fastener. The digital eddy-current reference signal compensates for slight differences in the test coil voltages after the automatic balance function is performed.

The preliminary MFEC tests indicated liftoff, the distance from the test coil to the inspection material, to be the most significant of the nuisance variables. Uniform liftoff was initially achieved by using a wide flange probe resting on plastic probe alignment devices which were fastened to the panels. Thickness variations in the plastic aligning devices caused liftoff variations, influencing the results of the measurements. Various alternatives were considered, with the result that the aligning devices were retained with the single function of aligning the test coil over the center of the fastener. The coil was recessed 10 mils within an encircling ring which made contact with the surface of the wing panel. This maintained the test coil a constant distance above the surface of the wing panel.

4. SAMPLE PREPARATION

The testing parameters (coil configuration, test frequencies, filtering, etc.) and the decision function used to transform raw eddy current data into inspection results for each MFEC inspection application must be determined in a learning phase. During this learning phase, actual samples of the parts to be inspected, e.g., the C-5A wing splice structures, are employed. Known defects, or simulations of these defects, are introduced into the samples; in this investigation, notches were machined to simulate cracks around the fastener holes. Similarly, all other variables which can be present in the part and which may affect the eddy currents, such as metallurgical structure and joint geometry must be represented in the sample parts, either by natural occurrence or by simulation. The exact nature of these variables and their measure need not be known.

The sample preparation task, therefore, consisted of introducing known simulations of cracks in typical C-5A wing splice structure supplied by the Air Force while assuring that all other joint variables that could affect the eddy current results were present. Possible joint variables which were considered initially are:

(1) Materials Variables
    (a) Fastener materials (H-11 Steel and Titanium 1Al-8V-5Fe)
    (b) Sheet material 7075-T6 Aluminum
    (c) Web stiffener material 7079-T6 Aluminum
    (d) Conductivity variation in materials due to heat treatment

(2) Surface Preparation Variables
    (a) Shot peening
    (b) Anodize
    (c) Paint

(3) Sheet Separation Variables
    (a) Sealant
    (b) Filings in sealant
    (c) Sheet spacing

(4) Joint Geometry Variables
    (a) Sheet material thickness
    (b) Fastener diameter

(c) Fastener spacing

(d) Fastener-to-edge distance

(e) Fastener fit

(5) Environment Variables

(a) Temperature

(b) Accessibility to joint

(c) Position.

In addition to these joint variables there are a number of test variables including coil liftoff, coil centering, and equipment stability which can affect the eddy current results.

Some of the above variables could be disregarded a priori. For example, the presence of sealant in the gaps between layers could be disregarded since it is nonconducting. Also, the surface preparation variables could be considered as primarily a coil liftoff effect and the methods used to handle coil liftoff would accommodate variations in surface preparation. Based on a preliminary evaluation using laboratory MFEC equipment, the effect of filings in the sealant and conductivity variation within the normal range experienced for a given alloy and heat treat condition was also found to be negligible. Some variables from previous work were known to be major variables requiring generation of separate decision functions, e.g., fastener material and major changes in joint geometry. The effect of other variables, e.g., minor variation in the joint geometry variables such as the thickness change in a tapered sheet, tolerance on nominal hole location, sheet separation, temperature variation, coil liftoff and equipment stability must be accommodated using the MFEC analysis.

Most of the variables that could affect the eddy current response occurred naturally in the sample C-5A wing splice joint provided by the Air Force. Samples were provided with both titanium and steel fasteners. These samples exhibited variations in material thickness, hole-to-hole distance, hole-to-edge distance, and fastener fit which was considered representative of normal fabrication variance. The simulated cracks had to be introduced and, to assure the presence of sheet separation covering the full range that might occur in normal fabrication, this variable was also introduced.

The wing splice panels were cleaned to remove the sealant on the surface and disassembled. Each fastener was identified during disassembly so that it could be replaced in the same hole. Care was taken not to damage the fasteners or the aluminum panels so that extraneous variables due to surface damage would not be introduced.

Variation in the separation between panels was achieved by inserting sheets of 0.010- and 0.020-inch mylar at certain locations along the joint as well as leaving some sections of the splice with no spacing material. The mylar material was chosen because of its electrical properties and its compressive strength. The separation between the faying surface for each fastener is listed in Tables 1 through 4.

The steel fasteners used in Panels 1-1 and 1-2 were TLH specifications H-11 Steel with 60-degree flush heads. The titanium fasteners used in Panels 1-3 and 1-4 contained double rows of fasteners resulting in distinct distance variations.

Figure 3 shows sketches of typical cross sections of test panels having a single row (bottom) and double row (top) of fasteners.

A. Artificial Cracks. Extreme care was exercised in the preparation of the artificial cracks because the validity of the decision function developed is dependent upon exact knowledge of the crack geometry and location. All reasonable efforts were made to assure that these artificial cracks resembled naturally occurring cracks as closely as possible.

The simulated cracks were machined in three locations as shown in Figure 4. The crack sizes introduced at each location were as follows:

Location A - Bottom panel faying surface, 0.050, 0.100, 0.200, 0.300, and 0.400 inch

Location B - Top panel faying surface, 0.025, 0.050, 0.100, and 0.200 inch

Location C - Counter sink, 0.025, 0.050, 0.075, and 0.100 inch.

TABLE 1. DIMENSIONS OF SPECIMEN NO. 1-1 SINGLE ROW OF STEEL FASTENERS JOINING TWO 3/16-INCH THICK ALUMINUM PIECES

Fastener No.	Separation Sheet Thickness (inches)	Location and Nominal Crack Length (inches)	Hole to Edge Distance (inches)	Actual Measured Crack Length Along Faying Surface (inches)	Actual Measured Crack Length Inside Hole (inches)
1	None	--	0.275	--	--
2	--	--	0.265	--	--
3	--	B-0.025	0.270	0.040	0.041
4	--	--	0.262	--	--
5	--	A-0.100	0.267	0.103	0.109
6	--	--	0.265	--	--
7	--	A-0.300	0.270	0.289	0.285 (b)
8	--	--	0.263	--	--
9	--	A-0.400	0.278	0.404	0.409 (b)
10	--	--	0.254	--	--
11	--	B-0.100	0.246	0.093	0.103
12	--	--	0.243	--	--
13	--	A-0.200	0.242	0.202	0.136 (b)
14	--	--	0.233	--	--
15	--	A-0.05	0.229	0.061	0.065
16	--	--	0.232	--	--
17	--	--	0.222	--	--
18	--	B-0.075	0.226	0.074	0.068
19	--	--	0.213	--	--
20 (a)	--	--	0.186	--	--
21	--	--	0.174	--	--
22	--	--	0.190	--	--
23	--	--	0.189	--	--
24	--	--	0.178	--	--
25	--	--	0.175	--	--
26	--	--	0.220	--	--

(a) Fasteners 20-26 are titanium and holes were not tested.
(b) Crack goes through thickness of the panel; measured crack length along bottom surface.

TABLE 2. DIMENSIONS OF SPECIMEN NO. 1-2 SINGLE ROW OF STEEL FASTENERS JOINING TWO 3/16 INCH THICK ALUMINUM PIECES

Fastener No.	Separation Sheet Thickness (inches)	Location and Nominal Crack Length (inches)	Hole to Edge Distance (inches)	Actual Measured Crack Length Along Faying Surface (inches)	Actual Measured Crack Length Inside Hole (inches)
1	None	--	0.356	--	--
2	--	--	0.372	--	--
3	--	--	0.375	--	--
4	--	A-0.300	0.385	0.303	0.306[a]
5	--	B-0.075	0.397	0.074	0.078
6	--	--	0.400	--	--
7	--	A-0.200	0.400	0.204	0.100[a]
8	--	--	0.387	--	--
9	--	A-0.400	0.370	0.401	0.402[a]
10	0.10	A-0.300	0.358	0.282	0.294[a]
11	Ditto	--	0.353	--	--
12	"	A-0.10	0.370	0.094	0.105
13	"	--	0.365	--	--
14	"	B-0.050	0.374	0.053	0.052
15	"	--	0.365	--	--
16	"	--	0.360	--	--
17	"	A-0.200	0.362	0.197	0.120[a]
18	"	--	0.357	--	--
19	0.20	B-0.050	0.365	0.051	0.042
20	Ditto	--	0.365	--	--
21	"	A-0.100	0.371	0.101	0.115
22	"	--	0.382	--	--
23	"	B-0.077	0.370	0.077	0.084
24	"	--	0.370	--	--
25	"	A-0.400	0.370	0.391	0.395[a]
26	"	--	0.366	--	--
27	"	--	0.372	--	--

(a) Crack goes through thickness of the panel; measured crack length along bottom surface.

TABLE 3. DIMENSIONS OF SPECIMEN NO. 1-3
TWO ROWS OF TITANIUM FASTENERS JOINING
TWO 1/4-INCH THICK ALUMINUM PIECES

Hole No.	Separation Sheet Thickness (inches)	Nominal Crack Length (inches)	Hole-to-Edge Distance (inches)	Hole-to-Hole Specimen (inches)	Actual Measured Crack Length Along Faying Surface (inches)	Actual Measured Crack Length Inside Hole (inches)
1	0.02	--	0.38	--	--	--
2	Ditto	--	--	0.52	--	--
3	"	--	0.365	--	--	--
4	"	--	--	0.54	--	--
5	"	--	0.355	--	--	--
6 (b)	"	A-0.30	--	0.54	0.296	0.301 (c)
7	"	--	0.375	--	--	--
8	"	B-0.05	--	0.525	0.060	0.057
9	"	B-0.19	0.38	--	0.190	0.163
10	"	--	--	0.53	--	--
11	"	--	0.37	--	--	--
12	"	--	--	0.53	--	--
13 (a)	"	A-0.05	0.34	--	0.065	0.073
14 (a)	"	A-0.20	--	0.495	0.200	0.090 (c)
15	"	A-0.40	0.355	--	0.400	0.400
16	"	B-0.075	--	0.54	0.080	0.073
17	0.010	--	0.359	--	--	--
18	Ditto	--	--	0.53	--	--
19	"	--	0.39	--	--	--
20	"	--	--	0.505	--	--
21	"	--	0.395	--	--	--
22	"	A-0.40	--	0.505	0.370	0.372 (c)
23	"	A-0.40	0.36	--	0.390	0.400 (c)
24	"	--	--	0.517	--	--

TABLE 3. (continued)

Hole No.	Separation Sheet Thickness (inches)	Nominal Crack Length (inches)	Hole-to-Edge Distance (inches)	Hole-to-Hole Specimen (inches)	Actual Measured Crack Length Along Faying Surface (inches)	Actual Measured Crack Length Inside Hole (inches)
25	0.010	--	0.33	--	--	--
26	Ditto	--	--	0.517	--	--
27	"	B-0.075	0.358	--	0.112	0.090
28 (b)	"	A-0.30	--	0.550	0.304	0.303
29	"	B-0.10	0.37	--	0.130	0.089
30	"	A-0.20	--	0.53	0.178	0.080
31	"	A-0.10	0.345	--	0.120	0.122
32	"	--	--	0.52	--	--
33	None	--	0.36	--	--	--
34	Ditto	--	--	0.548	--	--
35 (b)	"	A-0.30	0.344	--	0.302	0.303
36	"	B-0.025	--	0.525	0.066	0.043
37	"	--	0.363	--	--	--
38	"	A-0.20	--	0.54	0.176	0.086 (c)
39	"	--	0.355	--	--	--
40	"	--	--	0.54	--	--
41	"	--	0.342	--	--	--
42	"	B-0.19	--	0.545	0.175	0.169
43	"	B-0.05	0.342	--	0.065	0.067
44	"	--	--	0.54	--	--
45	"	--	0.37	--	--	--
46	"	B-0.10	--	0.534	0.115	0.119
47	"	A-0.40	0.332	--	0.396	0.420 (c)
48	"	--	--	0.552	--	--

TABLE 3. (continued)

Hole No.	Separation Sheet Thickness (inches)	Nominal Crack Length (inches)	Hole-to-Edge Distance (inches)	Hole-to-Hole Specimen (inches)	Actual Measured Crack Length Along Faying Surface (inches)	Actual Measured Crack Length Inside Hole (inches)
49	--	--	0.34	--	--	--
50(b)	--	A-0.30	--	0.545	0.298	0.296
51	--	--	0.36	--	--	--
52	--	--	--	0.52	--	--

(a) Total aluminum thickness around Hole No. 13 and 14 = 0.75 inch.
(b) Holes 6, 28, 35, and 50 were originally prepared with 0.10, 0.05, 0.10, and 0.05 cracks respectively in location A. These were later enlarged to 0.30 inch.
(c) Crack goes through thickness of the panel; measured crack length along bottom surface.

TABLE 4. DIMENSIONS OF SPECIMEN NO. 1-4
TWO ROWS OF TITANIUM FASTENERS JOINING
TWO 1/4-INCH THICK ALUMINUM PIECES

Hole No.	Separation Sheet Thickness (inches)	Nominal Crack Length (inches)	Hole-to-Edge Distance (inches)	Hole-to-Hole Specimen (inches)	Actual Measured Crack Length Along Faying Surface (inches)	Actual Measured Crack Length Inside Hole (inches)
1	0.020	--	0.356	--	--	--
2	Ditto	--	--	0.541	--	--
3	"	C-0.025	0.360	--	--	--
4	"	A-0.20	--	0.521	0.200	0.090
5	"	C-0.025	0.347	--	--	--
6	"	C-0.05	--	0.528	--	--
7	"	B-0.10	0.326	--	0.114	0.121
8	"	--	--	0.556	--	--
9	"	--	0.355	--	--	--
10	"	B-0.075	--	0.514	0.090	0.094
11	"	B-0.025	0.377	--	0.037	0.048
12	"	C-0.075	--	0.497	--	--
13	"	--	0.346	--	--	--
14[b]	"	A-0.30	--	0.535	0.295	0.299
15[b]	"	A-0.30	0.356	--	0.301	0.298
16	"	--	--	0.526	--	--
17	"	A-0.20	0.364	--	0.220	0.100[c]
18	"	A-0.40	--	0.545	0.410	0.410[c]
19	0.010	--	0.350	--	--	--
20	Ditto	--	--	0.520	--	--
21	"	A-0.40	0.352	--	0.450	0.450[c]
22	"	C-0.025	--	0.520	--	--
23	"	C-0.05	0.338	--	--	--
24	"	C-0.10	--	0.532	--	--

TABLE 4. (continued)

Hole No.	Separation Sheet Thickness (inches)	Nominal Crack Length (inches)	Hole-to-Edge Distance (inches)	Hole-to-Hole Specimen (inches)	Actual Measured Crack Length Along Faying Surface (inches)	Actual Measured Crack Length Inside Hole (inches)
25	0.010	C-0.075	0.340	--	--	--
26	Ditto	--	--	0.554	--	--
27	"	--	0.342	--	--	--
28	"	B-0.05	--	0.551	0.077	0.077
29(a)	"	A-0.05	0.404	--	0.070	0.096
30(a)	"	A-0.20	--	0.528	0.200	0.058
31	"	B-0.075	0.342	--	0.086	0.104
32	"	--	--	0.544	--	--
33	"	--	0.370	--	--	--
34	"	A-0.40	--	0.510	0.400	0.400(c)
35(b)	"	A-0.30	0.375	--	0.309	0.301
36	"	--	--	0.493	--	--
37	0.00	--	0.348	--	--	--
38	Ditto	--	--	0.528	--	--
39	--	C-0.05	0.321	--	--	--
40	--	C-0.025	--	0.550	--	--
41	--	C-0.05	0.346	--	--	--
42	--	A-0.10	--	0.521	0.100	0.106
43	--	A-0.20	0.346	--	0.205	0.080(c)
44	--	C-0.10	--	0.535	--	--
45	--	--	0.359	--	--	--
46(b)	--	A-0.30	--	0.505	0.297	0.295
47	--	B-0.05	0.360	--	0.068	0.085
48	--	--	--	0.525	--	--

TABLE 4. (Continued)

Hole No.	Separation Sheet Thickness (inches)	Nominal Crack Length (inches)	Hole-to-Edge Distance (inches)	Hole-to-Hole Specimen (inches)	Actual Measured Crack Length Along Faying Surface (inches)	Actual Measured Crack Length Inside Hole (inches)
49	0.00	--	0.354	--	--	--
50	Ditto	B-0.10	--	0.527	0.110	0.107 (c)
51	"	A-0.40	0.293	--	0.425	0.420 (c)
52	"	--	--	0.594	--	--
53	"	--	0.337	--	--	--
54	"	--	--	0.508	--	--

(a) Total aluminum thickness around Holes Nos. 29 and 30 = 0.75 inch.
(b) Holes 14, 15, 35, and 46 were originally prepared with 0.100, 0.050, 0.100 and 0.050 cracks respectively in location A. These were later enlarged to 0.300 inch.
(c) Crack goes through thickness of the panel; measured crack length along bottom surface.

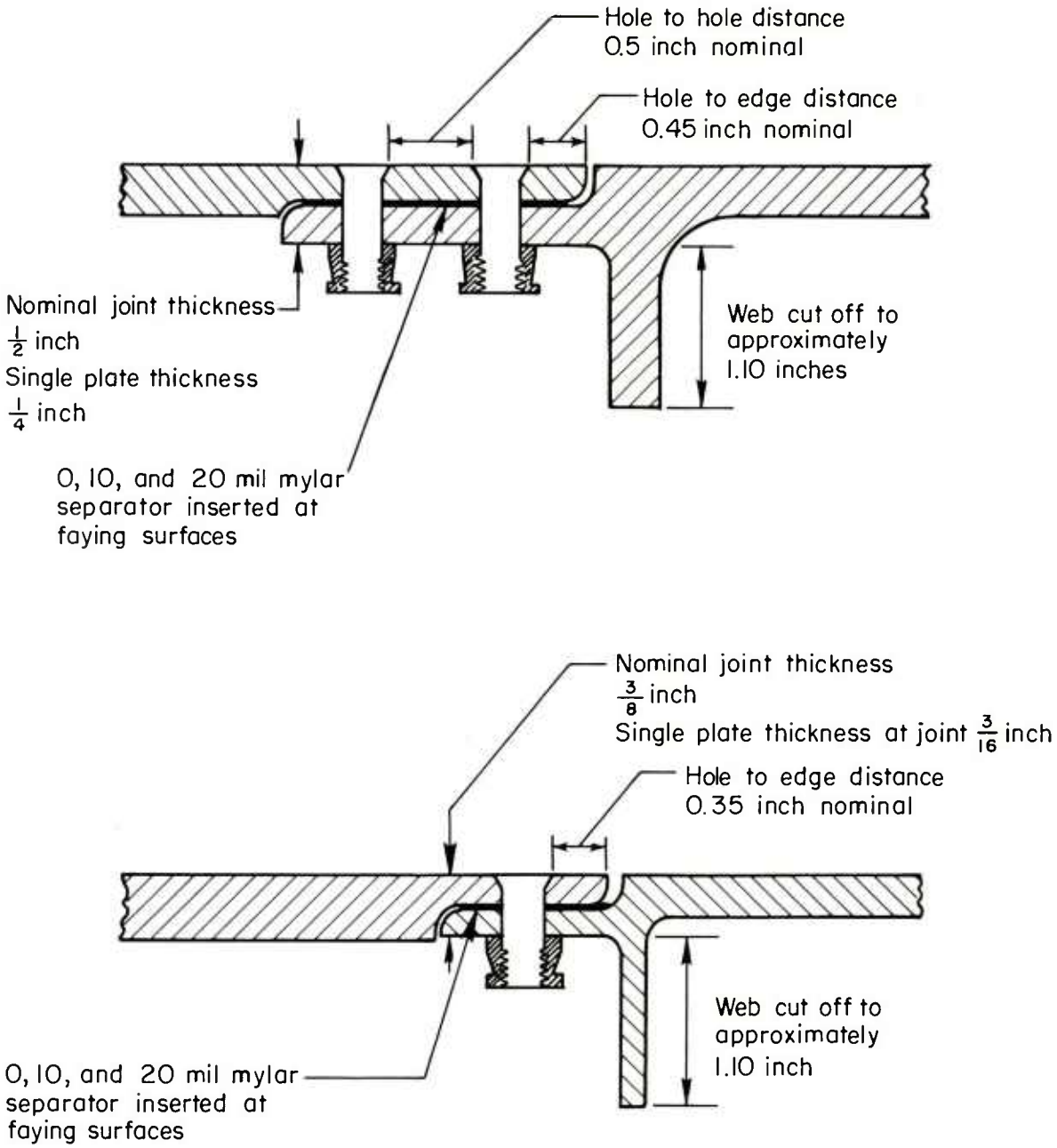

FIGURE 3. CONFIGURATION AND NOMINAL DIMENSIONS OF C-5A WING-SPLICE JOINT SPECIMENS

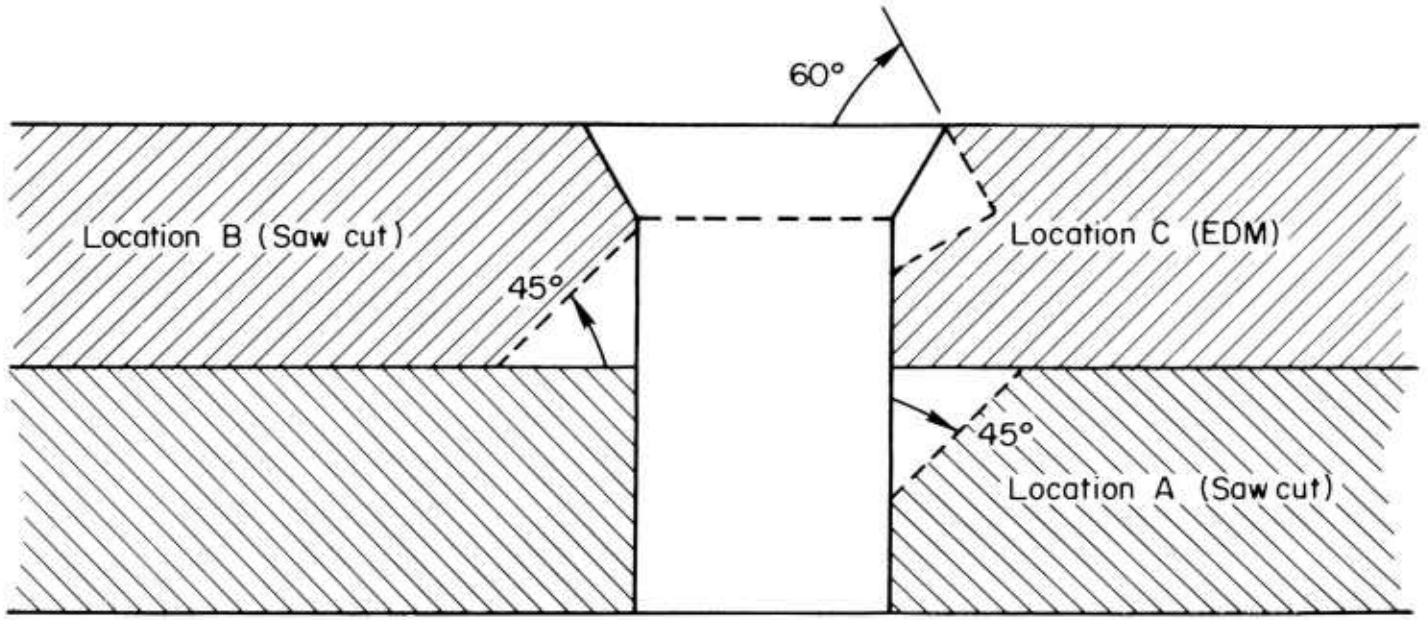

FIGURE 4. THREE LOCATIONS OF SAW CUTS AND EDM CRACKS IN FASTENER HOLES

where the crack length is measured along the faying surface in locations A and B, or the maximum depth for location C. All of the cracks were oriented along the centerline of the row of fasteners. The smaller cracks were cut from the faying surface to the hole at a 45-degree angle (Figure 4). When propagation occurred far enough to become a "through" crack, the crack was assumed to run in a linear pattern. Because of the large increase in crack area at 0.200 inch, the cracks were cut at 22.5 degrees, and at 0.300 inch they were cut so that the crack front was perpendicular to the faying surface. The faying surface-cracks were all cut with jeweler's blades for minimum width.

The cracks at the counter sink were EDM cuts at 60 degrees to the surface as shown in Figure 4. Although a square tip is shown for the EDM slots, this type of cutting produces slightly rounded corners which more closely resembles the eliptical shape of a propagated crack.

All of the cracks were measured with an optical enlarger and a depth micrometer to determine true crack area. The measured and planned crack lengths are listed in Tables 1 through 4 for each fastener.

B. Coil Positioning. For testing fastener holes on aircraft it is important that a means be developed to permit rapid centering of the test coil on the fastener within 0.005 to 0.010 inches tolerance. Optical or electromechanical devices are being considered and will be developed later in the program, however, these devices were not available for the Phase I effort.

For this program, V wedges as shown in Figure 5 were adhesively bonded to the surface of the panel so that when the cylindrical shaped coil holder was seated into the vee, the coil was centered on the fastener to be tested. The bottom of the coil holder rested on the panel surface so that the wedges did not affect coil lift-off.

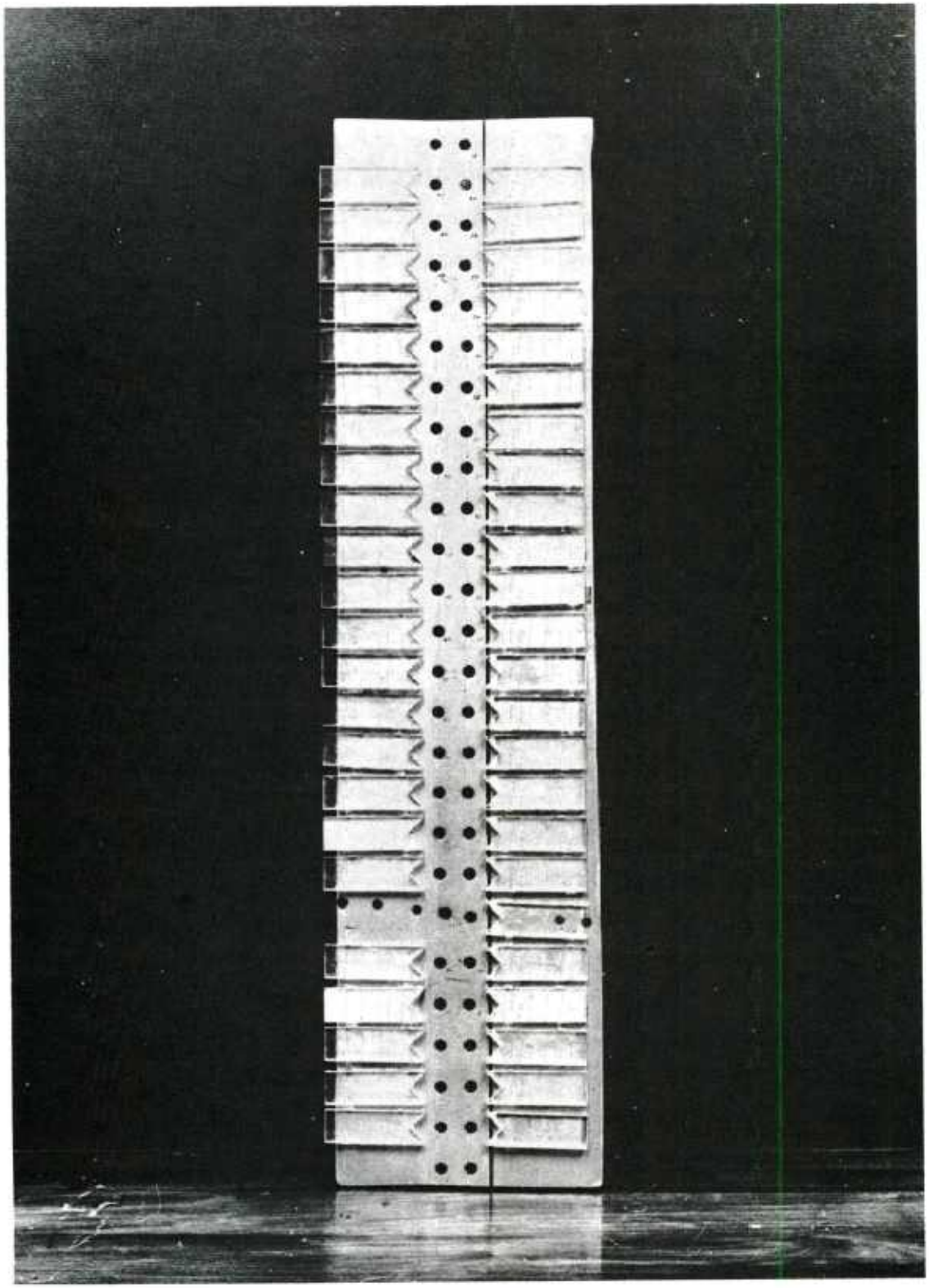

FIGURE 5. TYPICAL DOUBLE ROW WING-SPLICE PANEL WITH COIL CENTERING TEMPLATES IN PLACE

5. METHODS OF MFEC DATA ANALYSIS

The multiple frequency eddy-current (MFEC) approach used in this research yields six output voltage measurements for each attempt at crack detection. The six measurements consist of one inphase voltage component and one quadrature voltage component taken at each of three eddy-current frequencies. Depending upon the size, orientation, and depths of the cracks, some of these output voltage measurements tend to deviate from the measured values obtained when no crack is present. In this setting, the analysis of the data resulting from each measurement requires several steps. First, measurements must be taken under conditions when cracks are known to be absent and when cracks are known to be present. This step is required to determine whether the voltage measurements can be used to predict the presence or absence of a crack. This step involves the question of whether the best predictor is a single voltage measurement or some combination of the six voltage measurements. This step must also determine whether certain transformations (sums, products, ratios, etc.) of the six voltage measurements can yield improved predictions of the presence or absence of a crack.

Once the best predictor variables are obtained from the voltage measurements, the results can be expressed in the form of a predictor model:

$$Y = f(X1, X2, \ldots, Xn), \qquad (1)$$

where $X1, \ldots, Xn$ are the predictor independent variables and Y is the criterion variable. Ideally, the function f would be determined from the data in such a way that Y would be equal to convenient values, such as +1 or -1, depending on whether the X-values were obtained when a crack was present or absent, respectively. If the appropriate predictor variables and the appropriate function can be learned from the data obtained under conditions where cracks are known to be present or absent, then the same variables and function can be applied to other locations where

the presence or absence of a crack is not known. To do this, the appropriate voltage measurements would be measured, and transformed if necessary. These would then be substituted into the function f. The function indicates if a crack is present or absent depending on whether the calculated Y-value is sufficiently close to +1 or -1, respectively. Clearly, these predictor functions should be tested and verified to obtain assurance that the predictions are valid. If this verification step is successful, then the approach may be routinely applied with minimal field monitoring or updating to maintain the quality of the predictions.

In summary, this brief description shows that the data analysis problem consists of several steps: (1) a "learning" stage in which the important predictors, transforms, and predictive functional relations are identified; (2) a "verification" stage in which the resulting predictive relation is applied to data not used in generating the relation; and (3) an "implementation" stage in which a validated predictive relation may be routinely applied in the field.

The research reported below is related to the learning and verification steps of two different methods of data analysis: linear discriminant analysis (LDA) and automatic interaction detection (AID). Both methods have characteristics that are applicable to the MFEC detection of cracks. These characteristics include the following:

(1) Training sets of data are required to obtain the best variables for predicting the presence or absence of a crack.

(2) Several variables may be simultaneously involved in the multivariate predictive relations.

(3) The statistical strengths of the resulting predictive relations can be quantitatively assessed.

(4) The algorithms that generate the predictions are objective and can be mathematically derived from known assumptions.

(5) Both methods are statistical in that predictions are generated that have known probabilities of being correct.

As the MFEC crack detection research progressed it became evident that the crack predictions yielded by the AID algorithm were frequently better than those yielded by the linear discriminant. For this reason, the AID analysis and capabilities are described in greater detail, although the linear discriminant analysis is most conventional, has a longer history of application, and is more familiar to a broad group of researchers. The AID analysis is a more recent development than LDA and makes fewer assumptions concerning the relationships among the variables. AID provides a graphical display (AID "tree") that exhibits the interrelationships among the variables. The AID algorithm begins by making an exhaustive examination to determine the best predictor variable. Once determined, the algorithm then determines the next best predictors and continues in a sequential manner until all good predictors have been identified. The algorithm is structured so that complex interactions among the variables are routinely identified and exhibited. More detailed descriptions of both AID and LDA are given in the Appendices and References.

Many questions are not currently answered regarding field implementation of the AID algorithm. For example, it is not clear how representation of the AID output can be most efficiently implemented by a computer. Both arithemical and logical representations are possible. In the effort described in this report, a logical representation and implementation of the AID analysis was used. The representation used appears to be of minor concern.

A more important unresolved issue concerns whether the AID algorithm can be deliberately biased to control the probabilities of prediction errors. Such biasing is often desired in order to reduce the probability of missing a crack by increasing the number of false indications of cracks. Such biasing may be desirable because the cost of missing a crack is frequently much greater than the cost of a false indication. It is believed that such biasing is possible with the AID algorithm. However, no specific investigation of this issue was made under the effort described in this report.

In contrast to AID, linear discriminant analysis aims to determine an optimum set of numerical weights for combining the various predictor variables. Ideally, the numerical weights would be determined in such a way that the discriminant would take the value 1/2 when a crack is present and would take the value -1/2 when a crack is absent. In practice, such ideal weights do not exist. Instead, a least-squares procedure is used to obtain approximate estimates for the weights, together with the corresponding probabilities of correctly predicting the presence or absence of a crack.

Table 5 shows a listing of the candidate variables that were treated. In a typical AID run, all of these variables "competed" with each other to determine which candidates yielded the best predictions. Variables X2 through X7 consist of the 6 basic voltage measurements (3 frequencies and 2-phase components per frequency). Variables X23 through X28 are "normalized" forms with zero means and unit standard deviations. Variables X29 through X34 represent a different normalization in which the deviations from the means are expressed as fractions of the mean. These normalized variables were formed in order to obtain variables that are less sensitive to uniform increases or decreases in voltage levels. Variables X38, X36, and X37 represent computed modulus values (i.e., signal amplitude) for the low, intermediate, and high frequencies, respectively. Variables X41 through X46 are normalized versions of these modulus ratios. Variables X47 through X58 involve arcsine functions and their normalized forms; similar forms for arctan are included for variables X63 through X77. Variables X75 through X107 involve the use of the voltages obtained at high frequencies as "reference" voltages. In addition to variables shown in the list, variables X11 through X19 are computer-defined random variables. These variables "compete" with the real predictors in the AID runs. The random variables were introduced in order to provide some protection against incorrect inferences due to small sample sizes, especially for the later splits in the AID tree.

TABLE 5. LIST OF PREDICTORS INVESTIGATED BY AID PROGRAM

Predictor	Definition
	Basic voltage measurements
X2	Frequency = 90 Hz; Inphase Component
X3	Frequency = 90 Hz; Quadurature Component
X4	Frequency = 330 Hz; Inphase Component
X5	Frequency = 330 Hz; Quadurature Component
X6	Freqnency = 1219 Hz; Inphase Component
X7	Frequency = 1219 Hz; Quadurature Component
	Basic computed statistics
X20	Average of (X2, ···, X7)
X21	Standard Deviation of (X2···,X7)
X22	Coefficient of Variation, X21/X20
	Normalized voltage measurements with zero means and unit standard deviating
X23	(X2-X20)/X21
X24	(X3-X20)/X21
X25	(X4-X20)/X21
X26	(X5-X20)/X21
X27	(X6-X20)/X21
X28	(X7-X20)/X21
	Non-dimensional voltage measurements
X29	(X2-X20)/X20
X30	(X3-X20)/X20
X31	(X4-X20)/X20
X32	(X5-X20)/X20
X33	(X6-X20)/X20
X34	(X7-X20)/X20
	Modulus transformations with associated statistics
X35	SQRT ((X2 * X2) + (X3 * X3))
X36	SQRT ((X4 * X4) + (X5 * X5))
X37	SQRT ((X6 * X6) + (X7 * X7))
X38	Average of (X35, X36, X37)
X39	Standard Deviation of (X35, X36, X37)
X40	Coefficient of Variation, X39/X38

TABLE 5. (continued)

Predictor	Definition
	Normalized modulus transformations
X41	(X35-X38)/X39
X42	(X36-X38)/X39
X43	(X37-X38)/X39
X44	(X35-X38)/X38
X45	(X36-X38)/X38
X46	(X37-X38)/X38
	Phase angle transformations with associated statistics
X47	ASIN (X3/X35)
X48	ASIN (X5/X36)
X49	ASIN (X7/X37)
X50	Average of (X47, X48, X49)
X51	Standard Deviation of (X47, X48, X49)
X52	Coefficient of Variation, X51/X50
	Normalized phase angle transformations
X53	(X47-X50)/X51
X54	(X48-X50)/X51
X55	(X49-X50)/X51
X56	(X47-X50)/X50
X57	(X48-X50)/X50
X58	(X49-X50)/X50
	Generalized modulus transformation
X59	X2 + X4 + X6
X60	X3 + X5 + X7
X61	SQRT ((59 * X59) + (X60 * X60))
X62	ATAN (X60/X59)

TABLE 5. (continued)

Predictor	Definition
	Phase angle transformations with associated statistics
X63	ATAN (X3/X2)
X64	ATAN (X5/X4)
X65	ATAN (X7/X6)
X66	Average of (X63, X64, X65)
X67	Standard Deviation of (X63, X64, X65)
X68	Coefficient of Variation, X67/X66
	Normalized phase angle transformations
X69	(X63-X66)/X67
X70	(X64-X66)/X67
X71	(X65-X66)/X67
X72	(X63-X66)/X66
X73	(X64-X66)/X66
X74	(X65-X62)/X66
X75	(X63-X62)/X62
X76	(X64-X62)/X62
X77	(X65-X62)/X62
	Transformations using high frequency voltage measurement as a reference measurement
X78	X2-X7
X79	X3-X7
X80	X4-X7
X81	X5-X7
X82	X6-X7
X83	X78/Standard Deviation of (X78,···, X82)
X84	X79/Standard Deviation of (X78,···, X82)
X85	X80/Standard Deviation of (X78,···, X82)
X86	X81/Standard Deviation of (X78,···, X82)
X87	X82/Standard Deviation of (X78,···, X82)
X88	X78/X7
X89	X79/X7
X90	X80/X7
X91	X81/X7
X92	X82/X7

TABLE 5. (continued)

Predictor	Definition
	Normalizing transformations using high frequency modulus as a reference
X93	(X2-X37)/X39
X94	(X3-X37)/X39
X95	(X4-X37)/X39
X96	(X5-X37)/X39
X97	(X6-X37)/X39
X98	(X2-X37)/X37
X99	(X3-X37)/X37
X100	(X4-X37)/X37
X101	(X5-X37)/X37
X102	(X6-X37)/X37
	Normalizing transformations using high frequency phase angle as a reference
X103	(X63-X65)/X65
X104	(X64-X65)/X65
	Modulus transformations using high frequency modulus as a reference
X105	(X35-X37)/X37
X106	(X36-X37)/X37
X107	X105/X106

6. RESULTS

A. Single Frequency Measurements. As mentioned previously, six eddy-current readings are taken on each fastener to provide input to the MFEC analysis algorithm. An in-phase and quadrature reading is taken at each of three test frequencies.

The frequencies employed for these experiments were selected by considering calculated penetration depth, followed by preliminary evaluations of response at various frequencies and results of preliminary AID analysis using two candidate sets of frequencies. The results of the AID analysis for the other sets of frequencies indicated that the best detection of crack could be obtained with the frequencies listed in Table 6.

The in-phase component of voltage and corresponding quadrature components were selected from a variety of choices covering 360 degrees in approximately 5 degree increments depending on frequency of exictation. In-phase components were selected so that the assortment of fasteners in the test sample would provide approximately the same range of voltage responses in the in-phase and quadrature data storage registers. A balanced response between in-phase and quadrature reading takes advantage of the full response range of the digital eddy current equipment without altering the content of the information obtained at each frequency. The in-phase component was selected by typing the desired phase angle on the keyboard terminal. The quadrature component is automatically determined by the computer to be 90 degrees from the in-phase component for each frequency.

Eddy-current readings were then taken on each fastener in the titanium fastener panels 1-3 and 1-4 (except the four fasteners at the end of the sample and two fasteners which protruded excessively). Similarly, MFEC readings were taken on the steel fastener panel (the last seven fasteners were titanium). Measurements were then taken on panel 1-2, except the end fasteners. In each case, this procedure was repeated four times for a complete data set.

TABLE 6. TEST FREQUENCIES AND PHASE ANGLES SELECTED FOR TESTING TITANIUM AND STEEL FASTENER JOINTS

Fastener Material	Frequency, Hz	In-Phase Angle Measurements	Quadrature Angle Measurements
Titanium	90	44.3	134.3
	330	45	135
	1219	18	108
Steel	90	1.3	91.3
	330	5.0	95
	1219	18.0	108

The above procedure therefore resulted in the following data points at each frequency and phase angle for the steel and titanium fastener panels:

Fastener Material	Total Number of Data Points				
		Crack Size (inches)*			
	No Cracks	0.4	0.3	0.2	0.1
Steel	179	12	12	12	12
Titanium	174	32	32	20	8

* All cracks are in location A (See Figure 4).

Initial balance of the digital MFEC system was obtained before acquisition of each data set. Balance is a condition in which the signal generated by the MFEC system is nulled to less than 10 millivolts. The balance stability was checked before and after each set. The balance stability refers to the ability of the system to maintain the nulled signal. The balance stability is checked by returning to the standard (no crack) fastener on which the balance was originally taken.

Plots of each in-phase and quadrature reading were then obtained for each frequency. A sorting routine was used to group the data in crack sizes for AID and LDA processing and analysis. Two computer generated plots for the titanium and steel fastener panels at 90 Hz, in-phase, are shown in Figures 6 and 7, respectively. The two complete sets of plots of single frequency data from both the steel and titanium fastened panels at each frequency and phase are contained in Appendix D.

B. MFEC Classification of Titanium Fasteners. Any one of the single-frequency measurements is a relatively poor indication of the presence of cracks under the titanium as illustrated in Figure 6 and Appendix Figures D-1 through D-6. This is realized by observing the relatively broad variation in measurements taken on fasteners that do not have cracks which are designated as "no cracks" and the similar overlapping scatter in readings taken on fasteners with cracks. In comparison Figure 8 is a plot of the computer

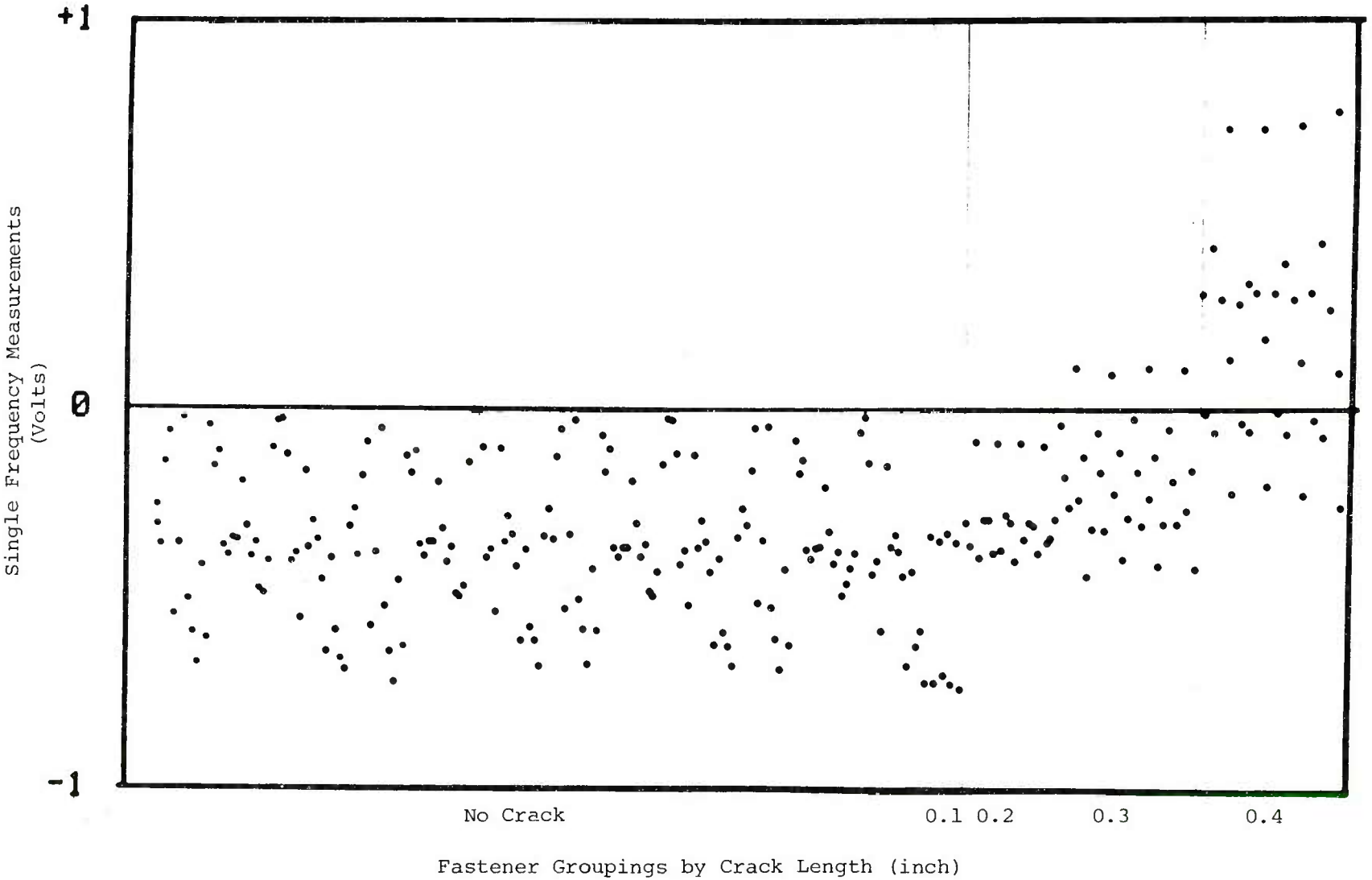

FIGURE 6. SINGLE FREQUENCY MEASUREMENTS FOR MFEC ANALYSIS ON TITANIUM FASTENERS — 90 HZ, INPHASE

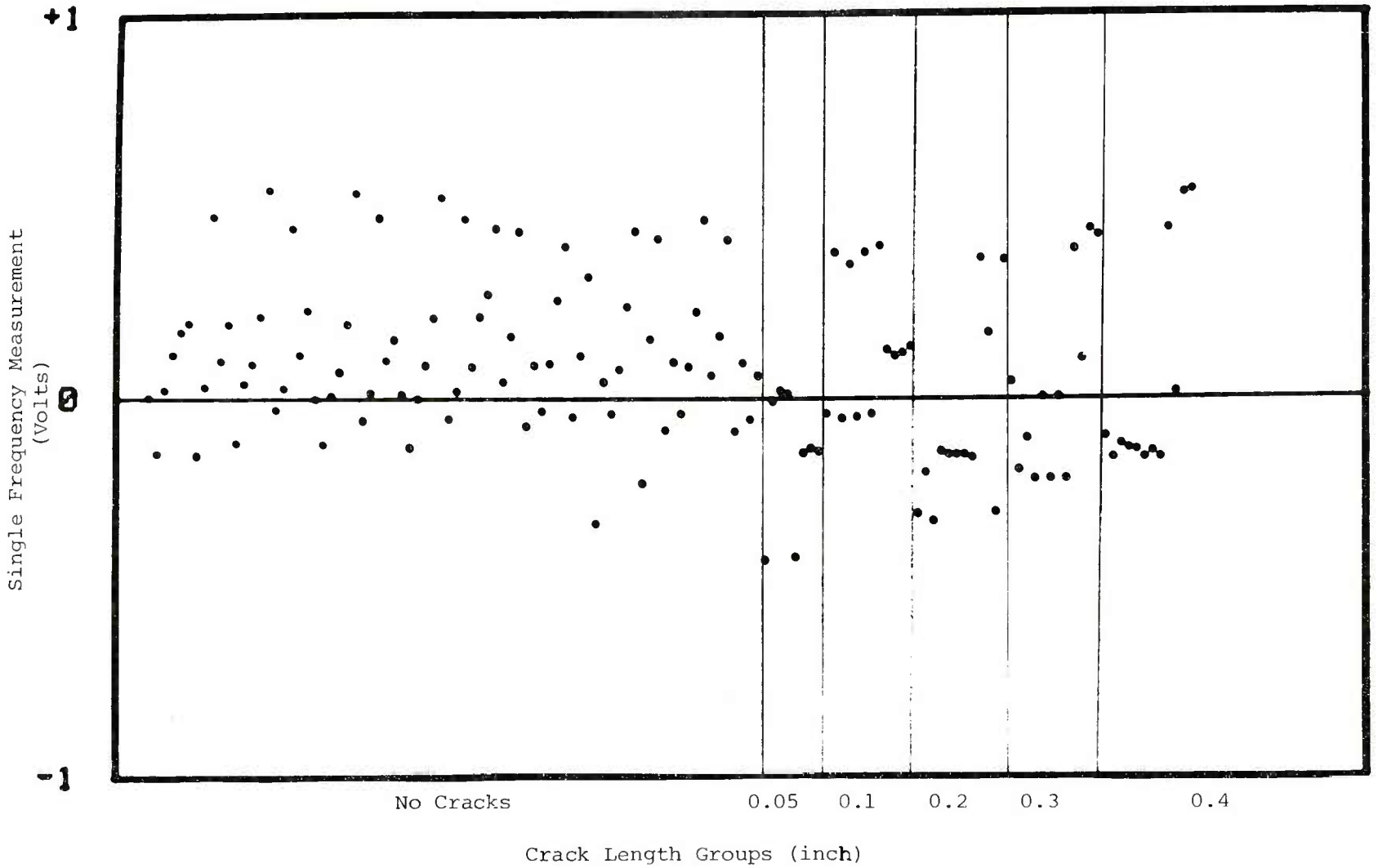

FIGURE 7. SINGLE FREQUENCY MEASUREMENTS FOR MFEC ANALYSIS ON STEEL FASTENERS - 90HZ, INPHASE

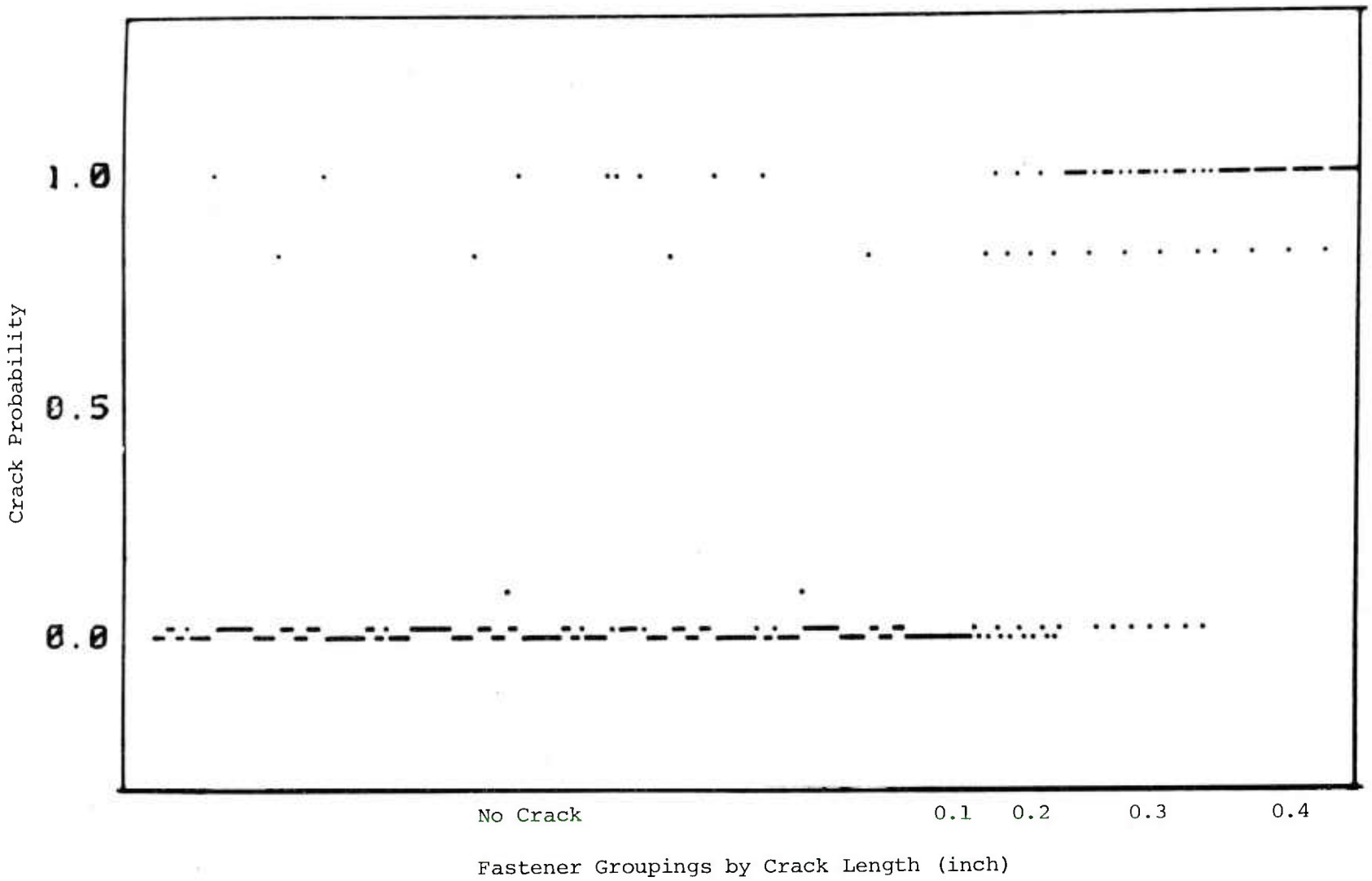

FIGURE 8. MFEC DECISION PROCESS USING AID IMPLEMENTATION TO CLASSIFY (MFEC) MEASUREMENTS ON TITANIUM FASTENERS

output provided by processing the single-frequency measurement with the decision algorithm.

The decision algorithm is derived from the AID analysis discussed in the following section. In brief, the single-frequency measurements are transformed to generate several new predictor variables. These transformed values are examined in a prescribed sequence which puts the particular set of readings into one of several groups determined from the AID analysis. Each group has an associated probability that a crack exists for the fastener in question. Fasteners that fall into groups that have probabilities greater than 0.5 are said to have cracks. Those fasteners that fall in groups below 0.5 are said to be crack-free.

The algorithm used to determine the detection of cracks under titanium fasteners classifies each fastener in one of five groups based on the single-frequency measurements associated with that fastener. As indicated on the diagram, three groups have low probabilities 0.0, 0.02, and 0.10. The other two have relatively high probabilities, 0.84 and 1.00. Fasteners that are placed in the high probability group are identified as cracks. Figure 8 shows those readings which were classified correctly and those which were misclassified. Although some of the no crack fasteners were classified as cracks; there were relatively few misclassifications. Notice that the computer was able to correctly classify most of the 0.4-inch-long cracks and most of the 0.3-inch-long cracks. Evidently, the 0.2- and 0.1-inch-long cracks were too small to be classified correctly with any reliability.

C. MFEC Classification of Steel Fasteners. Computer processing of the single-frequency data taken on steel fasteners plotted in Figure 7 and Appendix Figures D-7 through D-12 were used in the AID analysis to derive the decision algorithm. The AID analysis provided a fairly simple decision tree described in the following section using the single-frequency data taken on fasteners containing 0.1-, 0.2-, 0.3-, and 0.4-inch cracks and several no-crack fasteners to generate the AID tree.

Figure 9 illustrates the ability of the computer to classify the single frequency measurement using the derived decision algorithm. All but one of the single-frequency data were classified correctly with most of the no cracks falling in the group that has zero probability and most of the fasteners that contain cracks falling in the group having 1.0 probability. Although no additional measurements on steel fasteners containing cracks have been evaluated. These results indicate the potential of the digital MFEC system to detect cracks as small as 0.1 inch under 3/16 inch thick aluminum top plate when steel fasteners are involved.

D. Statistical Analysis of Data

(1) AID Analysis for Titanium Fasteners. Figures 10 through 12 depict the results of AID analyses of titanium fasteners data. Figure 10 shows the AID tree for the analysis of only the 0.4-inch cracks. This data set consists of 176 no cracks and 32 cracks. The first two splits, on X55 and X39 (see Table 5) correctly classified 31 of 32 total cracks, yielding a probability of correct classifications of 0.97 for cracks. Similarly, the first splits have a correct classification for non-cracks of 0.99. The remaining three splits shown on this tree each turned out to be equivalent to splits on purely random variables, and therefore should not be included in a classification algorithm based on this AID run.

The AID tree shown in Figure 11 shows the results of adding 32 cases involving 0.3-inch cracks to the data. This AID tree is more complex mainly because of the larger sample size and, to some extent, the fact that the 0.3-inch cracks are more difficult to distinguish from noncracks than are the 0.4-inch cracks. The first split in this tree is on variable X76 producing groups of sizes 186 and 54. The 54 cases in the smaller group includes 45 of the 64 cracks in the sample and the other group contains 19 cracks and 167 noncracks. The next split on the group of size 54 using X99 produces groups of size 44 and 10. The group of size 44 consists entirely of cracks; the other group

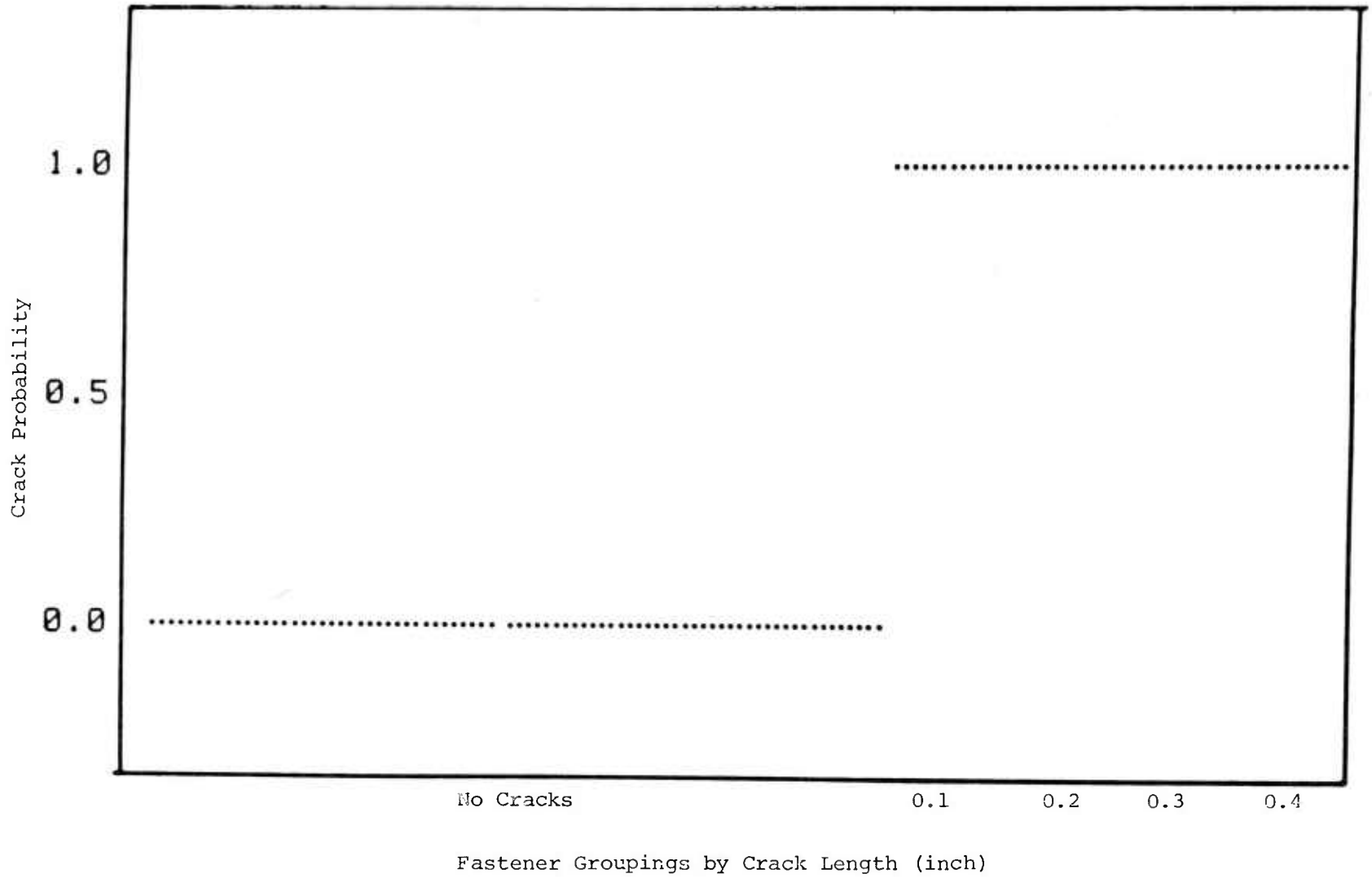

FIGURE 9. MFEC DECISION PROCESS USING AID IMPLEMENTATION TO CLASSIFY (MFEC) MEASUREMENTS ON STEEL FASTENER

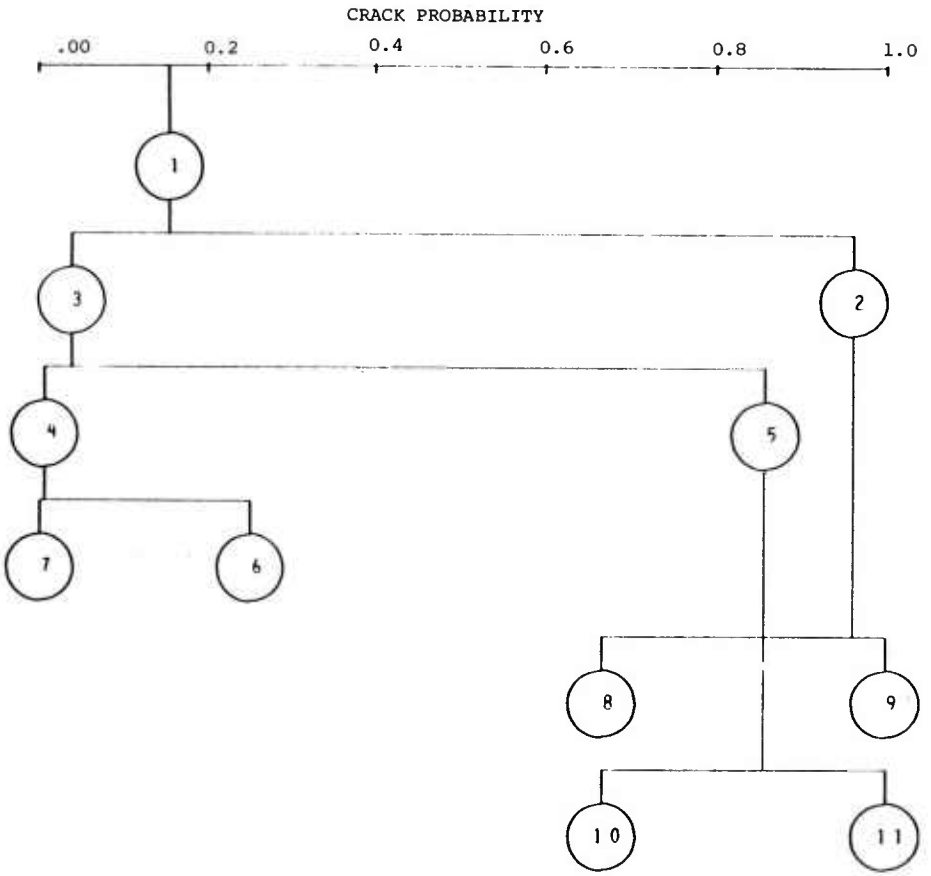

SUMMARY TABLE

---TOTAL GROUP---			
CRITERION - CRACK			
TOTAL GROUP N = 208			
MEAN = 0.15			
STO. DEV. = 0.36			
PARENT 1 SPLITTING VARIABLE - X55			
Mean = 0.04	N = 182	Mean = 0.96	N = 26
PARENT 3 SPLITTING VARIABLE - X39			
Mean = 0.01	N = 175	Mean = 0.86	N = 7
PARENT 4 SPLITTING VARIABLE - X100			
Mean = 0.00	N = 171	Mean = 0.25	N = 4
PARENT 2 SPLITTING VARIABLE - X102			
Mean = 0.67	N = 3	Mean = 1.00	N = 23
PARENT 5 SPLITTING VARIABLE - X107			
Mean = 0.67	N = 3	Mean = 1.00	N = 4

FIGURE 10. AID ANALYSIS OF DATA TAKEN ON TITANIUM FASTENERS HAVING 0.4 INCH CRACKS

DEPENDENT VARIABLE = CRACK PROBABILITY

CRACK PROBABILITY

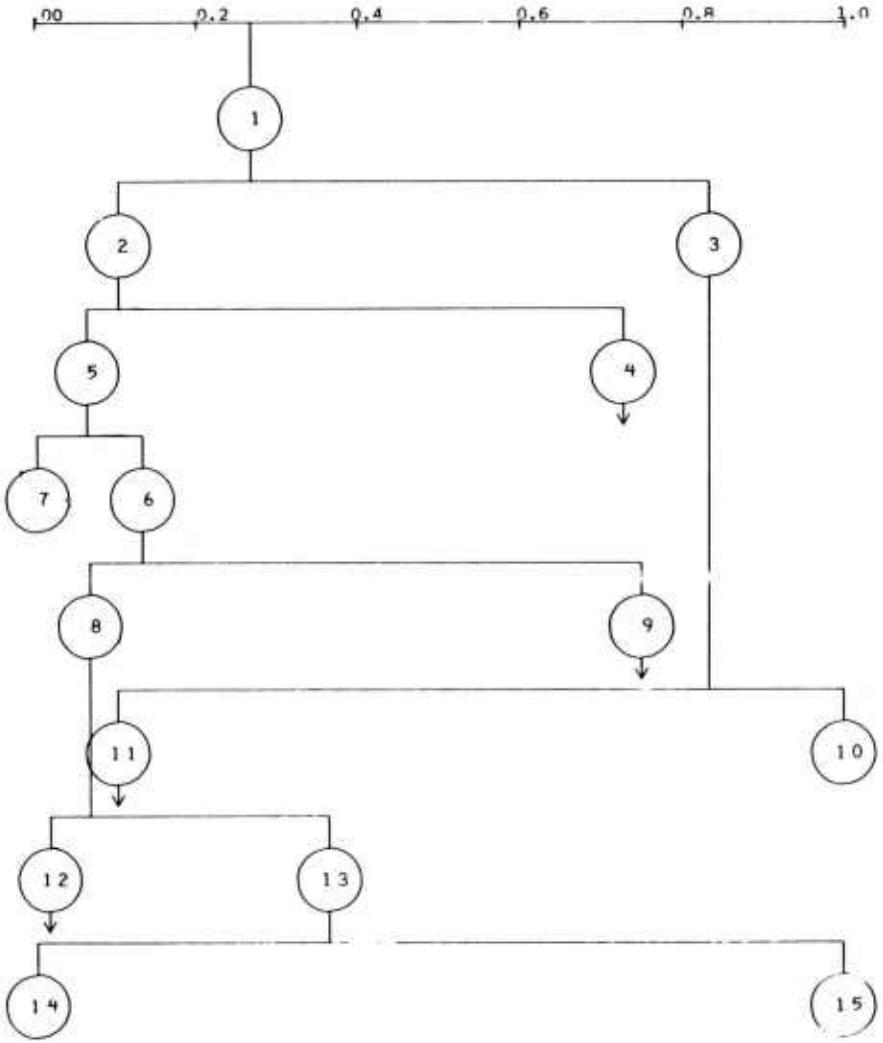

SUMMARY TABLE

---TOTAL GROUP---			
CRITERION - CRACK			
TOTAL GROUP N = 240			
MEAN = 0.27			
STD. DEV. = 0.44			
PARENT 1 SPLITTING VARIABLE - X76			
Mean = 0.10	N = 186	Mean = 0.83	N = 54
PARENT 2 SPLITTING VARIABLE - X33			
Mean = 0.06	N = 175	Mean = 0.73	N = 11
PARENT 5 SPLITTING VARIABLE - X22			
Mean = 0.00	N = 91	Mean = 0.13	N = 84
PARENT 6 SPLITTING VARIABLE - X103			
Mean = 0.07	N = 76	Mean = 0.75	N = 8
PARENT 3 SPLITTING VARIABLE - X99			
Mean = 0.10	N = 10	Mean = 1.00	N = 44
PARENT 8 SPLITTING VARIABLE - X66			
Mean = 0.02	N = 65	Mean = 0.36	N = 11
PARENT 13 SPLITTING VARIABLE - X106			
Mean = 0.00	N = 7	Mean = 1.00	N = 4

FIGURE 11. AID ANALYSIS OF DATA TAKEN ON TITANIUM FASTENERS HAVING 0.4 INCH AND 0.3 INCH CRACKS

DEPENDENT VARIABLE = CRACK PROBABILITY

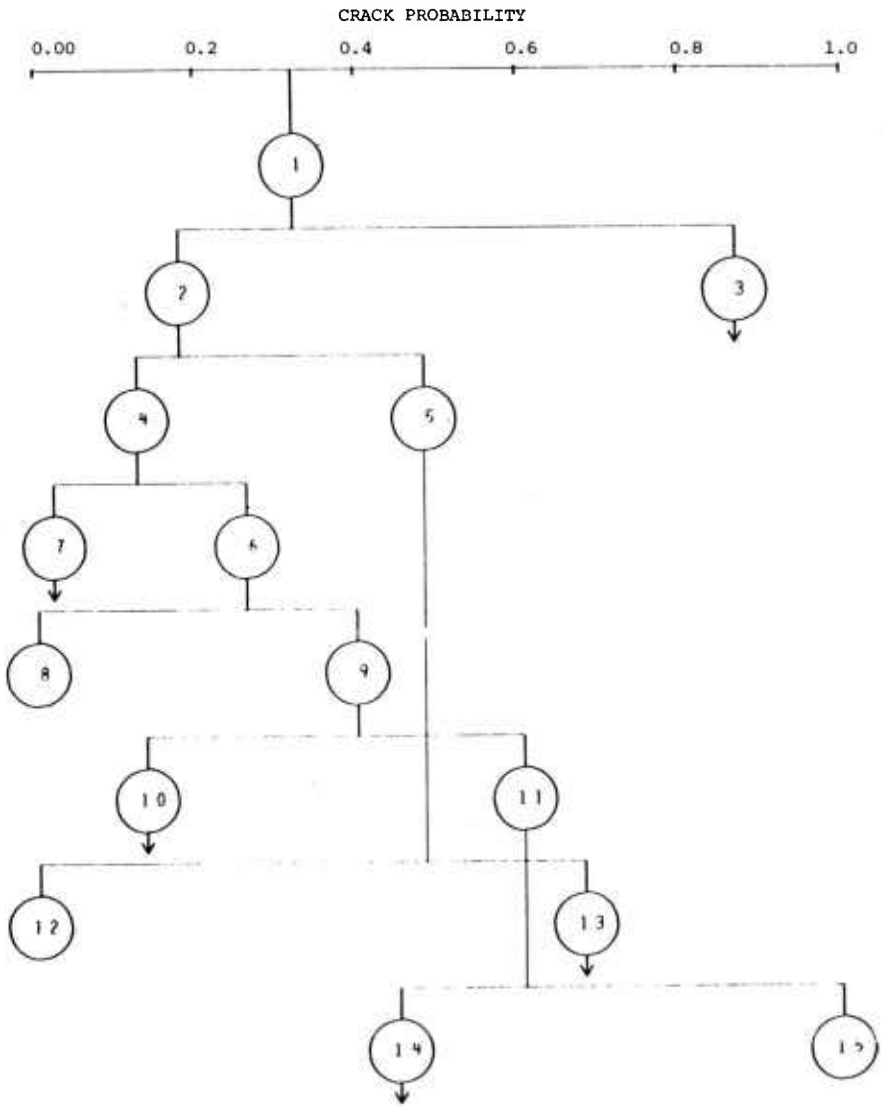

SUMMARY TABLE

---TOTAL GROUP---			
CRITERION - CRACK			
TOTAL GROUP N = 260			
MEAN = 0.32			
STD. DEV. = 0.47			
PARENT 1 SPLITTING VARIABLE - X62			
Mean = 0.13	N = 206	Mean = 0.87	N = 54
PARENT 2 SPLITTING VARIABLE - X82			
Mean = 0.13	N = 175	Mean = 30	N = 31
PARENT 4 SPLITTING VARIABLE - X97			
Mean = 0.02	N = 99	Mean = 0.26	N = 76
PARENT 6 SPLITTING VARIABLE - X87			
Mean = 0.00	N = 26	Mean = 0.40	N = 50
PARENT 9 SPLITTING VARIABLE - X36			
Mean = 0.14	N = 22	Mean = 0.61	N = 28
PARENT 5 SPLITTING VARIABLE - X104			
Mean = 0.00	N = 9	Mean = 0.68	N = 22
PARENT 11 SPLITTING VARIABLE - X67			
Mean = 0.45	N = 20	Mean = 1.00	N = 8

FIGURE 12. AID ANALYSIS OF DATA TAKEN ON TITANIUM FASTENERS HAVING 0.4 INCH, 0.3 INCH, AND 0.2 INCH CRACKS

DEPENDENT VARIABLE = CRACK PROBABILITY

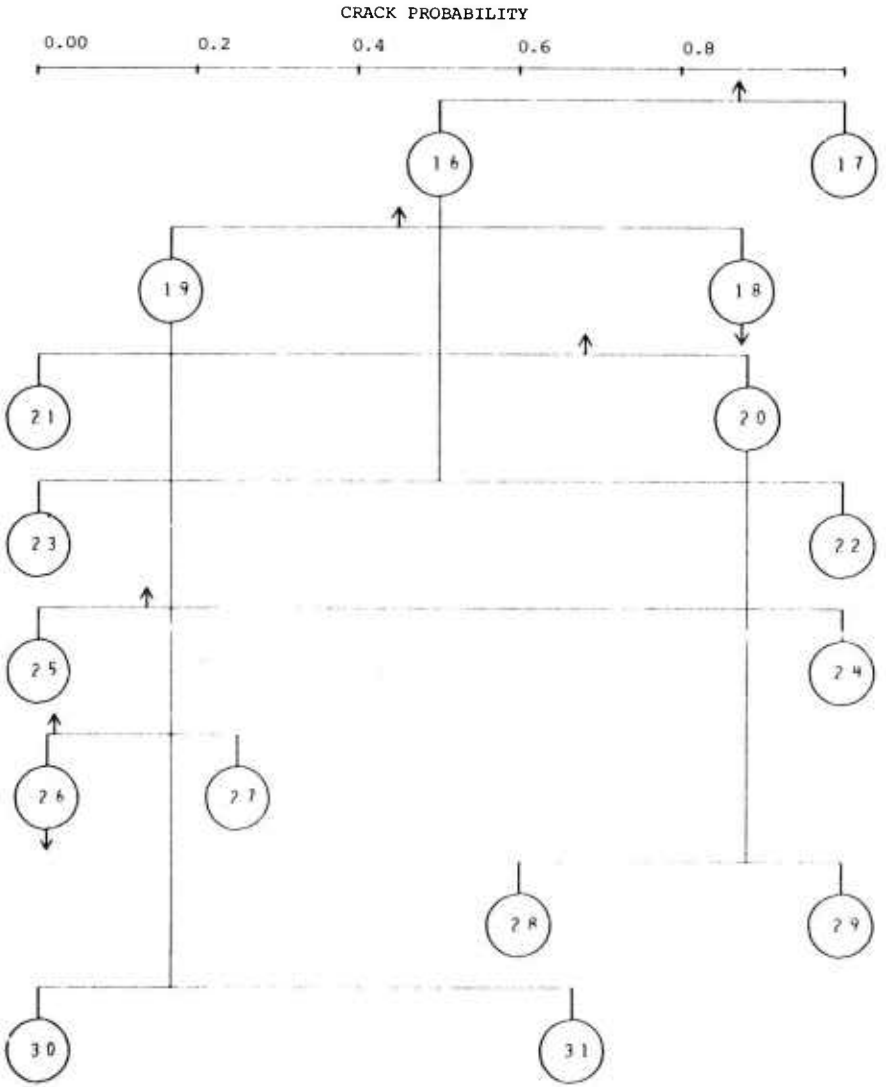

SUMMARY CONTINUED			
PARENT 3 SPLITTING VARIABLE - X73			
Mean = 0.90	N = 14	Mean = 1.00	N = 40
PARENT 14 SPLITTING VARIABLE - X106			
Mean = 0.14	N = 12	Mean = 0.87	N = 8
PARENT 13 SPLITTING VARIABLE - X106			
Mean = 0.00	N = 5	Mean = 0.88	N = 17
PARENT 16 SPLITTING VARIABLE - X106			
Mean = 0.00	N = 7	Mean = 1.00	N = 7
PARENT 10 SPLITTING VARIABLE - X100			
Mean = 0.00	N = 19	Mean = 1.00	N = 3
PARENT 7 SPLITTING VARIABLE - X97			
Mean = 0.01	N = 95	Mean = 0.25	N = 7
PARENT 28 SPLITTING VARIABLE - X37			
Mean = 0.60	N = 5	Mean = 1.00	N = 12
PARENT 19 SPLITTING VARIABLE - X17			
Mean = 0.00	N = 9	Mean = 0.67	N = 3

FIGURE 12. (Continued)

includes 1 crack and 9 no-cracks.

In Figure 11 by discarding splits that occur "too far down the tree", i.e., beyond the point of having any statistical significance, we are left with the following groups as terminal groups: 4, 7, 8, 9, 10, 11. A classification rule based on this AID tree with these six terminal groups would identify any members of groups 4, 9, or 10 as a crack and members of groups 7, 8, and 11 as non-cracks. This classification rule correctly identified 58 of 64 total cracks giving a probability of correct classification of cracks of 91 percent. Similarly the probability of correct classification of non-cracks is 97 percent.

In Figure 12 we see that the addition of 20 data points on 0.2-inch cracks produces some differences, although there are some similarities with respect to the previous AID tree. The first split is on X62 producing one group predominantly comprised of cracks and another group including most of the non-cracks. Group 3 contains 47 of the 84 cracks in the sample and 7 non-cracks. Group 2 has 37 cracks and 169 non-cracks. Group 3 eventually splits on X73 and then on X106. On the left side of the tree, the AID program is attempting to separate relatively small cracks fron noncracks and the results in this area are not particularly impressive. Many steps are required to identify these cracks and, furthermore, only a few cracks are identified at any one step.

In addition to the AID analysis discussed above which included tests made on fastener holes with cracks only in the lower layer, several analyses were conducted on MFEC measurements made on the titanium fastened panels in which the holes having cracks in the upper layer were included. These measurements were made early in the program before the AID analysis methodology had been well established. The MFEC measurement for these experiments included fasteners in the top layer containing cracks 0.025, 0.050, 0.075, and 0.100 inch in length at the counter sink and faying surface and fasteners in the bottom layer contain cracks 0.050, 0.100, 0.200, and 0.400 inch long at the faying surface. The bottom layer had no 0.300 inch cracks when these data were acquired.

The analysis indicated difficulty in correctly classifying fastener condition except for the 0.400 inch cracks in the bottom layer. Approximately 55 percent correct classification was achieved on four analyses made on panels 1-3 and 1-4. Since there were so many false classifications with the top crack and smaller bottom cracks included, it was decided to test the panels progressively, starting with an assortment of non-cracked holes and holes having the largest (0.4 inch) cracks in the bottom layer. Progressive development of the AID analysis was continued by including 0.3 inch and then 0.2 inch cracks in the lower layer and comparing the results of these successive AID runs. It was intended to add the larger cracks in the upper panel and conduct a similar progressive AID analysis during the program but these plans were not fulfilled in this Phase I project.

(2) AID Analysis for Steel Fasteners. Figures 13 through 18 show the results of AID analysis of steel fasteners. The AID tree shown in Figure 13 is a result of the AID analysis using a data set of steel fasteners consisting of the 79 measurements with no cracks and 12 measurements on 0.4-inch cracks. The tree shows that only one split is required to completely separate the cracks from the no cracks defined in Figure 13. This split is based on predictor X106. A more detailed examination of the output of this AID run shows that exactly the same split is produced by 27 of the 105 predictor variables (X3, X4, X5, X20, X22, X31, X33, X34, X36, X38, X39, X40, X45, X46, X59, X60, X61, X76, X80, X81, X89, X90, X91, X99, X100, X101, X106). In case of ties among predictor variables the AID algorithm simply selects the last one in the list, hence, X106.

The reasons that the AID analysis of the 0.4-inch cracks for steel fasteners yielded a perfect first split on so many of the predictor variables are several. First of all, the eddy-current system is more sensitive to cracks under steel fasteners than it is to cracks under titanium fasteners. Secondly, with a relatively small number of crack measurements there is a rather small amount of resolution in the data set and the predictor variables, all being related in varying degrees

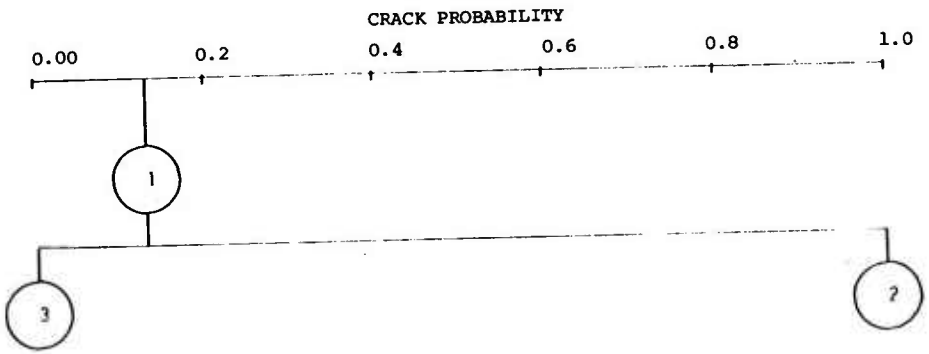

SUMMARY TABLE

---TOTAL GROUP---			
CRITERION - CRACK			
TOTAL GROUP N = 91			
MEAN = 0.13			
STD. DEV. = 0.34			
PARENT 1 SPLITTING VARIABLE - X10A			
Mean = 0.00	N = 74	Mean = 0.00	N = 12

FIGURE 13. AID ANALYSIS OF DATA TAKEN ON STEEL FASTENERS HAVING 0.4 INCH CRACKS

DEPENDENT VARIABLE = CRACK PROBABILITY

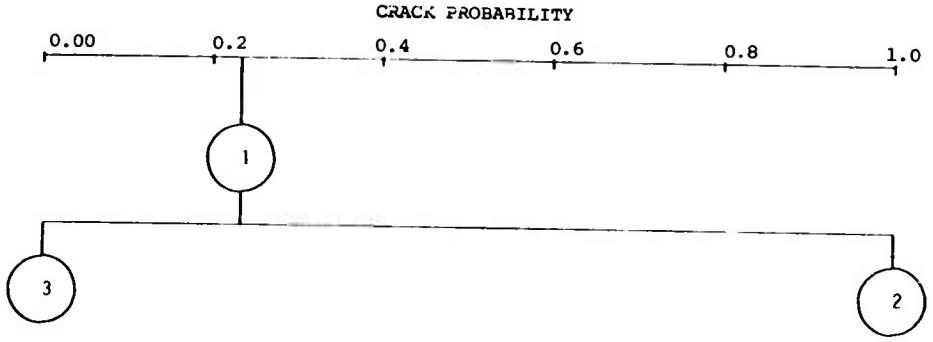

SUMMARY TABLE

---TOTAL GROUP---			
CRITERION - CRACK			
TOTAL GROUP N = 103			
MEAN = 0.23			
STD. DEV. = 0.42			
PARENT 1 SPLITTING VARIABLE - X61			
Mean = 0.00	N = 79	Mean = 1.00	N = 24

FIGURE 14. AID ANALYSIS OF DATA TAKEN ON STEEL FASTENERS HAVING 0.4 INCH AND 0.3 INCH CRACKS

DEPENDENT VARIABLE = CRACK PROBABILITY

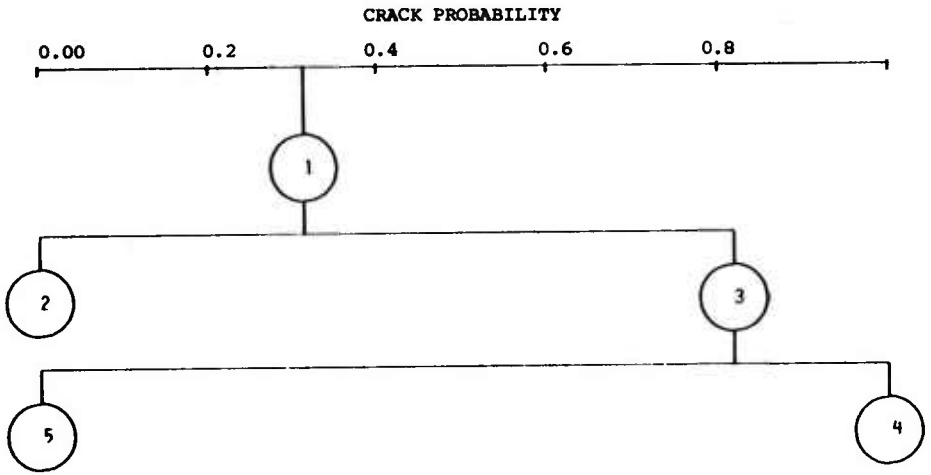

SUMMARY TABLE

---TOTAL GROUP---			
CRITERION - CRACK			
TOTAL GROUP N = 115			
MEAN = 0.31			
STD. DEV. = 0.46			
PARENT 1 SPLITTING VARIABLE - X33			
Mean = 0.00	N = 71	Mean = 0.82	N = 44
PARENT 3 SPLITTING VARIABLE - X83			
Mean = 0.00	N = 8	Mean = 1.00	N = 36

FIGURE 15. AID ANALYSIS OF DATA TAKEN ON STEEL FASTENERS HAVING 0.4 INCH, 0.3 INCH, and 0.2 INCH CRACKS

DEPENDENT VARIABLE = CRACK PROBABILITY

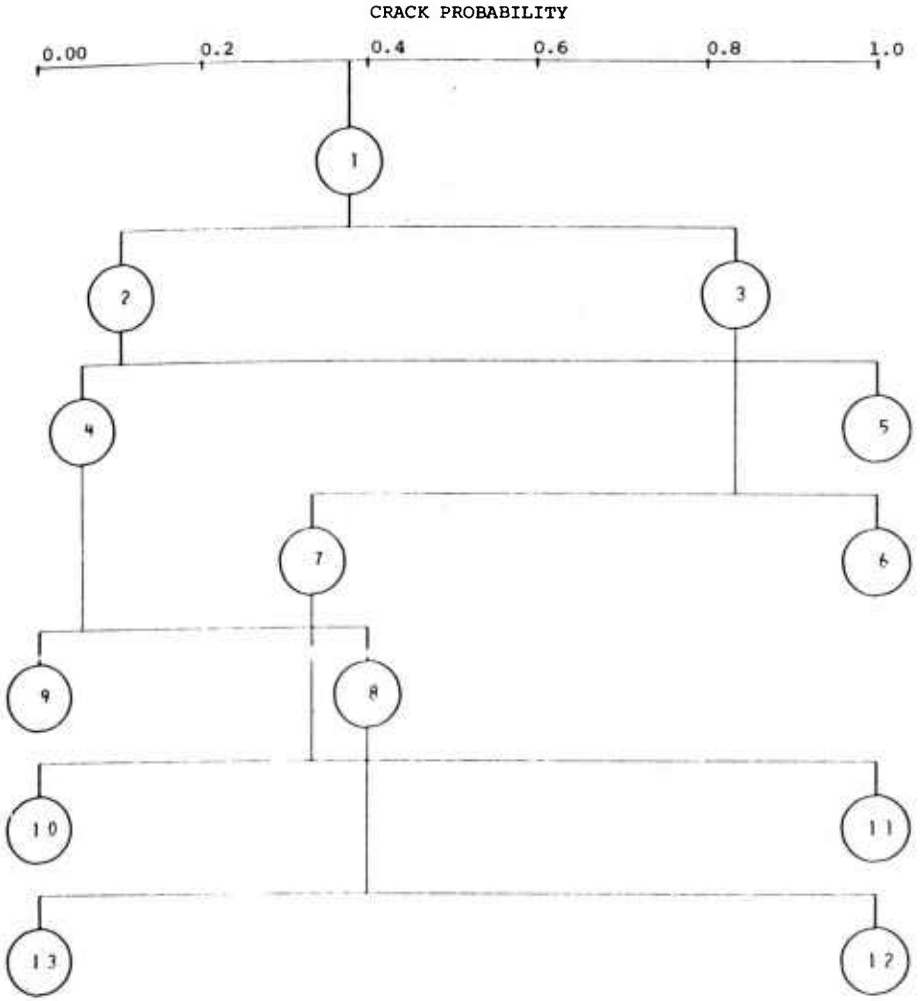

SUMMARY TABLE

---TOTAL GROUP---			
CRITERION - CRACK			
TOTAL GROUP N = 127			
MEAN = 0.38			
STD. DEV. = 0.48			
PARENT 1 SPLITTING VARIABLE - X33			
Mean = 0.10	N = 79	Mean = 0.83	N = 48
PARENT 2 SPLITTING VARIABLE - X25			
Mean = 0.05	N = 75	Mean = 1.00	N = 4
PARENT 3 SPLITTING VARIABLE - X83			
Mean = 0.33	N = 12	Mean = 1.00	N = 36
PARENT 4 SPLITTING VARIABLE - X55			
Mean = 0.00	N = 65	Mean = 0.40	N = 10
PARENT 7 SPLITTING VARIABLE - X105			
Mean = 0.00	N = 8	Mean = 1.00	N = 4
PARENT 8 SPLITTING VARIABLE - X94			
Mean = 0.00	N = 6	Mean = 0.00	N = 4

FIGURE 16. AID ANALYSIS OF DATA TAKEN ON STEEL FASTENERS HAVING 0.4 INCH, 0.3 INCH, 0.2 INCH, and 0.1 INCH CRACKS

DEPENDENT VARIABLE = CRACK PROBABILITY

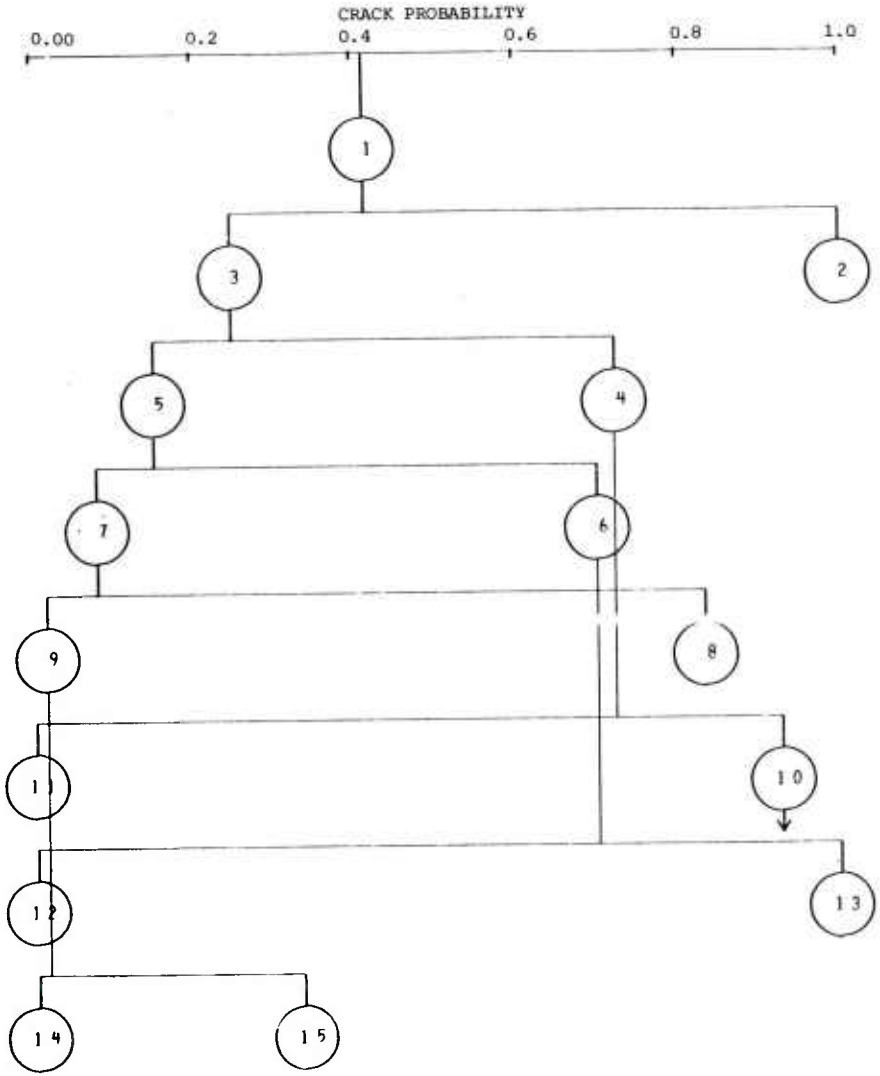

SUMMARY TABLE

---TOTAL GROUP---			
CRITERION - CRACK			
TOTAL GROUP N = 135			
MEAN = 0.41			
STD. DEV. = 0.49			
PARENT 1 SPLITTING VARIABLE - X38			
Mean = 0.25	N = 105	Mean = 1.00	N = 30
PARENT 3 SPLITTING VARIABLE - X105			
Mean = 0.15	N = 87	Mean = 0.72	N = 18
PARENT 5 SPLITTING VARIABLE - X43			
Mean = 0.08	N = 77	Mean = 0.70	N = 10
PARENT 7 SPLITTING VARIABLE - X88			
Mean = 0.01	N = 71	Mean = 0.83	N = 6
PARENT 4 SPLITTING VARIABLE - X66			
Mean = 0.00	N = 4	Mean = 0.93	N = 14
PARENT 6 SPLITTING VARIABLE - X106			
Mean = 0.00	N = 3	Mean = 1.00	N = 7
PARENT 9 SPLITTING VARIABLE - X87			
Mean = 0.00	N = 68	Mean = 0.33	N = 3

FIGURE 17. AID ANALYSIS OF DATA TAKEN ON STEEL FASTENERS HAVING 0.4 INCH, 0.3 INCH, 0.2 INCH, 0.1 INCH, AND 0.05 INCH CRACKS

DEPENDENT VARIABLE = CRACK PROBABILITY

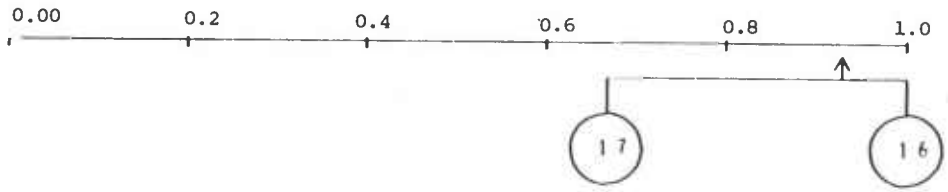

SUMMARY CONTINUED			
PARENT 10 SPLITTING VARIABLE - X98			
Mean = 42	N = 3	Mean = 63	N = 11

FIGURE 17. (Continued)

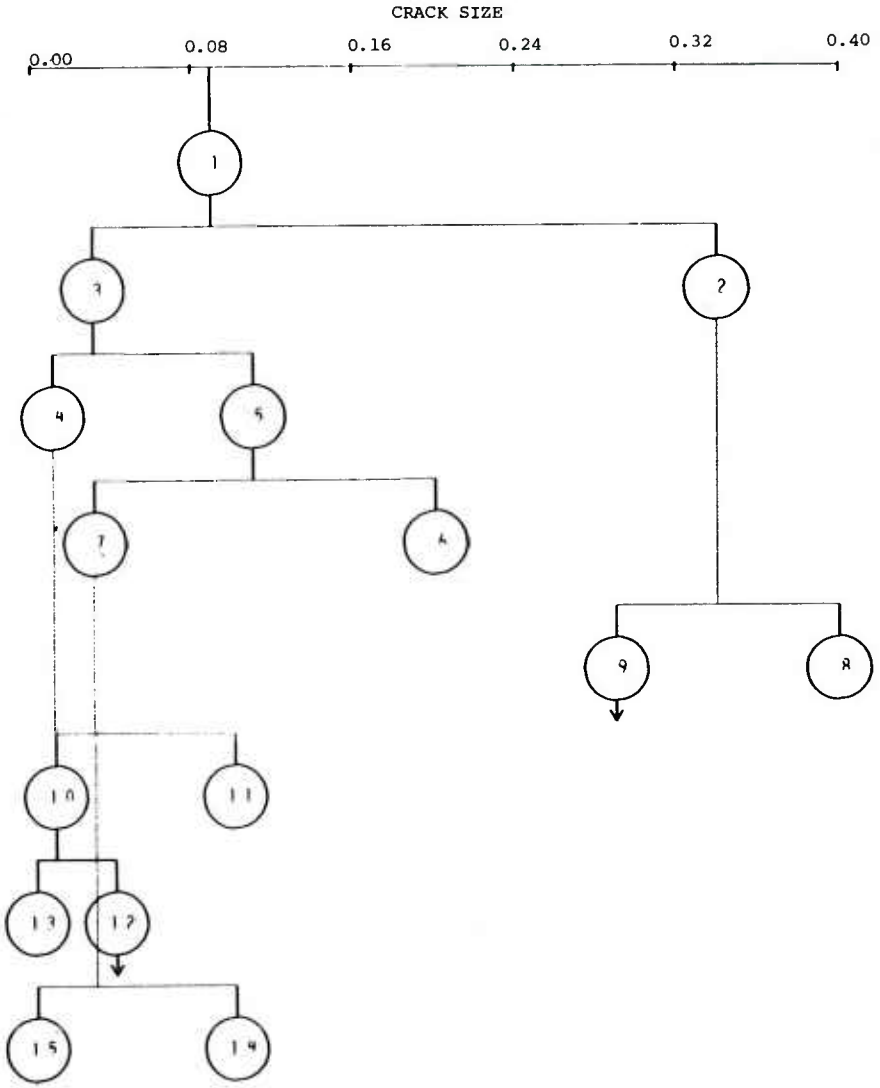

SUMMARY TABLE

---TOTAL GROUP---			
CRITERION - CRACK			
TOTAL GROUP N = 127			
MEAN = 0.09			
STD. DEV. = 0.14			
PARENT 1 SPLITTING VARIABLE - X59			
Mean = 0.03	N = 102	Mean = 0.34	N = 25
PARENT 3 SPLITTING VARIABLE - X33			
Mean = 0.01	N = 79	Mean = 0.11	N = 23
PARENT 5 SPLITTING VARIABLE - X83			
Mean = 0.03	N = 12	Mean = 0.20	N = 11
PARENT 2 SPLITTING VARIABLE - X38			
Mean = 0.29	N = 13	Mean = 0.40	N = 12
PARENT 4 SPLITTING VARIABLE - X25			
Mean = 0.01	N = 75	Mean = 0.10	N = 4
PARENT 10 SPLITTING VARIABLE - X55			
Mean = 0.00	N = 65	Mean = 0.04	N = 10
PARENT 7 SPLITTING VARIABLE - X104			
Mean = 0.00	N = 8	Mean = 0.10	N = 4

FIGURE 18. AID ANALYSIS OF DATA TAKEN ON STEEL FASTENERS HAVING 0.4 INCH, 0.3 INCH, 0.2 INCH, AND 0.1 INCH CRACKS

DEPENDENT VARIABLE = CRACK SIZE

(all are functions of the original six measurements, X2 through X7), are difficult to distinguish from one another in terms of the variance of dependent variable.

Enlarging the data set by including measurements on smaller cracks will tend to counteract the analytical anomalies described above. The AID tree shown in Figure 14 corresponds to the analysis of the data set formed by adding 12 measurements of 0.3-inch cracks to the previous data set. In this case a perfect split is obtained on X20, X38, X59, as well as X61. The fact that a perfect discrimination between the cracks and no cracks is still achieved with one split shows that the larger cracks associated with steel fasteners are still easily detected by this method. The slightly larger data set containing more information on cracks is better able to distinguish among the many predictor variables and not yield quite so many ties.

For the AID tree shown in Figure 15, we further enlarged the data base by adding 12 measurements on 0.2-inch cracks. In this case, two splits yield a complete identification of cracks versus no cracks. The first split on X33 forms one group comprised of 71 no cracks and another group containing 8 no cracks and 36 cracks. The next split separates these 8 no cracks from the 36 cracks and complete identification is achieved.

The next analysis, Figure 16, includes 0.4-, 0.3-, 0.2-, and 0.1-inch cracks. The addition of the 0.1 inch cracks makes it more difficult to distinguish cracks from no cracks which is indicated by gradually growing complexity of the AID tree. Although this AID tree still yields complete separation of cracks from no cracks, six splits are required. The analysis illustrated and summarized in Figure 17 corresponds to the complete data set for steel fasteners including eight 0.05-inch cracks. The addition of the 0.05-inch cracks causes a quite different AID tree to be produced. It was not possible to produce terminal groups all of which contain either all cracks or all noncracks.

Group 10 should be regarded as a terminal group since the variable which split this group, namely variable X98, turned out to be equivalent to many other predictor variables including a random variable.

Two additional AID runs were made on the steel fasteners cracks with the dependent variable equal to crack size rather than the dichotomous variable indicating occurrence or nonoccurrence of a crack regardless of size. Figure 19 shows the results of the AID analysis of the data including all cracks and Figure 18 shows the results for the case with the 0.05-inch cracks removed. The purpose of making these runs was to see if the AID program could do a better or more informative job of classifying cracks when the total sum of squares was a function of deviations of actual crack size from mean crack size rather than just the proportion of cracks. Examination of these runs shows that cracks do tend to be assigned to terminal groups of crack size and that the larger cracks are identified first. The results of these AID analyses are sufficiently encouraging that the use of crack size as the dependent variable should be considered and tested on a larger, more comprehensive set of data. For the 0.1 to 0.4 inch crack runs, the AID trees discussed above yielded probabilities of correct classification of 100 percent.

(3) Linear Discriminant Analysis for Steel Fasteners. Linear discriminant analysis (LDA) was applied to the same data sets on steel fasteners in the following manner. Candidate variables for forming the discriminant function were selected using, in part, the results of the AID runs. The discriminant analysis program then operated in a stepwise mode successively selecting variables to be either added or deleted from the discriminant function until significant further improvement is not attainable.

In general, LDA did not produce results as definitive as did AID on the data available. For example, in attempting to obtain a discriminant function representation of the AID tree of Figure 16, the variables producing splits in this AID tree as well as cross products representing interactions among the

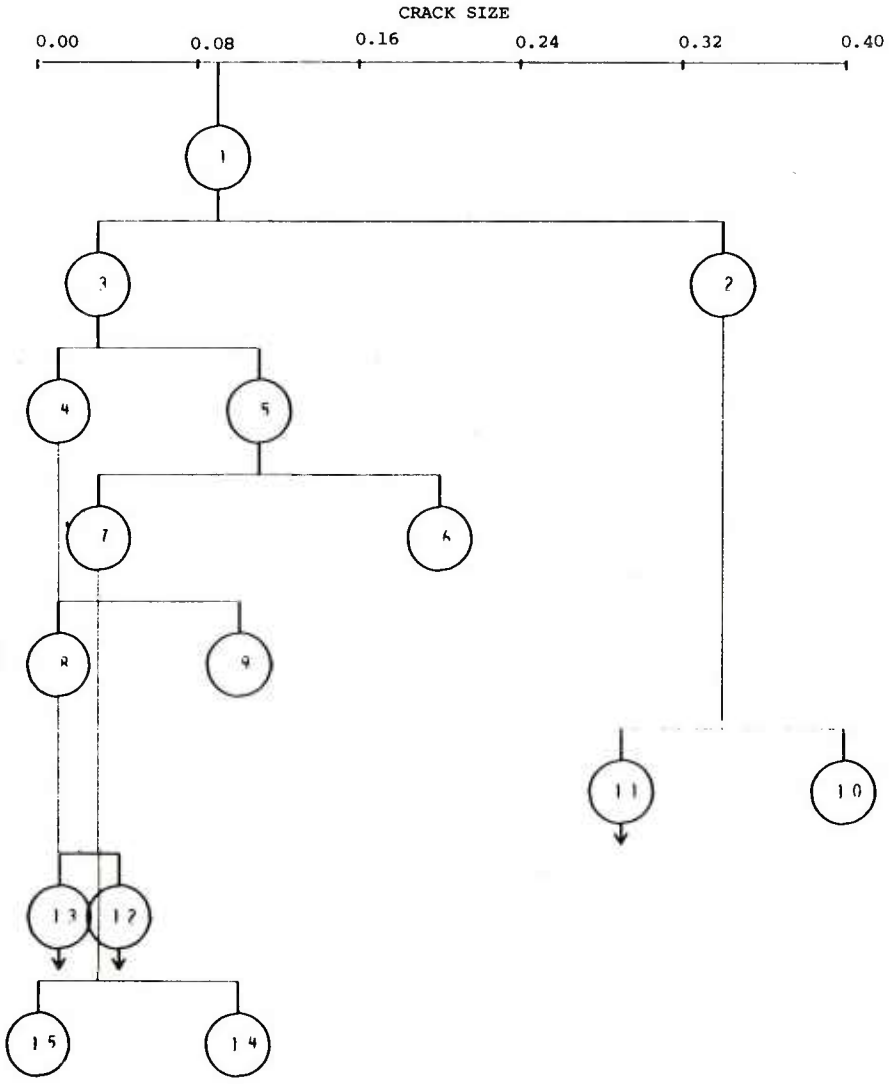

SUMMARY TABLE

---TOTAL GROUP---			
CRITERION - CRACK TOTAL GROUP N = 135 MEAN = 0.09 STD DEV = 0.14			
PARENT 1 SPLITTING VARIABLE - X59			
Mean = 0.03	N = 110	Mean = 0.34	N = 25
PARENT 3 SPLITTING VARIABLE - X33			
Mean = 0.01	N = 87	Mean = 0.11	N = 23
PARENT 5 SPLITTING VARIABLE - X83			
Mean = 0.03	N = 12	Mean = 0.20	N = 11
PARENT 4 SPLITTING VARIABLE - X25			
Mean = 0.01	N = 83	Mean = 0.10	N = 4
PARENT 2 SPLITTING VARIABLE - X38			
Mean = 0.29	N = 13	Mean = 0.40	N = 12
PARENT 8 SPLITTING VARIABLE - X55			
Mean = 0.10	N = 73	Mean = 0.04	N = 10
PARENT 7 SPLITTING VARIABLE - X104			
Mean = 0.00	N = 8	Mean = 0.10	N = 4

FIGURE 19. AID ANALYSIS OF DATA TAKEN ON STEEL FASTENERS HAVING 0.4 INCH, 0.3 INCH, 0.2 INCH, 0.1 INCH, AND 0.05 INCH CRACKS

DEPENDENT VARIABLE = CRACK SIZE

splitting variable for the first two splits were specified for stepwise LDA. The results of these analyses are summarized in Table 7. This discriminant function correctly classified all noncracks. The crack group included 12 of each of the following crack sizes (total of 48) 0.4, 0.3, 0.2, and 0.1 inch. The discriminant function correctly classified all 24 of the 0.3- and 0.4-inch cracks. Thus, the LDA method correctly classified 72.9 percent of the cracks.

7. DISCUSSION OF RESULTS

The experimental investigation using AID has involved three steps described below:

(1) Generation of an AID decision tree using a training set of data

(2) Implementation of the AID decision tree as a classification algorithm on the PDP 11/40 minicomputer

(3) Evaluation of the implementation algorithm using the training set and additional sets of data.

Evolving from this investigation is the trainable, adaptive classification process derived from the AID analysis technique. AID has provided a relatively simple decision structure, i.e., AID tree, which is easily implemented on a small computer. Hard-wired versions of the classification function are also feasible when a large number of inspection devices are required. However, the small computer can provide a variety of additional functions including initial balance, calibration, stable digital eddy-current signal generation and process control. The minicomputer implementation provides the rapid selection or modification of the required classification algorithm where test parameters such as plate thickness and fastener size are changed.

TABLE 7. DISCRIMINANT ANALYSIS OF STEEL FASTENERS

Step	Variable Entered	Discriminant Function Coefficient
1	X33	-11.8424
2	X83	0.6905
3	X33 X25	-5.7485
4	X94	-0.0534
5	X55	-0.9196
6	X25	-0.3928
7	X33 X83	1.7896
	(Constant)	-0.0705

The data described in the preceding section indicate the capability of digital MFEC to detect cracks in the subsurfaces of the aluminum alloy structure near titanium and steel fasteners in the C-5A aircraft. Comparison of the single frequency measurements illustrated in Figures D-1 through D-6 with the MFEC process data of Figure 8 illustrate the improvement in detectability realized by a combination of measurements taken at more than one frequency on titanium fasteners. Even greater improvements are observed when comparing the single frequency measurements of Figures D-7 through D-12 on steel fasteners to the results obtained with a combination of these single frequency measurements illustrated in Figure 9.

The statistical analysis of the single frequency measurements taken on titanium fasteners indicated that cracks 0.3 and 0.4 inch long can be detected with a reasonable reliability by implementing the AID tree illustrated in Figure 11. In all cases the classification algorithm based on AID was superior to the algorithm based on LDA. From the AID analysis it was estimated that the probability of detecting 0.3 inch crack under a 1/4-inch-thick top plate near titanium fasteners is 0.81 with a 95 percent confidence interval of 0.41 to 0.98. The probability of detecting 0.4 inch cracks in the run samples approaches 1.0 with a 95 percent confidence interval of 0.63 to 1.0. The overall probability of correct classification including the correct identification of fasteners with no cracks as well as those with 0.4 and 0.3 inch cracks is estimated to be 0.95. The 95 percent confidence interval for this probability is estimated to be 0.90 to 1.00.

The AID analysis was also used to estimate the probability of detecting cracks in steel fasteners. According to the AID analysis illustrated in Figure 16, the probability of detecting cracks under 3/16-inch-thick material around steel fasteners approaches 1.00 with a 95 percent confidence interval of 0.99 to 1.00. AID indicates that the overall probability of correct classification of steel fasteners with and without cracks also approaches 1.00 with a 95 percent confidence interval of 0.99 to 1.00 providing that the cracks are greater than 0.1 inch.

The classification algorithms were implemented directly on the PDP-11/40 from the AID tree diagrams of Figures 11 (titanium fasteners) and Figures 16 (steel fasteners). This simply involved programming the minicomputer to make a series of binary decisions using the splitting variables indicated by AID tree diagrams. For example, the first step in the implementation of classification algorithm for titanium fasteners requires calculation of variable X76. If X76 is greater than the threshold value, it is placed in Group 3 which subsequently splits on variable X99. If variable X76 is less than the threshold value, it is placed in Group 2 which subsequently splits on variable X33. These sequential decisions programmed as "if-statements" in FORTRAN on the PDP-11/40 are made until terminal groups are encountered. Therefore, the classification can be carried out in few rapid steps immediately after the MFEC measurements are taken by the digital eddy-current system.

It is important to note that the results of classification of the measurements with the implemented algorithm was not as good as the results predicted by the AID analysis. When the original training set of data was applied to the classification algorithm more than the anticipated number of fasteners were misclassified as illustrated in Figures 8 and 9. These additional misclassifications are attributed to small computational errors in the minicomputer. It is evident that the classification algorithm is sensitive to small changes in the threshold value and therefore may be sensitive to other small variations such as initial balance. For this reason one can regard the probabilities of correct classification determined from the AID analysis to be the maximum obtainable for the type of fasteners and plate thickness involved. The following paragraphs discuss other factors which support this conclusion.

The AIDTI computer code was also used to process additional data as illustrated in Figures 20 and 21. The first of these data sets processed by AIDTI was obtained by taking MFEC measurements on Panels 1-3 and 1-4 immediately after the training set of data was acquired. Figure 20 illustrates that most of the 0.3- and 0.4-inch cracks were correctly identified using this additional

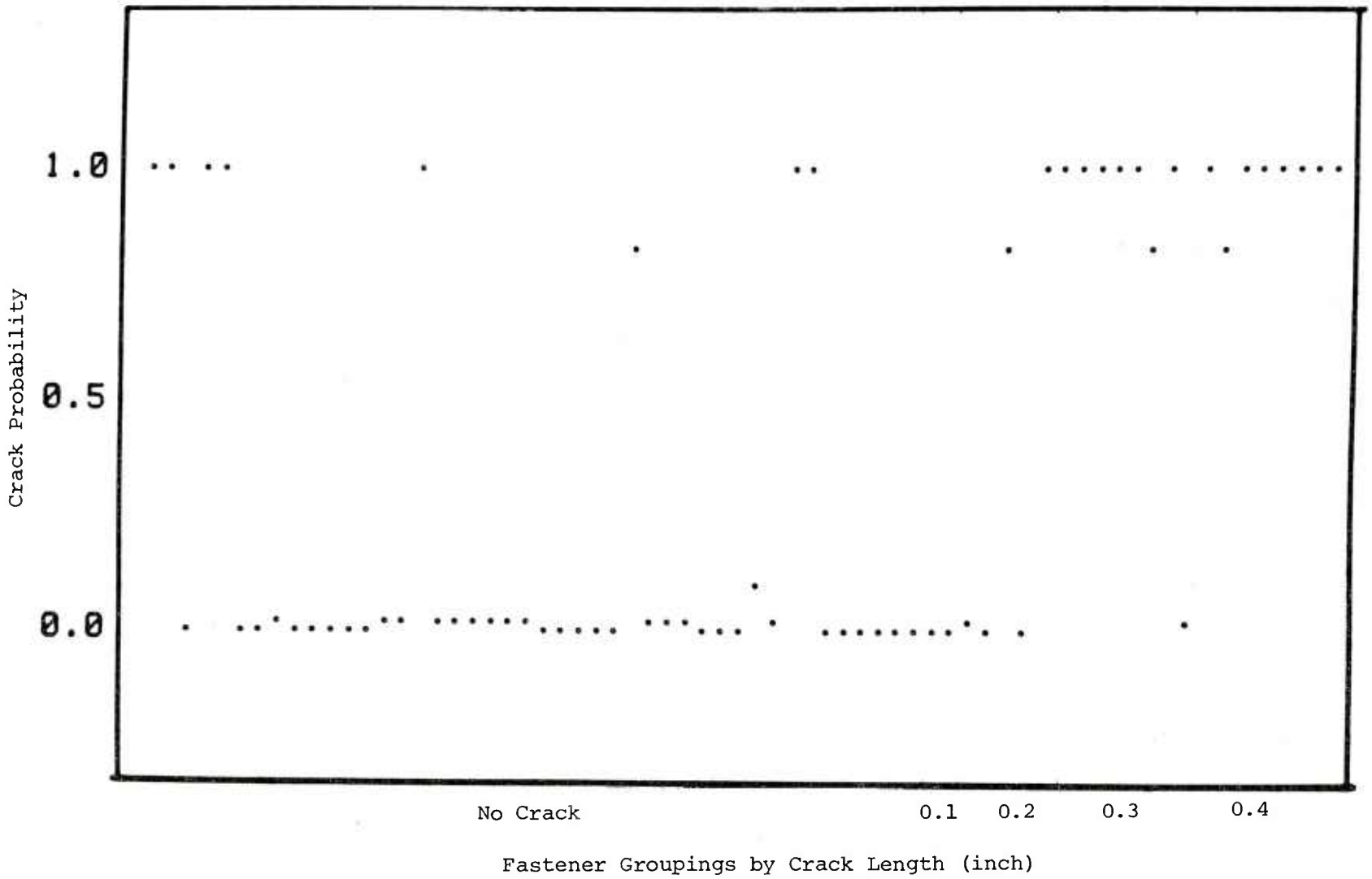

FIGURE 20. MFEC DECISION PROCESS USING AID IMPLEMENTATION TO CLASSIFY ADDITIONAL MEASUREMENTS ON TITANIUM FASTENERS

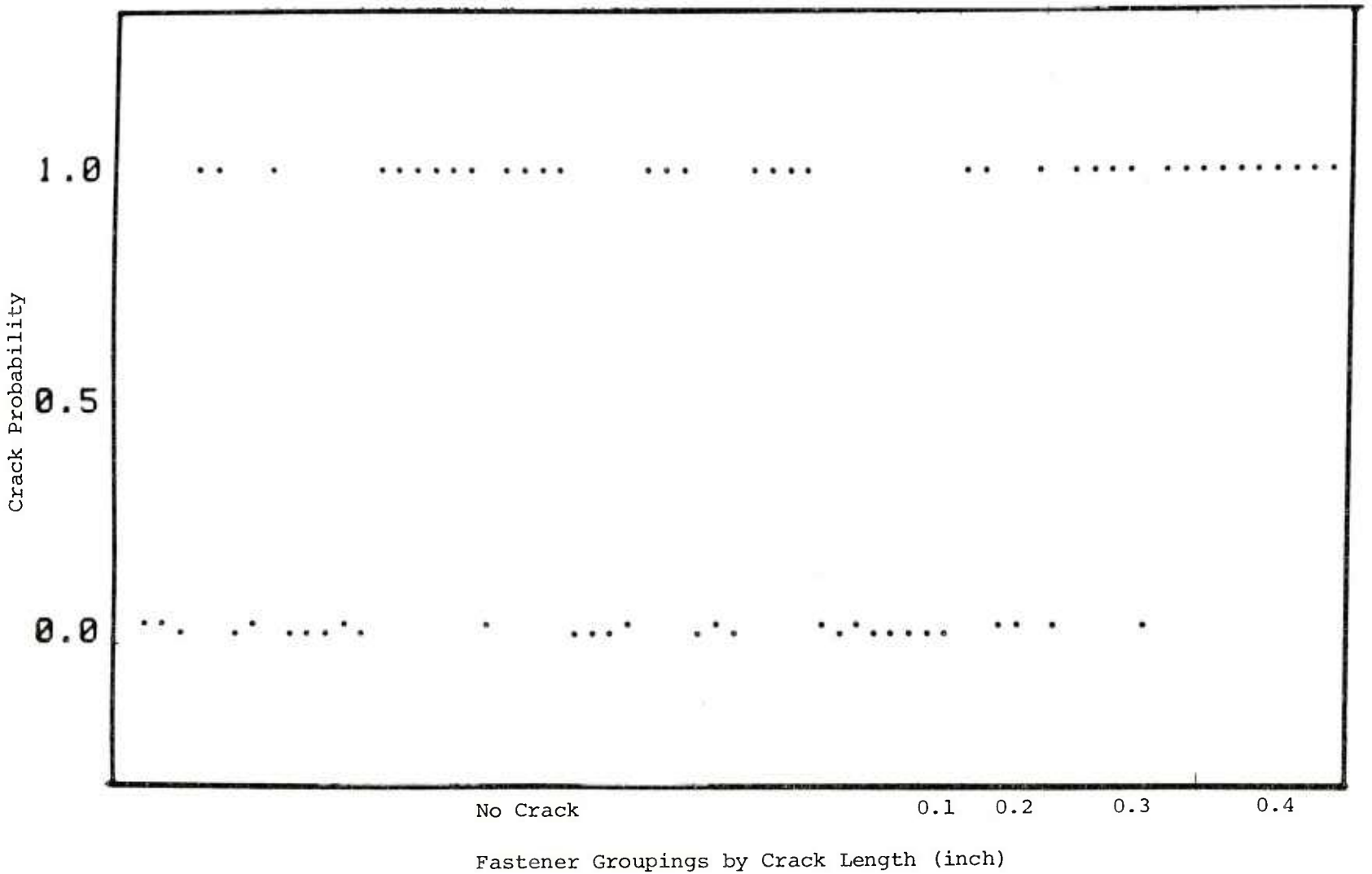

FIGURE 21. MFEC DECISION PROCESS USING AID IMPLEMENTATION TO CLASSIFY MEASUREMENTS ON TITANIUM FASTENERS AFTER 2 WEEK INTERVAL AND REBALANCE OF THE DIGITAL EDDY CURRENT EQUIPMENT

set of data. Also, there were only 8 false indications of cracks out of the 42 MFEC measurements taken on the titanium fasteners with no cracks.

The results illustrated in Figure 21 were obtained by using the code AIDTI to process data that were taken approximately two weeks after the training set of data were acquired on Panels 1-2 and 1-4. Before taking these data the digital eddy current system was assembled and rebalanced for each frequency with the test probe placed on the reference fastener, i.e., Fastener No. 10 on Panel 1-3. As illustrated in Figure 21, practically all of the 0.3- and 0.4-inch cracks were detected. However, there were 20 false indications of cracks out of 44 measurements taken on fasteners with no cracks.

The increase in the number of false indications of cracks that occurred two weeks after the initial AID analysis might be attributed to several factors. These include subtle changes in the electronic equipment or slight variations in the test coil sensitivity caused by a shift in the position of the test coil core with respect to the coil housing. Since the digital eddy-current system was rebalanced before the MFEC data were taken, it is likely that a slightly different balance was obtained. The present system is programmed to exit from the balance routine and hold balance drive levels when the output voltage is less than 1 percent, i.e., 10 mv, of full scale. The $\pm$ 10 mv random error may be sufficient to cause errors in the AID decision function.

Modification in computer procedures, software, and electronic equipment coupled with change in inspection calibration and procedure may reduce the classification errors. For example, a recalibration of the AID algorithm before each inspection of a new group of fasteners can be performed with minor difficulty using the available minicomputer. Modifications in the analog and digital equipment and automatic balance code can be made to provide a more precise initial balance and more stable response characteristics. These considerations should be of interest in the design and fabrication of a prototype inspection system.

SECTION IV
CONCLUSIONS

The following conclusions are derived primarily by analysis of the data taken on actual wing-splice samples containing artificial cracks. Limited additional data taken in subsequent experiments were processed by the decision algorithm derived from these analyses. However, the statements given below reflect the potential capabilities of the digital MFEC system to detect cracks in the actual C-5A aircraft. Experimental verification of a prototype system on additional samples and actual C-5A structures is of interest in the Phase II portion of this program.

(1) The digital MFEC system has the potential for reliably detecting cracks as small as 0.3 inch near titanium fasteners in the bottom layer of a two-layer aluminum joint under a 1/4 inch thick top layer of the aluminum alloy used in typical wing-splice sections of the C-5A aircraft. The AID analysis indicates a potential probability of detecting 0.3 inch cracks of 0.81 with a confidence interval of 0.41 to 0.98 and probability of detecting 0.4 inch cracks approaching 1.0 with a 95 percent confidence interval of 0.63 to 1.0.

(2) Digital MFEC has the potential of reliably detecting cracks as small as 0.1 inch near steel fasteners in the bottom layer of a two-layer aluminum joint under 3/16 inch thickness of the C5-A wing-splice sections. The AID analysis indicates a probability of nearly 1.0 for detecting cracks which are 0.1 inch and larger near the steel fasteners with a 95 percent confidence interval of 0.99 to 1.0.

(3) The adaptive decision algorithm based on the Automatic Interaction Detection (AID) analysis appears to be a superior method for detecting cracks under fasteners compared to the algebraic decision functions such as those derived from linear discriminant analysis (LDA).

SECTION V
RECOMMENDATIONS

The overall program is to be accomplished in two phases of activity. Phase I described in this report has involved the demonstration of the MFEC technique using laboratory equipment with actual wing splice samples. Phase II of the program is directed toward the development of prototype MFEC instrumentation that can be used to inspect actual C5-A aircraft.

Recommended is a portable digital eddy-current system incorporating a small computer such as the DEC PDP 11 and suitable peripheral equipment including D/A converters, A/D converters, test coil interface, pushbutton control unit and display. Simple digital storage such as tape cassette will probably be needed to facilitate system calibration and storage of data records. The digital storage will also provide record of system programs that will perform various useful functions during system operations including automatic balance, calibration, and test coil centering. Since a minicomputer offers the required flexibility at a lower cost compared to the equivalent hard-wired system a minicomputer based system is recommended.

Reliable and consistent performance of the MFEC system depends on a number of factors that warrant further investigation. For example, the results of the Phase I project data evaluated after a two-week interval indicated appreciable differences between data acquired immediately after acquisition of the training set of data. Potential causes of this inconsistent performance are small differences in the initial balance or unknown changes in the digital eddy-current instrument during the two-week interval between data acquisitions. Further investigation is recommended to identify the cause of these effects and associated changes in system design and operation that can minimize the resulting misclassification of fasteners.

Consistent performance may be realized by improvements in the system design to provide more accurate initial balance. This can be accomplished by the incorporation of more precise D/A, A/D converter, and better filtering of test coil signals to remove the harmonic distortion. More consistent operation might

also be provided by frequent retraining of the AID decision algorithms used in the MFEC detection process. Sets of training data can be obtained on standard fasteners immediately before inspection of fasteners in the aircraft structure to account for new balance conditions and time-dependent changes that alter system performance. Additional improvement in consistent operation might be realized by investigating various alternate classification algorithms that are less vulnerable to these changing conditions. For example, the transformed predictor variables and their sensitivity to initial variations in initial balance and other changing conditions would be of interest in continued investigation. The development of calibration standards that are used to generate the training set of data are also important in providing consistent reliable operation of the MFEC system.

The C5-A like most aircraft structures contains a variety of fastener sizes applied to a variety of layered structures of different thicknesses. It is not likely that the MFEC system can be used to inspect for cracks in all of the layers under all types of fasteners. On the other hand, it is believed that an MFEC system can be used to inspect the material under a large number of these fasteners resulting in considerable savings in maintenance cost to the U.S. Air Force.

Since all of the basic structures containing various fastener sizes and shapes were not thoroughly investigated in the Phase I project, these should be evaluated in Phase II. It is recommended that the prototype system that will be fabricated in the Phase II project be used to evaluate these various conditions. Also of interest is the determination of the ability of the prototype system to detect cracks that occur in the top plate as well as the subsurface plates under both titanium and steel fasteners.

The Phase I experiments have indicated the importance of test coil positioning over the fastener. The cup core coils must be positioned precisely with respect to the fastened surface and precisely aligned with respect to the center of the fastener head. It is estimated that coil liftoff variations should be less than 0.002 inch and coil centering should be within 0.010 inch.

Therefore, the development of precise mechanical positioning is important for the successful operation of the prototype system. It is recommended that potential centering techniques be investigated for use with the prototype system. These would include fiber optical techniques and the use of a single high-frequency excitation of the eddy-current coil to facilitate manual or automatic axial positioning. Mechanical fixturing that will assure a minimum constant coil liftoff should also be designed and evaluated.

APPENDIX A

DIGITAL EDDY CURRENT TECHNIQUE AND SOFTWARE DESCRIPTION

APPENDIX A
DIGITAL EDDY-CURRENT TECHNIQUE AND SOFTWARE DESCRIPTION

1. GENERAL DESCRIPTION

The digital eddy-current concept overcomes many of the shortcomings associated with the analog eddy current instrumentation. The digital eddy-current concept will be explained with reference to the block diagram shown in Figure A-1. The test coil drive signals are generated from digital arrays contained in the memory of a minicomputer. This is done by outputting the digital value of the voltage level required to the left-hand digital-to-analog converter (D/A). The output of the D/A is amplified and applied to the test coil. A single cycle of the drive signal is stored in the digital drive array. The frequency is determined by the number of words in the drive array used to describe the cycle and the period of time between the loading of one number into the D/A buffer and the loading of the next number. The stepwise nature of the wave form generated is smoothed out by limiting the response of the power amplifier.

The computer memory contains a second signal array, called the balance array. This balance signal is generated in the same manner as the drive signal, but the power amplification is not necessary. The amplitude and phase of the balance signal are adjusted with respect to the drive signal so that the sum of the output of the pickup coil and the balance signal is close to zero, when the test coil is placed on the standard specimen, i.e., no crack condition. The output of the summing amplifier is passed through a band pass filter and coded in digital form by the analog-to-digital converter (A/D). The band pass filters are used to remove the harmonics of the drive signal produced by the inherent nonlinearity of the test coil/specimen system. The measurements are stored in the computer memory for later processing, or processing may be done real time.

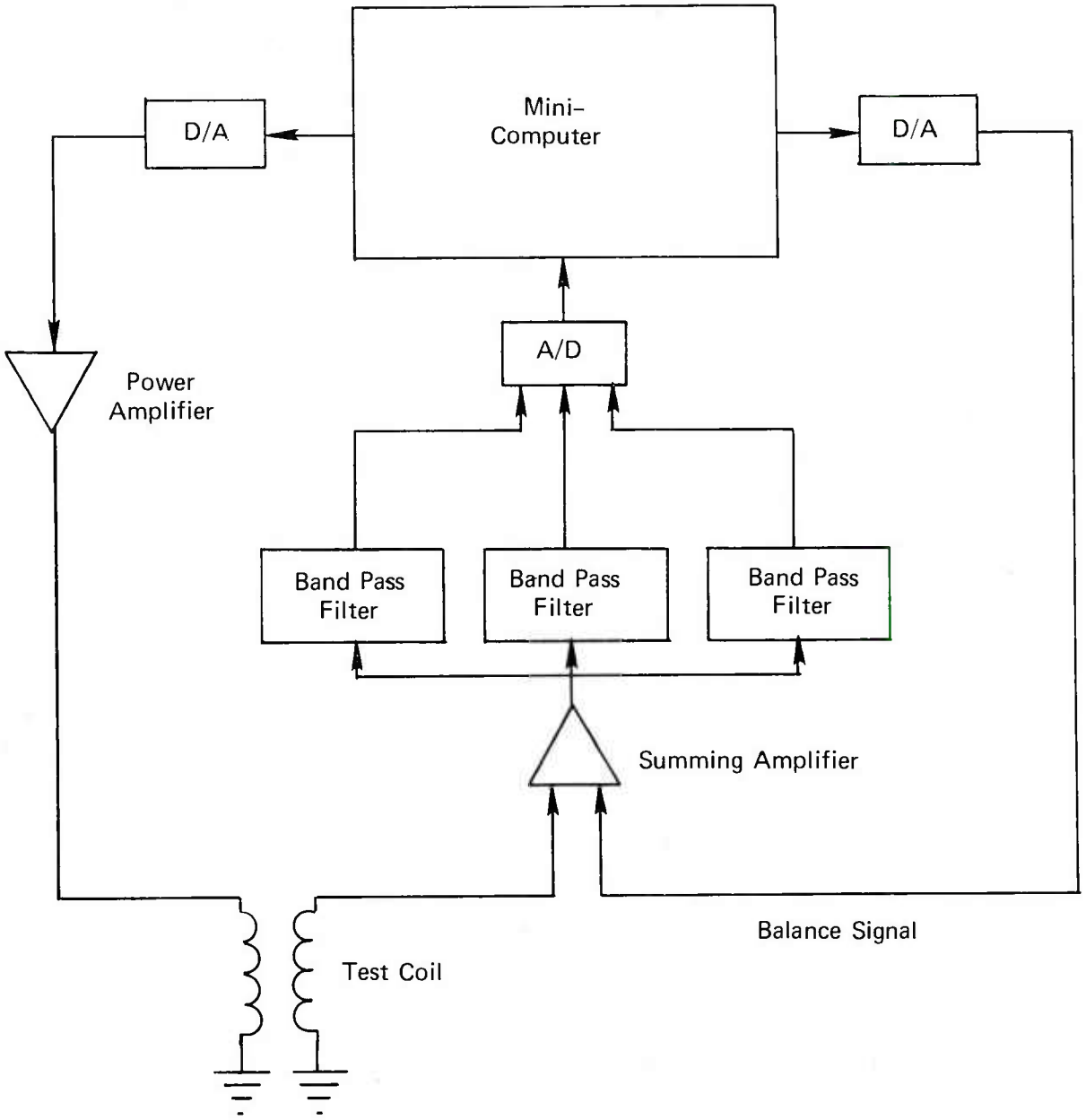

FIGURE A-1. DIGITAL EDDY-CURRENT SYSTEM

The problem of saturating the test coil by exciting it at all of the different frequencies at the same time is overcome by exciting the coil at the various frequencies sequentially. The coil is excited for several cycles to allow turn-on transients to decay. Measurements are then made during each of the next several cycles, both inphase and quadrature. Measurements are made at each of the frequencies so rapidly that for all practical purposes the measurements are simultaneous.

The stability of the phase of the measurement is high because of the digital generation. For example, suppose it is desired to make a measurement at 90 degrees, and that there are 400 words in the digital array. The measurement is made by the computer immediately after it has output the 100th word of the array. There is no significant phase variation since the measurement is always made at the same interval after the 100th word has been output. Quadrature measurements are exactly 90 degrees lagging the inphase measurement because the number of words in the drive arrays for the various frequencies is always a multiple of 4, so that in the above case a quadrature measurement would be made at the 200th word.

The operation of the present developmental system involves more operator interaction with the computer than a production system would require because of the great flexibility allowed for development purposes. For example, to generate the balance and drive arrays, the operator is asked to select the frequency, the angle of the inphase measurement, and the filter channel to be used. In a production system, the frequencies would have already been determined. The computer software for a production system would be a restricted version of the present flexible software.

2. SOFTWARE DESCRIPTION

The software used to drive and control the digital eddy-current system consists of two main programs and a number of sub-

routines. The main programs are:

Name	Language
BALANC	Fortran
MFEC3	Fortran

The subroutines are:

Name	Language
DACEDI	Macro*
DACZRO	Macro
SEEDAC	Macro
TRIGER	Macro
TRGSTP	Macro

The programs were run with a DEC RT-11 Disk Operating System on a PDP 11/40 and a DEC LPS (Lab Peripheral System) which contains the real-time clock, analog-to-digital converter, and digital-to-analog converters. The various routines perform the following functions:

BALANC: This routine permits the operator to select the desired operating frequency, the filter channel, and the phase angle of the inphase voltage measurement. With the test coil in place on a standard specimen, the drive and balance arrays are generated.

MFEC3: This program used three arrays generated by BALANC to make the eddy current measurements.

DACEDI: This routine generates the drive and balance voltages from the values contained in the digital arrays with the digital-to-analog converters, and makes the measurements of inphase and quadrature voltages at the prescribed phase angles of the drive signal.

DACZRO: Initially zeros the output of the DAC's.

SEEDAC: Produces a continuous output of a single frequency so that the balance conditions may be viewed with an oscilloscope.

TRIGER: Calls to DACEDI are preceeded by a call to TRIGER which senses the schnidt trigger of the LPS. This provides a means for the operator to signal when the test probe is in position. This function could equally well be performed using the buffered I/O.

---

* DEC Assembly Language

TRGSTP: The same function as TRIGER, except switch 15 on the control console is sensed and when switch 15 is set, a stop flag is set to terminate the measurement run. This also could be done with the buffered I/O.

The following material describes in more detail the operation of BALANC, MFEC3 and DACEDI. The operation of SEEDAC is apparent from the explanation of DACEDI. The operation of the remaining programs is obvious.

Program BALANC

Program BALANC closely simulates the manual operation of the balance controls on a multiplefrequency eddy-current inspection system. There are a number of parameters which are used to adjust the operating characteristics of the program. Some of these parameters are "touchy" and if they are not properly set the program becomes unstable and will never achieve a balance. Further development of this program will improve the efficiency of its operation. As it stands, we have achieved the objective of a workable balancing arguement.

Figure A-2 shows a simplified flow diagram of program BALANC. The loop for measuring the phase of the test coil output with no balance signal is not shown. This is used to determine the initial value of the balance signal phase angle.

This program is used as follows (the operator replies are underlined):

```
. R BALANC
WELCOME TO BALANC VERSION 6
ANGLE OF INPHASE MEASUREMENT?  III
[The program is requesting the phase angle at which the
inphase measurement is to be made.  The quadrature measure-
ment will be made exactly 90 degrees following this]
0
[The operator has selected zero degrees.  The III of the
request indicates the operator should enter no more than
three integer digits, no decimal point]
```

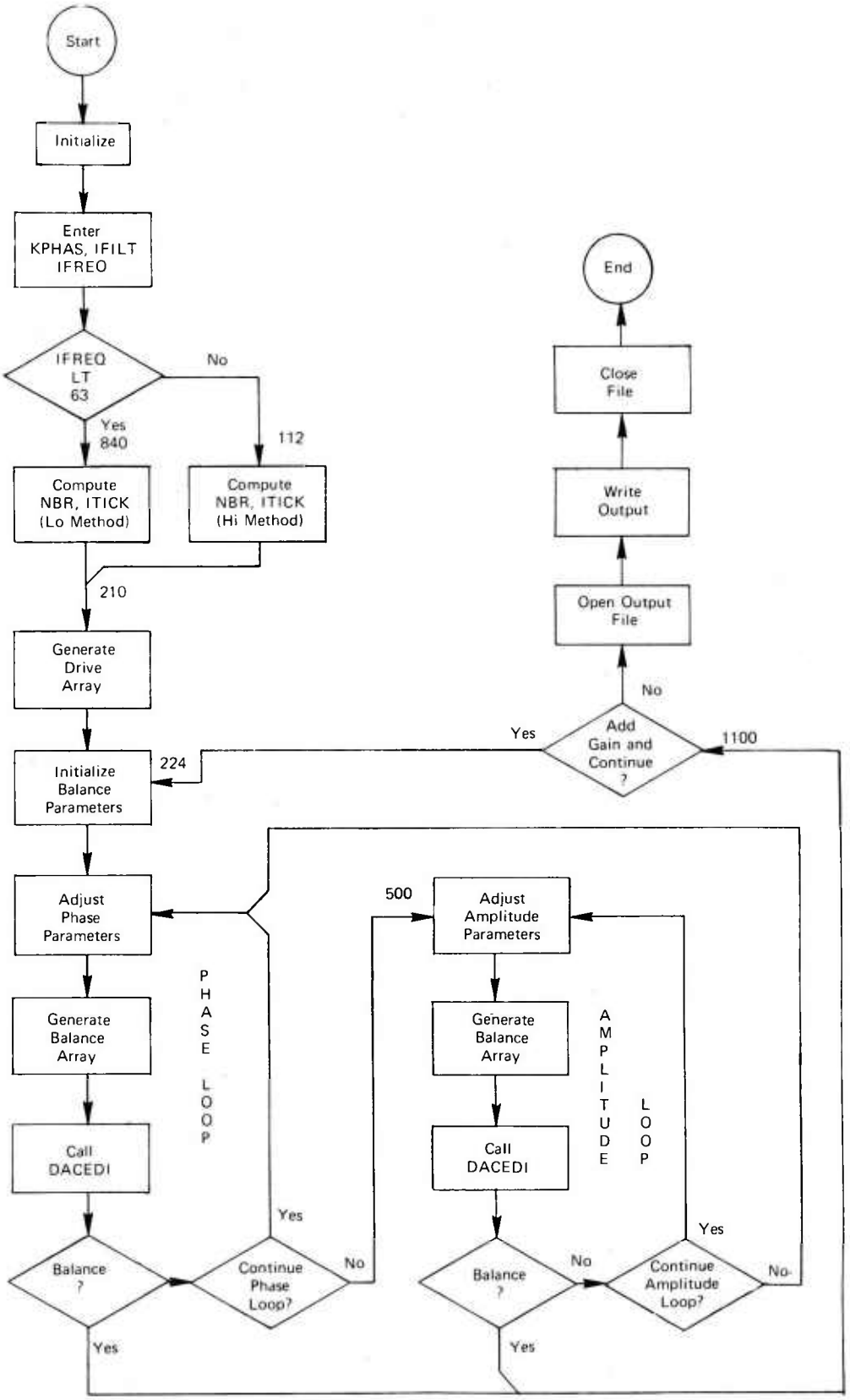

FIGURE A-2. BALANCE ROUTINE FLOW CHART

FILTER CHANNEL? 0 TO 7

1

[The operator has selected channel 1]

FREQUENCY? 1 TO 2000 HZ

950

FREQUENCY USED IS 946

[The operator selected 950 hertz. Under constraints imposed by a maximum of 400 words in the array and a minimum tick period of 40 microseconds, plus the fact that the number of words must be a multiple of 4, the closest the computer could get is 946 hertz--reasonably close]

FRACTIONAL AMPLITUDE? 0.XXXX

0.4

[The computer has requested the amplitude of the drive signal to be used in terms of the maximum output of the D/A]

POSITION PROBE. PRESS TRIGGER WHEN READY

[When the operator has positioned the probe on the standard specimen, he presses the trigger, in this case a foot switch]

OFF NULL ANGLE = 296.6

VX = 0.0155

VY = 0.0395

[Before beginning the generation of the balance array, inphase (VX) and quadrature (VY) voltages are measured, without the balance signal. This permits the initial phase adjustment of the balance array to be adjusted reasonably close to the proper angle]

[The program then proceeds to adjust the phase and the amplitude of the balance array so as to reduce the sum of the squares of the two measurements to something less than 10 millivolts. When this is done, the computer replies]

VALUE VECTOR SUM = 0.0050

ITERATIONS = 35

[The iterations indicates how many times the program reversed the direction of change of the balance voltage. If this number is too small, the operator can assume that the program "stumbled"

into the balance condition, and further balancing operations might have problems]

TYPE 1 TO SEE WAVE FORM
2 TO ADD GAIN AND RE-BALANCE
9 TO TERMINATE THIS FREQUENCY

[If the operator enters a 1, the test coil drive current and the balance voltages are turned on so that the operator may observe them on an oscilloscope. If he enters a 2, he is directed to increase the system gain and the balance process is continued]

9

DRIVE ARRAY NAME? RKØ:AIIIII,MF3

*RKØ:F946.MF3

[The operator has been requested to enter the name of the disk file where the program is to store the generated array for later use by the measurement program]

TYPE 9 TO CONTINUE, OR 1 TO TERMINATE

[If the operator replies with a 9, the program will continue for the generation of an array for another frequency]

1

END BALANCE MFEC

.

[The period indicates that control has been returned from the program to the system monitor]

For the entire operation shown above, the operator has typed a total of 22 characters.

When a sufficient number of drive arrays for the various frequencies have been generated by BALANC, the operator proceeds with the measurement program MFEC3.

Program MFEC3

The straight-forward operation of this program is indicated by the flow chart of Figure A-3. The subroutine CATLOG is used locally at Battelle to open the output (data) files with a common name and

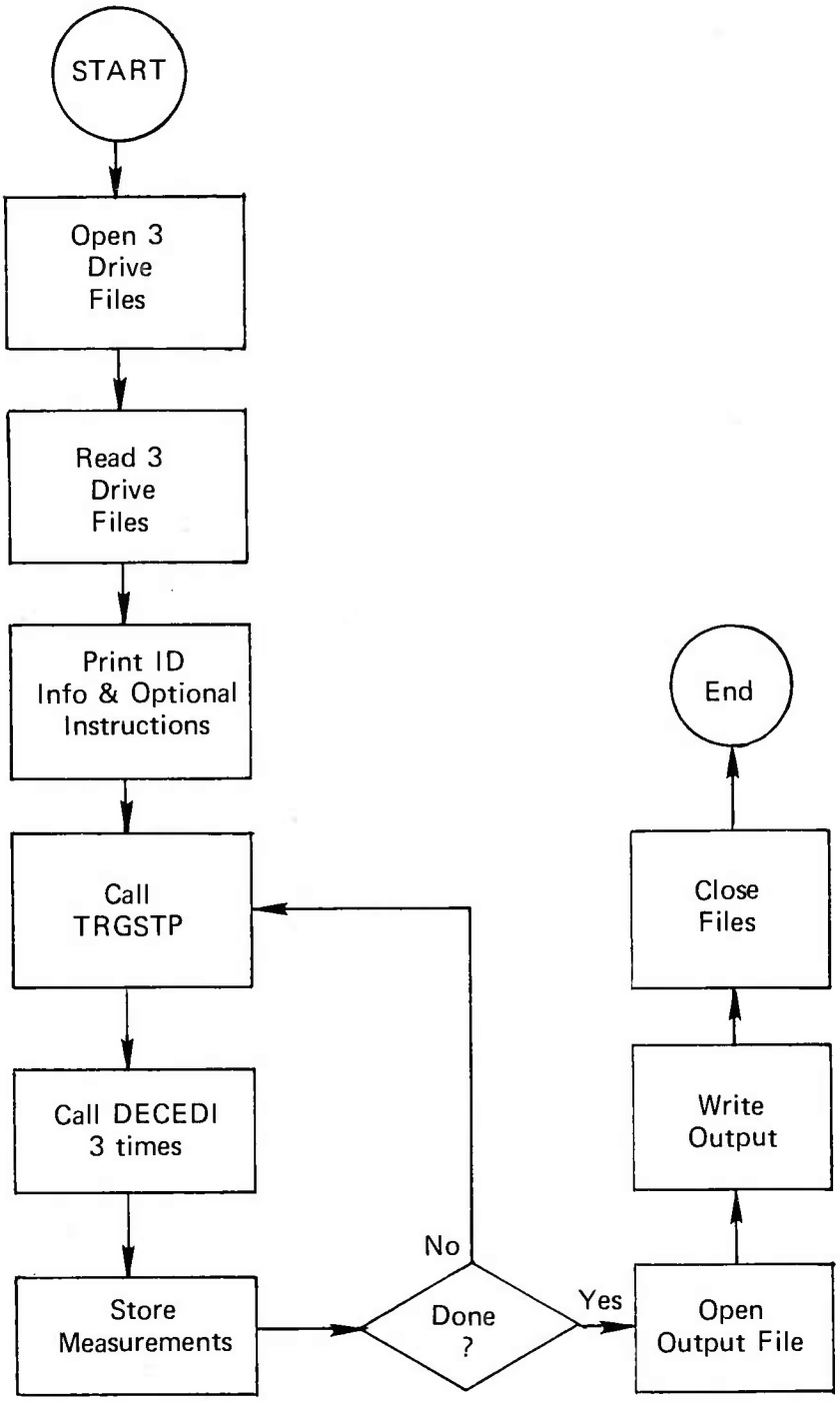

FIGURE A-3. MEASUREMENT ROUTINE FLOW CHART

sequential number extension, as well as maintain a file directory containing identification supplied by the operator.

The program proceeds as follows (again operator replies are underlined):

```
.RUN MFEC3
WELCOME TO MFEC3-V5
FREQ 1 DRIVE ARRAY FILE NAME?  *F90.MF3
FREQ 2 DRIVE ARRAY FILE NAME?  *F330.MF3
FREQ 3 DRIVE ARRAY FILE NAME?  *F793.MF3
```

[The operator has entered the file names of the three drive arrays he wishes to use. Invalid entries or naming disk files which do not exist illicitates appropriate diagnostic replys and an opportunity for the operator to correct his errors. The program then summarizes the frequency and phase data (stored at the end of the array)]

```
FREQUENCIES   AND   ANGLES USED ARE
FREQ 1 =  90        ANGLE 1 =  1.3
FREQ 2 = 330        ANGLE 2 =  5.0
FREQ 3 = 793        ANGLE 3 = 12.9
TYPE 9 TO SEE INSTRUCTIONS
     1 TO PROCEED
9
********** OPERATING INSTRUCTION **********
1- CLEAR SWITCH 15 PDP-11 CONTROL PANEL.
2- PLACE PROBE ON SPECIMEN AND PRESS TRIGGER WHEN READY.
   HOLD PROBE STILL UNTIL BELL SOUNDS.
3- WHEN BELL SOUNDS, MOVE PROBE TO NEW SPECIMEN AND
   REPEAT STEP 2.
4- WHEN FINISHED, SET SWITCH 15 AND PRESS TRIGGER TO
   TERMINATE MEASUREMENT.
PRESS TRIGGER WHEN YOU ARE READY WITH PROBE IN PLACE.
```

[The measurement process then proceeds until the operator sets switch 15 and presses the trigger. Switch 15 was used to terminate since its position can be readily sensed by software. A remote terminating switch can be arranged with a little more effort, which was not warranted at this stage. The program then types]

THIS DATA WILL BE CATALOGED AS CRACKS.032
TYPE UP TO 46 CHARACTERS OF ID INFORMATION
THE OPERATOR THEN TYPES IDENTIFICATION INFORMATION
DATA HAVE BEEN STORED ON DISK FILE. GOOD BYE.
END MFEC3

The last operation is part of an automatic cataloging routine. The data files are stored on disk in consecutive file names CRACKS.001, CRACKS.002, and so forth. The cataloging subroutine keeps a directory of the files which includes (1) the file name, (2) the date, and (3) the identification information entered by the operator. This directory is maintained across power-downs.

Routines are also available to display the data in graphic form on the CRT, plot the data on the line printer, and print the data formated for the line printer.

Subroutine DACEDI

This program provides drive and balance voltages to the analog portion of the multiple frequency eddy-current system from the two DAC's, and makes the inphase and quadrature measurements at the proper time during the cycle. DACEDI is called at least one time for each frequency. Figure A-4 is a flow chart of DACEDI.

Subroutine SEEDAC

This subroutine outputs drive and balance voltages continuously until the operator terminates with the schmidt trigger. This permits the observation of the balance condition with an oscilloscope. The program is very similar to DACEDI, but there are no measurements.

Subroutines DACZRO, TRIGER, TRGSTP

Subroutine DACZRO zeros the x and y output of DAC
Subroutine TRIGER monitors Schmidt trigger ST1 until

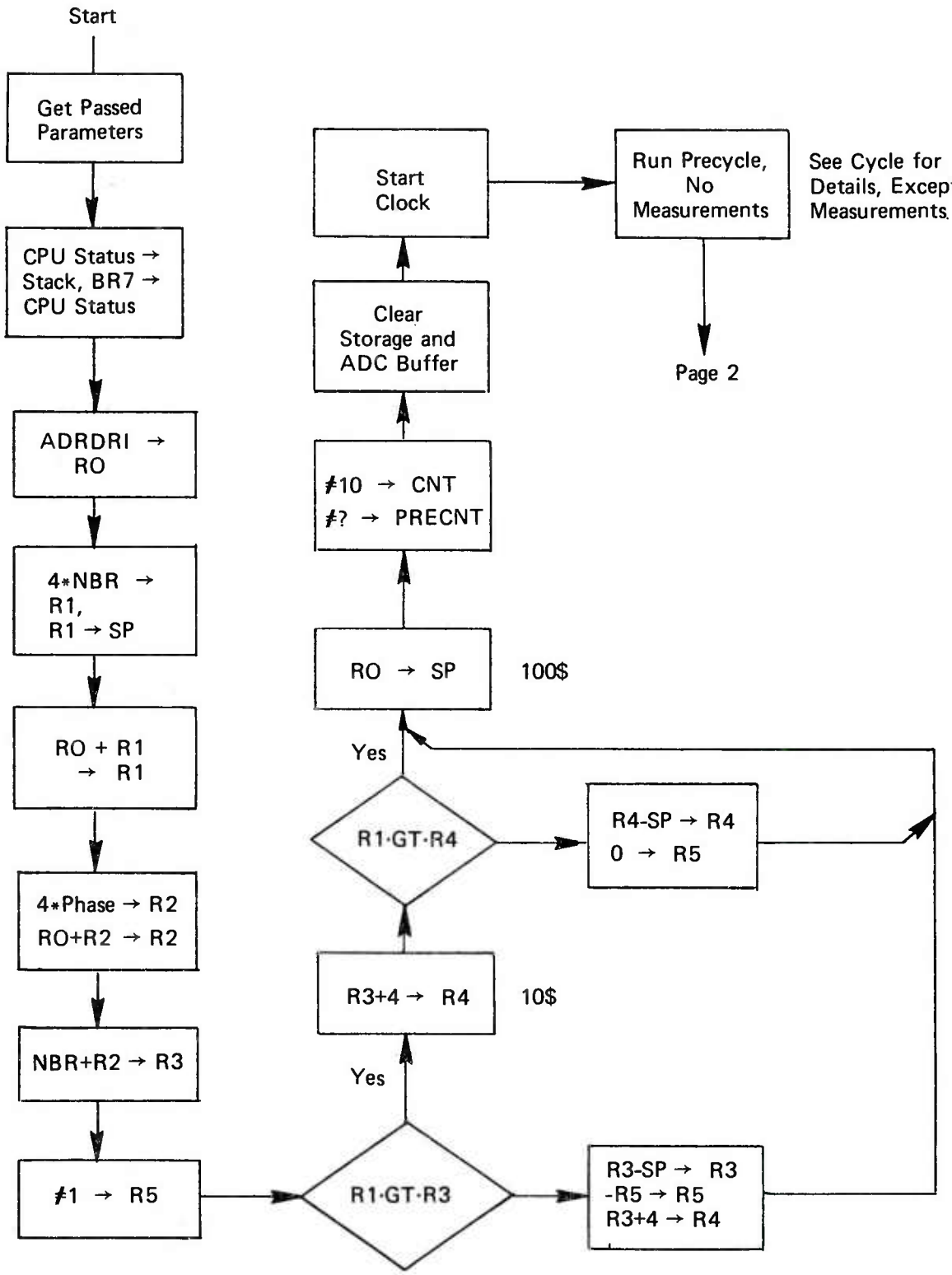

FIGURE A-4. DACEDI ROUTINE FLOW CHART

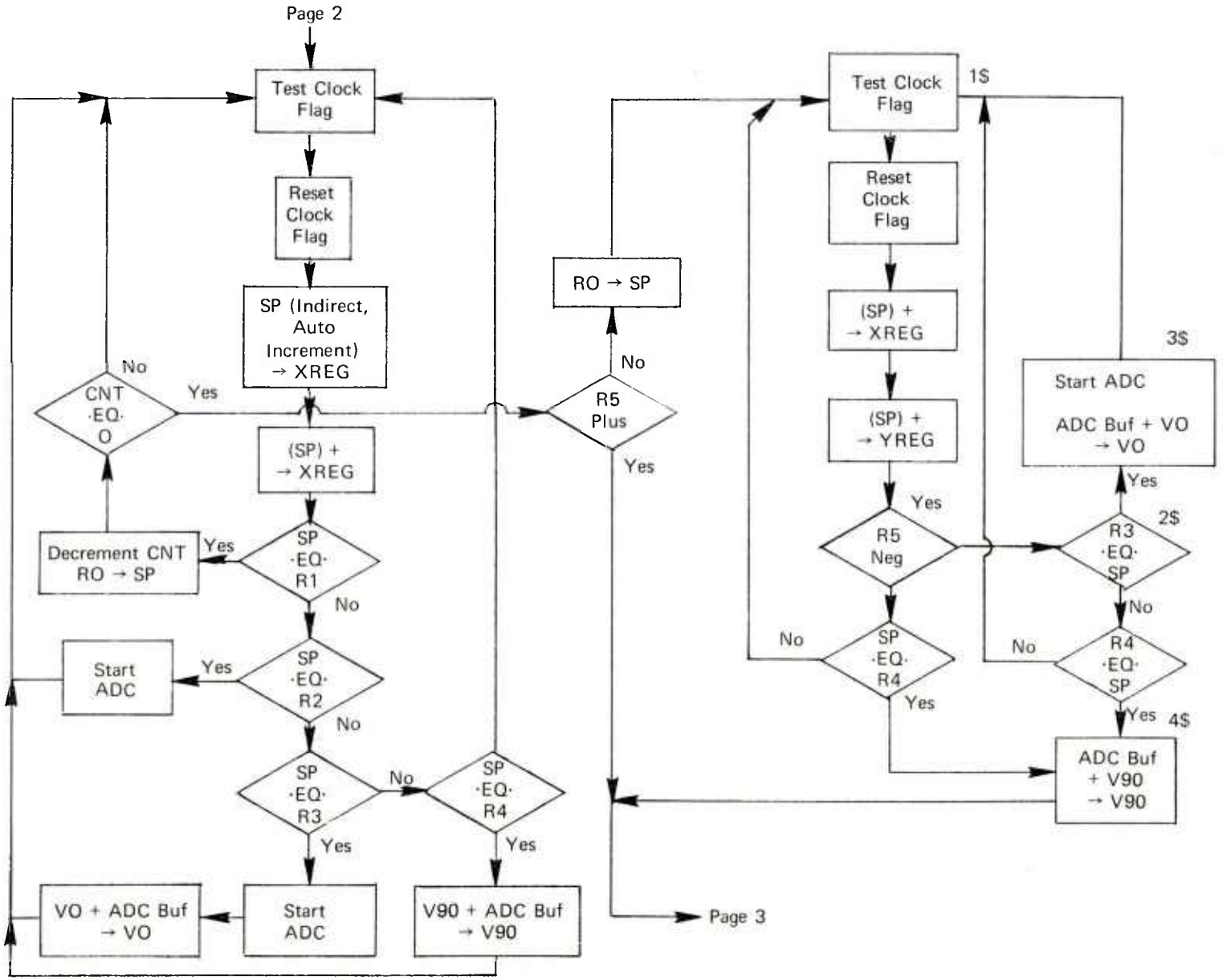

FIGURE A-4. (Continued)

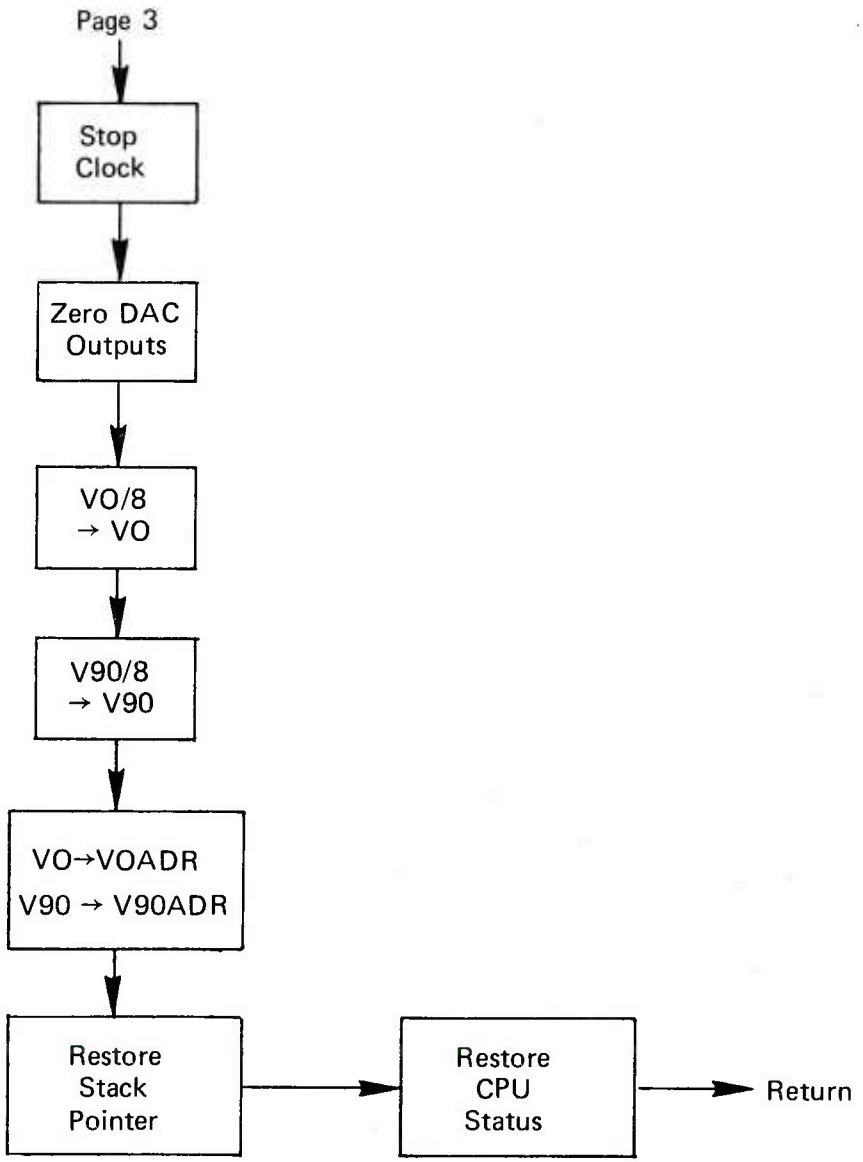

FIGURE A-4. (Continued)

triggered, then returns

Subroutine TRGSTP monitors Schmidt trigger and console switch 15, returns when triggered. If switch 15 is set prior to trigger, then a stop flag is set.

3. TEST COIL INTERFACE

Figure A-5 illustrates the digital eddy-current interface unit constructed for use in the laboratory on this program. This unit was designed to be flexible and therefore somewhat more complicated than a production system would be.

The D/A output from the computer was amplified by a 50-watt operational amplifier (not shown). The output of the operational amplifier was connected to the two series aiding drive coils through a series resistor approximately 100 times greater in resistance than the impedence of the two coils. Since the operational amplifier represents essentially a constant voltage source, the series resistor provides a relatively constant current source to drive the test coil.

The pickup and balance coils were connected to the remainder of the analog circuit as shown in Figure A-5. The variable input resistor from the balance coil was used to obtain a null in the output signal at the middle frequency with the test coil in place on a specimen, with no balance input from the computer.

The system gain was controlled by varying the feedback resistance in the second operational amplifier to the right of Figure A-5. Changing the value of the feedback resistor changes the gain for both the error signal from the input amplifier and the balance signal by proportionate amounts. The balance signal gain changes only the gain of the balance signal and permits the software of the computer to adjust the amplitude of the balance signal near the middle or upper half of the range of the D/A, to provide good resolution of adjustment. The RC filter in the balance signal input removes the higher frequency components of the balance signal introduced by the stepwise changes from the D/A.

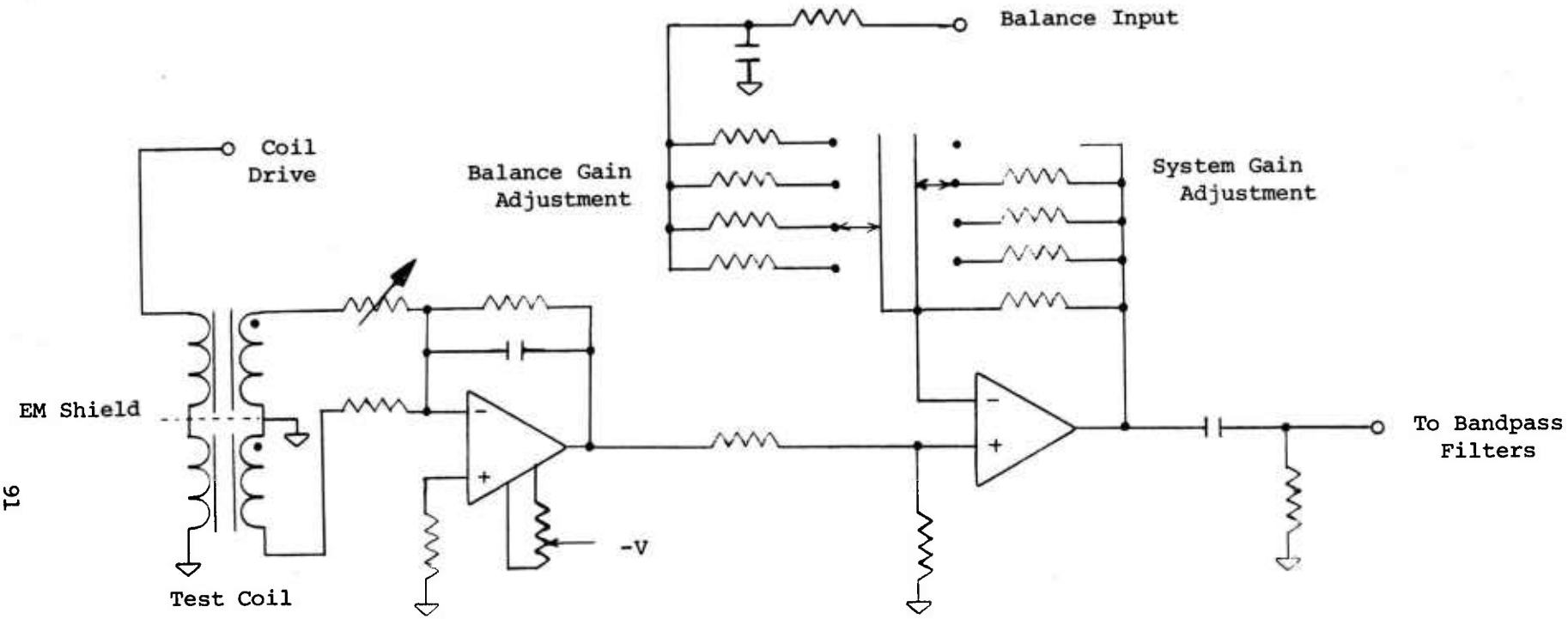

FIGURE 5. SCHEMATIC OF TEST COIL INTERFACE NETWORK

The output of the system is AC coupled to the various band pass filters through a 1000 microfarad capacitor. The resistor to ground at the output is a high resistance which prevents any charge from building up on the capacitor.

With the exception of the test coil interface, the digital eddy-current system consists of general purpose laboratory computer (Digital Equipment Corporation PDP 11/40) and software. Figure 6 is a photograph of the laboratory system showing the test coil on a typical wing-splice sample with the laboratory instrumentation in the background.

APPENDIX B

TEST COIL DESIGN

APPENDIX B
TEST COIL DESIGN

1. DESIGN PHILOSOPHY

The eddy-current test coil design is primarily determined by the application of interest. Test coils for general applications of necessity sacrifice high defect sensitivity for general versatility, whereas eddy-current test coils for specific applications sacrifice general applicability for higher defect sensitivity.

There are portions of two circuits contained in an eddy-current test coil. The total magnetic circuit is made up of the core material of the test coil (usually a ferrite material) and the magnetic path through the object to be inspected. The total electrical circuit is made up of the coil windings of the test coil and the circuit in the eddy-current test instrument. Both the magnetic and electrical circuits must be considered in an eddy-current test coil design.

The geometry of the magnetic core material in the eddy-current test coil is governed by the geometry of the part being inspected, and the nature and location of the defect to be detected. For example, if the defect is expected to be located on the surface of the part, and high location resolution is desired, the poles of the magnetic core material of the test coil should be close together. The test coil should also be designed to accommodate energization at a relatively high frequency. For the case where the defect to be detected is located deeper within the part, the poles of the core material should be further apart, the frequency lower, and the excitation current higher. These factors will be discussed further in connnection with the specific coil designs.

There are two basic electrical circuits which may be used: a single-coil and a double-coil circuit. The single-coil circuit uses the same coil for excitation of the eddy currents and for the detection of the defect. The double-coil circuit has one coil connected to the current source and the second coil connected to the detection circuit. The impedance of the coils should be designed to match the internal impedance of the eddy-current test instrument. For the instrumentation used for the present work (and for many other eddy-current instruments), the coil reactance should be on the order of 100 ohms inductive reactance, and the resistance should be less than the reactance, preferably one-fourth to one-half the reactance value. In practical situations it is not always possible to achieve these conditions, so some compromise is necessary. This is acceptable as long as the eddy-current test-coil electrical characteristics are within the adjustment range of the balancing circuits and the coil does not saturate within the range of test conditions encountered. For example, assume that the 100 ohms inductive reactance can be achieved with 800 turns at the frequency of interest. This requires the use of 42 AWG wire because of physical constraints. While the desired inductive reactance is achieved, the resistance is too great. It is therefore necessary to compromise with fewer turns of a large size wire until the resistance is something less than the inductive reactance at the frequency of interest. This situation is further complicated if the test coil is to be used at more than one frequency.

2. COIL DESIGN DESCRIPTIONS

Three coil designs were used for the present investigation: cup coil, side coil, and straddle coil. The names are descriptive of the relationship of the eddy-current test-coil geometry to the

fastener. The cup core coil was the design finally chosen and is discussed in the body of the report. The coil core is cup-shaped and is centered over the fastener of interest. The magnetic field flows through the fastener, out into the aluminum, and returns to the outer edge of the ferrite cup. The field is relatively symmetrical around the fastener.

One method of increasing defect sensitivity is to confine the flow of the eddy currents to a smaller volume so that the defect causes a high percentage change in the current flow. This was accomplished with the side coil design shown in Figure B-1. In this case the inspection volume is reduced by using a U-shaped ferrite core with one pole centered on the fastener and the other pole to the side of the fastener. Inspection around the fastener is obtained by rotation of the test coil. The physical dimensions of the side coil are presented in Figure B-2.

One method of getting deeper magnetic field penetration is to separate the poles of the ferrite core, as was done with the straddle coil shown in Figure B-3. The straddle coil rotates about its center so that the poles rotate around the fastener symmetrically. While the magnetic flux should penetrate more deeply, a single defect would register twice during a 360-degree revolution of the straddle coil. The physical dimensions of the straddle coil are presented in Figure B-4.

3. RESULTS

The side coil and the straddle coil were evaluated by the MFEC analysis. Results of these evaluations indicated that the cup coil provides superior capability in detecting cracks in the second plate under fasteners.

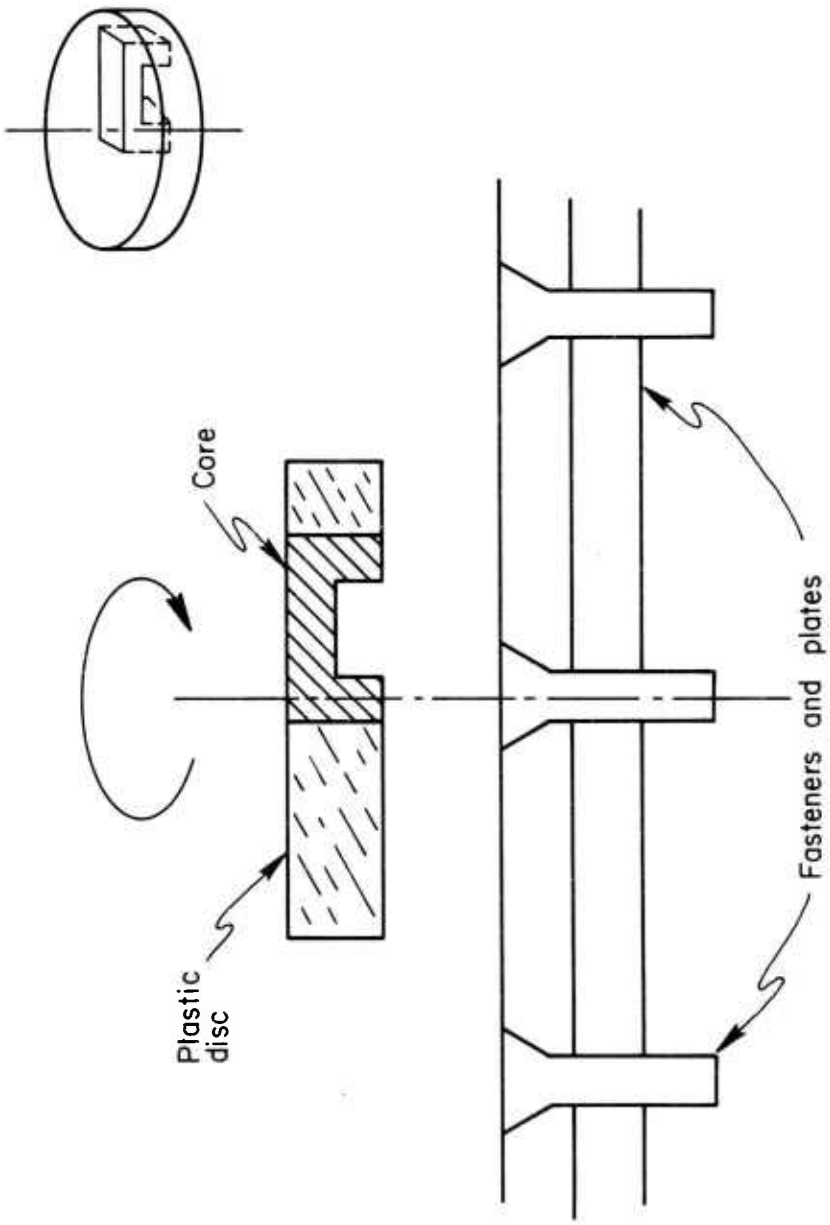

FIGURE B-1. SIDE COIL EXPERIMENTAL SETUP

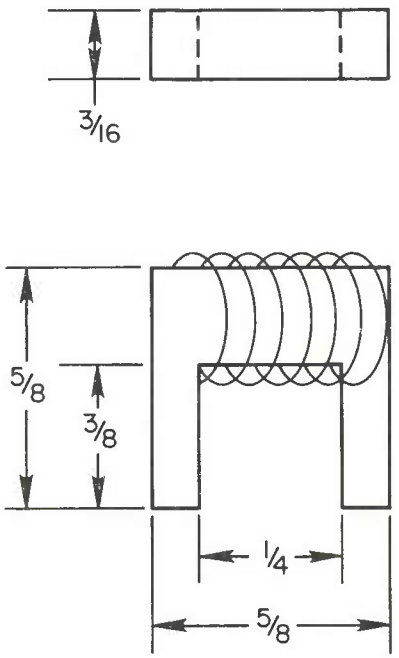

Winding: 525 bifilar turns
#32 awg copper

FIGURE B-2. SIDE COIL DIMENSIONS

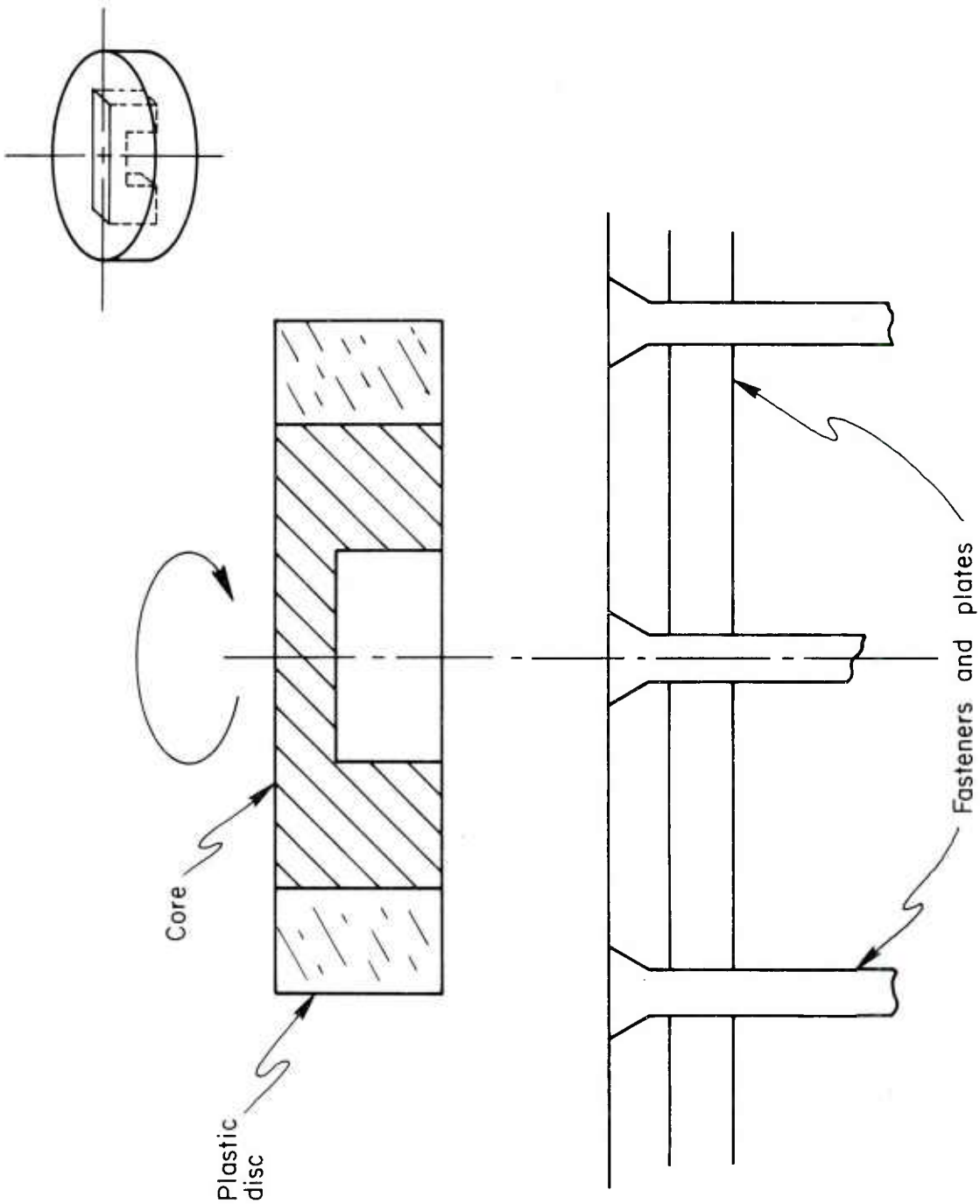

FIGURE B-3. STRADDLE COIL EXPERIMENTAL SETUP

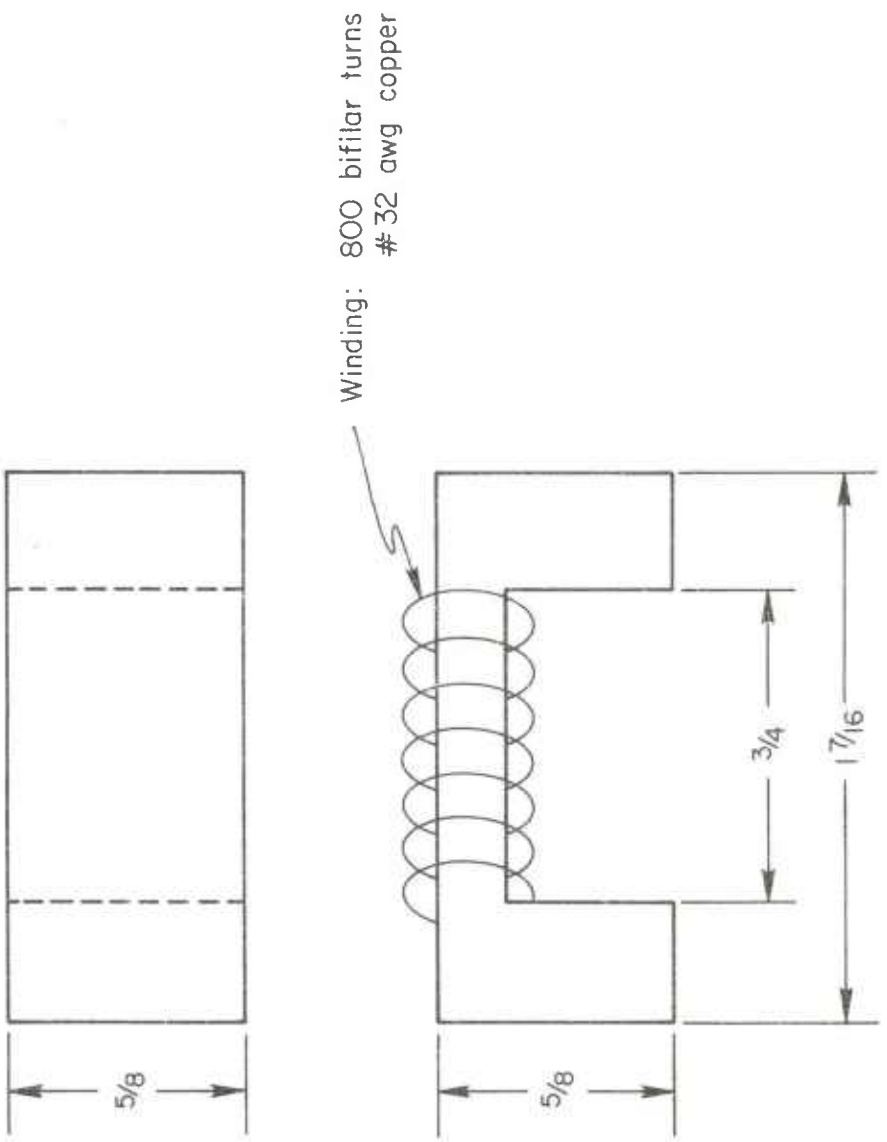

FIGURE B-4. STRADDLE COIL DIMENSIONS

Examination of the voltage reading for any one of the channel outputs corresponding to a particular frequency reveals a considerable variation in the signal voltage as the side coil or saddle coil is rotated about the center of the fastener. These variations are cyclical, having somewhat repeatable high and low values within a complete revolution of the side coil. The sources of these cyclical signal variations have not been identified. Possible causes include the proximity of the coil to the edges of the plates and the effect of adjacent fasteners.

APPENDIX C

CLASSIFICATION METHODOLOGIES BASED ON LINEAR DISCRIMINANT ANALYSIS AND AUTOMATIC INTERACTION DETECTION

APPENDIX C
CLASSIFICATION METHODOLOGIES BASED ON LINEAR DISCRIMINANT ANALYSIS AND AUTOMATIC INTERACTION DETECTION

In this appendix, brief discussions are given of linear discriminant analysis (LDA) and automatic interaction detection (AID).

1. LINEAR DISCRIMINANT ANALYSIS (LDA)

A. General Properties. As suggested by the label, linear discriminant analysis assumes a linear relation among the predictive variables:

$$Y = A0 + A1(X1-\overline{X1}) + \ldots + An(Xn-\overline{Xn}) \qquad (C1)$$

In this expression, the predictive variables and their respective mean values are given by $X1, \overline{X1}, \ldots, Xn, \overline{Xn}$. The method of data analysis yields optimum least-squares estimates for the weights $A1, A2, \ldots, An$. In general, the method of analysis is similar to regression analysis in which the dependent value Y is set equal to 1/2 for one subset of the data (say that portion associated with the presence of a crack), and is set equal to -1/2 for another subset of the data (say that portion associated with the absence of a crack). In applications, the values 1/2 and -1/2 are suitably modified to account for differences in sample size for the two subsets of data.

After the A-weights are determined, the linear discriminant may then be used to predict the presence or absence of a crack as follows. Suppose that $X1, \ldots, X6$ denote 6 voltage measurements obtained at a location where it is not known whether or not a crack exists. These 6 values are used to compute the numerical value of Y using Equation (C1) and the A-values obtained by least squares from the learning stage of data

analysis. This computed value of Y is next compared with a threshold value of Y, say Y*, as indicated by the following decision rule:

if $Y \geq Y^*$ predict the presence of crack;

if $Y < Y^*$ predict the absence of crack.

The value of Y* is obtained from the output of a linear discriminant analysis. It is customary in theory to choose Y* so that the probabilities of misclassification are equal. However, in many applications, including the present one, equal misclassification errors are not desired. The two misclassification errors are the following:

Type 1 Error -- declare a crack to be absent when, in fact, a crack is present;

Type 2 Error -- declare a crack to be present when, in fact, no crack is present.

If the Type 1 Error is judged to be more serious than the Type 2 Error, the threshold value Y* is sometimes adjusted to bias the discriminant to yield Type 1 Errors less frequently than the Type 2 Errors.

In strict terms the linear discriminant method requires the measured values of the X's to be multivariate normally distributed, with the same covariance matrix over each subset of data. In application to the MFEC crack detection, this means that the voltage measurements associated with cracks should be dispersed about their mean values in the same manner as those for the no crack data. Stated another way, the n-dimensional expressions of the voltage measurements are assumed to be statistically equal for the two subsets of data; the expressions differ only in the fact that the vector of mean values $(\overline{X1}, \ldots, \overline{Xn})$ for cracks differs from the vector of mean values for no cracks, so that the expressions are measured about different mean vectors. More sophisticated versions of linear discriminant analysis permit more than two subsets

of data to be considered. This would permit, for example, classification into three categories: No-crack, crack less than 0.2 inch, or crack exceeding 0.2 inch, depending on the measured voltage values. Stepwise versions of LDA are also available that first yield the best one-variable discriminant, then the best two-variable discriminant, etc.

In applications it is usually difficult to verify the correctness of the assumptions that underlie linear discriminant analysis. Typically, the analyses are performed as though the assumptions were valid, and then comparisions are made between the observed and expected performance of the discriminant in the learning and verification stages of the analysis. If the computed frequencies of correct classifications are approximately equal and relatively large, say greater than 85 percent, then it may often be concluded that the assumptions that underlie the analysis are not seriously violated. It must be noted, however, that the assumptions that underlie linear discriminant analysis are strong assumptions. These assumptions would not be expected to hold in all situations, so that verification efforts are essential.

B. Innovations for MFEC Crack Detection. In order to enhance the ability of the linear discriminant method for MFEC crack detection, the following alternative forms were used in addition to that given in Equation (C1):

$$Y = A1 \log X1 + A2 \log X2 + \ldots + An \log Xn \qquad (C2)$$

and

$$Y = A1 \log (X1/\overline{X1}) + A2 \log (X2/\overline{X2}) + \ldots + An \log (Xn/\overline{Xn}) \qquad (C3)$$

Both of these forms allow a nonlinear relation to hold between the X's and Y. For example, Equation (C3) may be rewritten to yield:

$$Y = \log(X1)^{A1} + \ldots + \log(Xn)^{An}$$

so that

$$EXP(Y) = X1^{A1} \ldots Xn^{An}$$

and the weights A1, . . . , An now appear as "powers", and Y is related to a product of powers of X's. This is an extremely flexible functional relation that may reasonably be expected to hold in many applications where the strict linear form shown in Equation (C1) would not be valid. The form shown in Equation (C3) serves to make each predictive variable nondimensional. This transformation is of value in those applications in which the predictor variables have different units of measure.

C. Software. The linear discriminant analyses were performed using SPSS (Statistical Package for the Social Sciences). Control card programs permit the transfer of data from PDP-11 disk files to the DCD 6400 or Cyber 70 for batch processing during the learning stages of the data analysis. Once the discriminant weights are determined, subsequent classification may be accomplished using the PDP-11.

2. AUTOMATIC INTERACTION DETECTOR (AID)

A. General Properties. In a general setting, the AID algorithm makes successive binary splits of a data set into groups. At each successive stage, the algorithm examines every predictor variable and every possible threshold for every predictor variable in order to determine that splitting variable and associated threshold that yields the best statistical prediction of the criterion variable. Algebraically, the AID algorithm maximizes, at each split, the between-set sum of squares (BSS) for the group that is split:

$$BSS = (N1*\overline{P1}^2 + N2*\overline{P2}^2) - N\overline{P}^2$$

where N and $\overline{P}$ denote the sample size and the probability of a crack for the group that is split, and N1, N2, $\overline{P1}$, $\overline{P2}$ denote the corresponding sample sizes and crack probabilities for the two groups formed by the splitting variable. Equivalently, it may be shown that the AID algorithm minimizes the within-set sum of squares (WSS), or residual sum of squares at each split. The between-set and within-set sums of squares are standard

statistical quantities that are conventionally used in analysis of variance, components of variance, and other statistical techniques based on least squares.

The AID approach to classification can be described in a variety of ways. A simple description is provided by examining a graphical representation of the AID output, usually called an AID "tree". Figure C-1 shows a simplified representation of an AID tree. The scale shown at the top of the AID tree gives the probability that a crack is present. The entire learning set of data is represented by the circle labeled 1. The location of this circle under 0.5 of the horizontal scale shows that, for this illustration, half of the learning data consist of measurements associated with cracks and half consist of measurements associated with no-cracks. The sketch shows that this set of data is split into two mutually exclusive groups, labeled 2 and 3. The location of Group 2 indicates that approximately 40 percent of the data in the Group 2 subset is associated with cracks; the location of Group 3 indicates that approximately 90 percent of the data in Group 3 are associated with cracks. The sketch shows that X4 is the splitting variable that is used to obtain Groups 2 and 3. That is, Group 2 is obtained from the learning set of data (Group 1) by taking all those measurements for which X4 is less than 4.5; Group 3 is obtained by taking all those measurements for which X4 is greater than 4.5. If a perfect prediction had existed in the data set, then the AID program would have found this predictor and Group 2 would have been located beneath 0.0 on the horizontal scale and Group 3 wuld have been located beneath 1.0 on the horizontal scale.

The AID algorithm examines every possible splitting variable, and every possible threshold for every possible variable, and chooses that variable and threshold that maximizes the horizontal separation between the two resulting groups as shown in the AID tree. In this example the best splitting variable is found to be X4. The horizontal separation shown between Groups 2 and 3 depends primarily on the difference between the crack probabilities obtained for the two groups, and also accounts for dispersion (as measured by standard

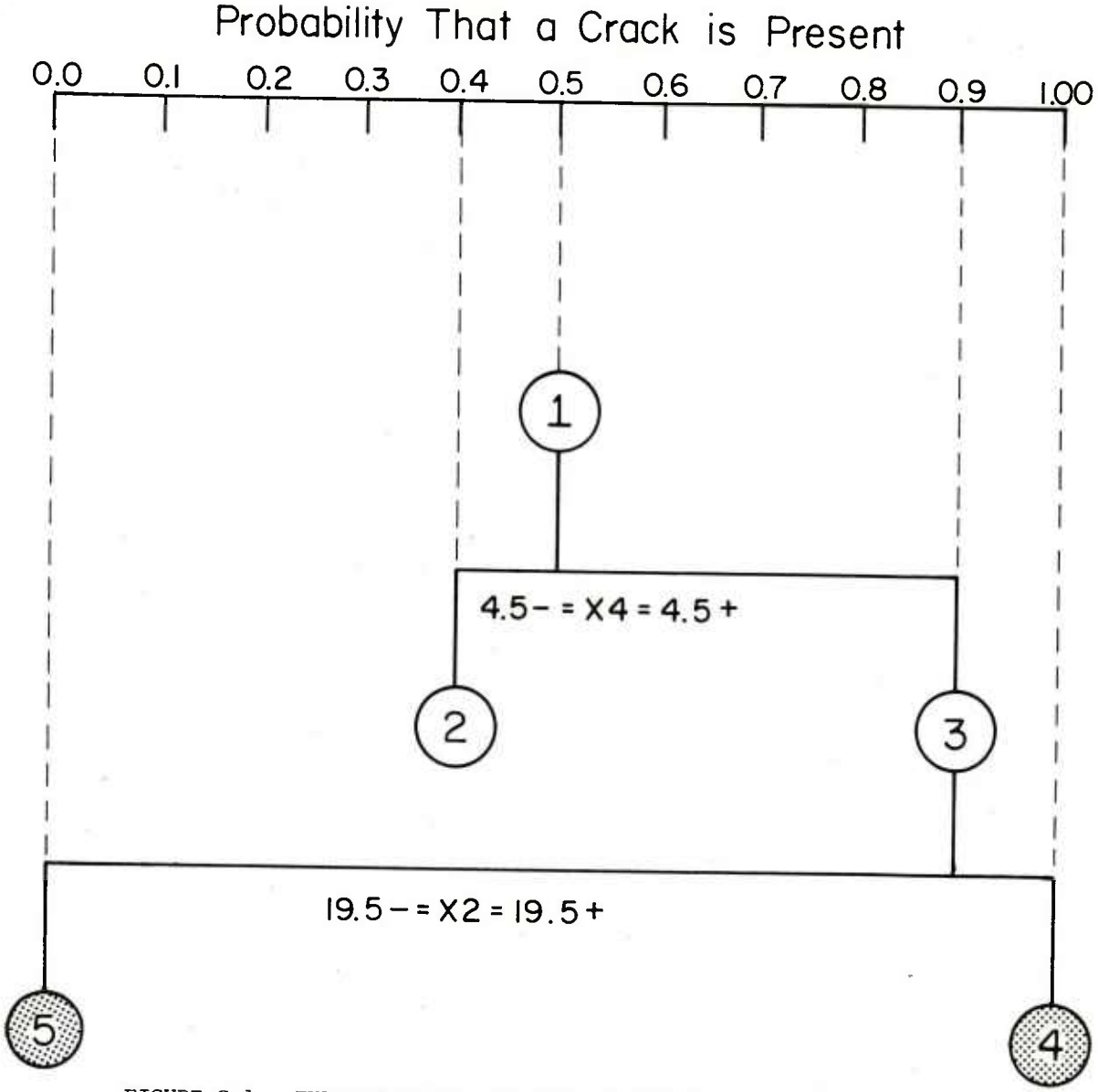

FIGURE C-1. EXAMPLE OF AN AID TREE IN WHICH TRANSFORMED PREDICTION VARIABLES X2 AND X4 SHOW THAT THE PROBABILITY THAT A CRACK IS PRESENT IS 1.0 IF X4 EXCEEDS 4.5 AND X2 EXCEEDS 19.5 AND IS 0.0 IF X4 EXCEEDS 4.5 AND X2 IS LESS THAN 19.5, AS INDICATED BY THE SHADED TERMINAL GROUPS

deviations within groups) and sample size. There is no necessity for the two groups that are formed to be of equal sample size.

The AID tree next shows a split of Group 3. Group 3 splits into Groups 4 and 5 with X2 as a splitting variable with a threshold of 19.5. The location of Group 4 under 1.0 shows that it is a "pure" group consisting entirely of data associated with cracks, whereas Group 5 consists of entirely no cracks because it is located under 0.0.

For this AID tree, Groups 2, 4, and 5 are called "terminal" groups because no further splits are made of these groups. These groups are also the groups involved in making subsequent predictions and verifications. The predictions are generated as follows. Measure X2 and X4 at a location where it is not known whether or not a crack exists. Then, apply the following decision rules:

(1) If X4 exceeds 4.5 and X2 exceeds 19.5, predict a crack is present (Prob(crack)=1.0);

(2) If X4 exceeds 4.5 and X2 is less than 19.5, predict no crack is present (Prob(crack) = 0.0);

(3) If X4 is less than 4.5, the probability that a crack is present is estimated to be 40 percent (Prob(crack)=0.4).

B. Innovations for MFEC Crack Detection. The initial aim in applying the AID algorithm to MFEC crack data was to assist in isolating those voltage measurements that might serve as good prediction variables in a linear discriminant. The algebraic and graphical features of the AID program made it ideally suited for the study of a large number of candidate predictor variables obtained by making various transformations of the basic 6 output voltage measurements. Over 100 variables were studied in this way.

C. Software. The original AID program was written by R. W. Hsieh at the University of Michigan, Ann Arbor, Michigan. The original program was written in MAD, and was subsequently translated into FORTRAN IV CDC 6000 version by R. Rockwell in 1967 at

the University of Texas. The program is now generally available. Manuals for its use may be ordered directly from the Institute for Social Research, The University of Michigan. The Battelle version of AID was obtained from The Ohio State University. In 1973 J. B. Miller of Battelle added a graphic capability to AID so that AID trees are computer generated when desired by the user.

BIBLIOGRAPHY RELATED TO AUTOMATIC INTERACTION DETECTOR (AID)

Assael, H., "Segmenting Markets by Group Purchasing Behavior: An Application of the AID Technique", Journal of Marketing Research, 7, pp. 153-158, (1970).

Doyle, P., "The Use of Automatic Interaction Detector and Similar Search Procedures", Operations Research Quarterly, 24, pp. 465-467, (1973).

Heald, G.I., "The Application of the Automatic Interaction Detector (AID) Program and Multiple Regression Techniques to the Assessment of Store Performance and Site Selection", Operational Research Quarterly, 23, pp. 445-457, (1972).

Heenan, D.A., Addleman, R. B., "Quantitative Techniques for Today's Decision Markets", Harvard Business Review, May-June, (1976).

Kass, G.V., "Significance Testing in Automatic Interaction Detection (AID)", Applied Statistics, 24, pp. 178-189, (1975).

Morgan, J.N., Sonquist, J.A., "Problems in the Analysis of Survey Data and a Proposal", Journal of the American Statistical Association, 58, pp. 415-435, (1963).

Morgan, J.N., Sonquist, J.A., "The Determination of Interaction Effects", Monograph No. 35, Ann Arbor: Survey Research Center, Institute for Social Research, University of Michigan, (1964).

Sonquist, J.A., "Multivariate Model Building", Institute for Social Research, Ann Arbor, Michigan, (1970); reprinted (1971).

Sonquist, J.A., Baker, E.L., Morgan, J.N., "Searching for Structure", Institute for Social Research, University of Michigan, Ann Arbor, Michigan, (1971); revised edition (1974).

BIBLIOGRAPHY RELATED TO LINEAR DISCRIMINANT ANALYSIS

Fisher, R.A., "The Use of Multiple Measurements in Taxonomic Problems", Ann. of Eugencies, 7, p. 179, (1936).

Fisher, R.A., "The Statistical Utilization of Multiple Measurements", Ann. of Eugencies, 8, p. 376, (1937).

Kullback, S., "Information Theory and Statistics", John Wiley and Sons, Inc., New York, Chapter 13, pp. 342-352, (1959).

APPENDIX D

SINGLE FREQUENCY EDDY CURRENT RESULTS

APPENDIX D
SINGLE FREQUENCY EDDY CURRENT RESULTS

This appendix contains the computer produced plots of the individual in-phase and quadrature eddy current readings obtained on each fastener. Figure D-1 thru D-6 illustrate the readings obtained on titanium fastener panels 1-3 and 1-4. Figures D-7 thru D-12 illustrate the readings obtained on steel fastener panels 1-1 and 1-2.

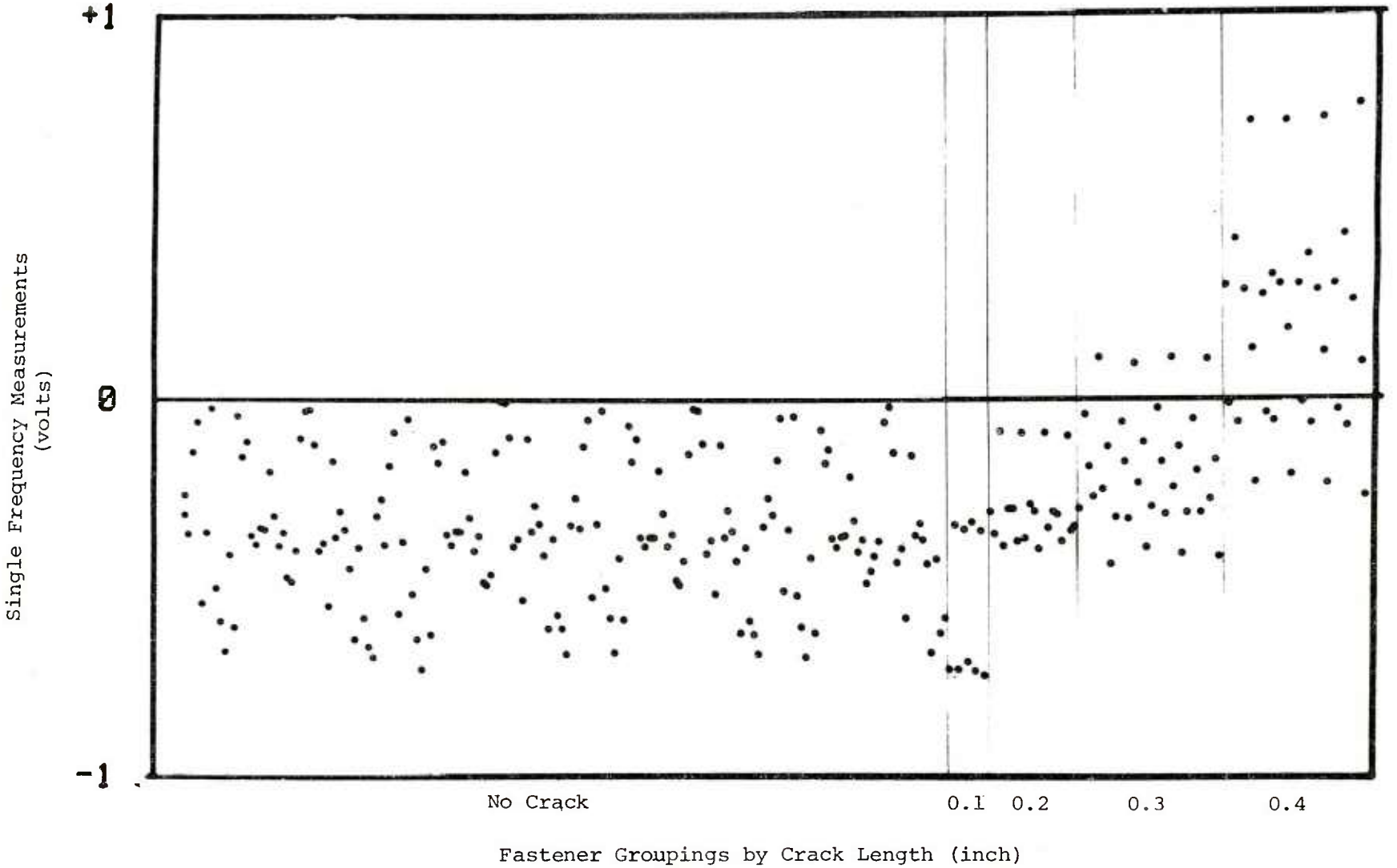

FIGURE D-1. SINGLE FREQUENCY MEASUREMENTS FOR MFEC ANALYSIS ON TITANIUM FASTENERS — 90 HZ, INPHASE

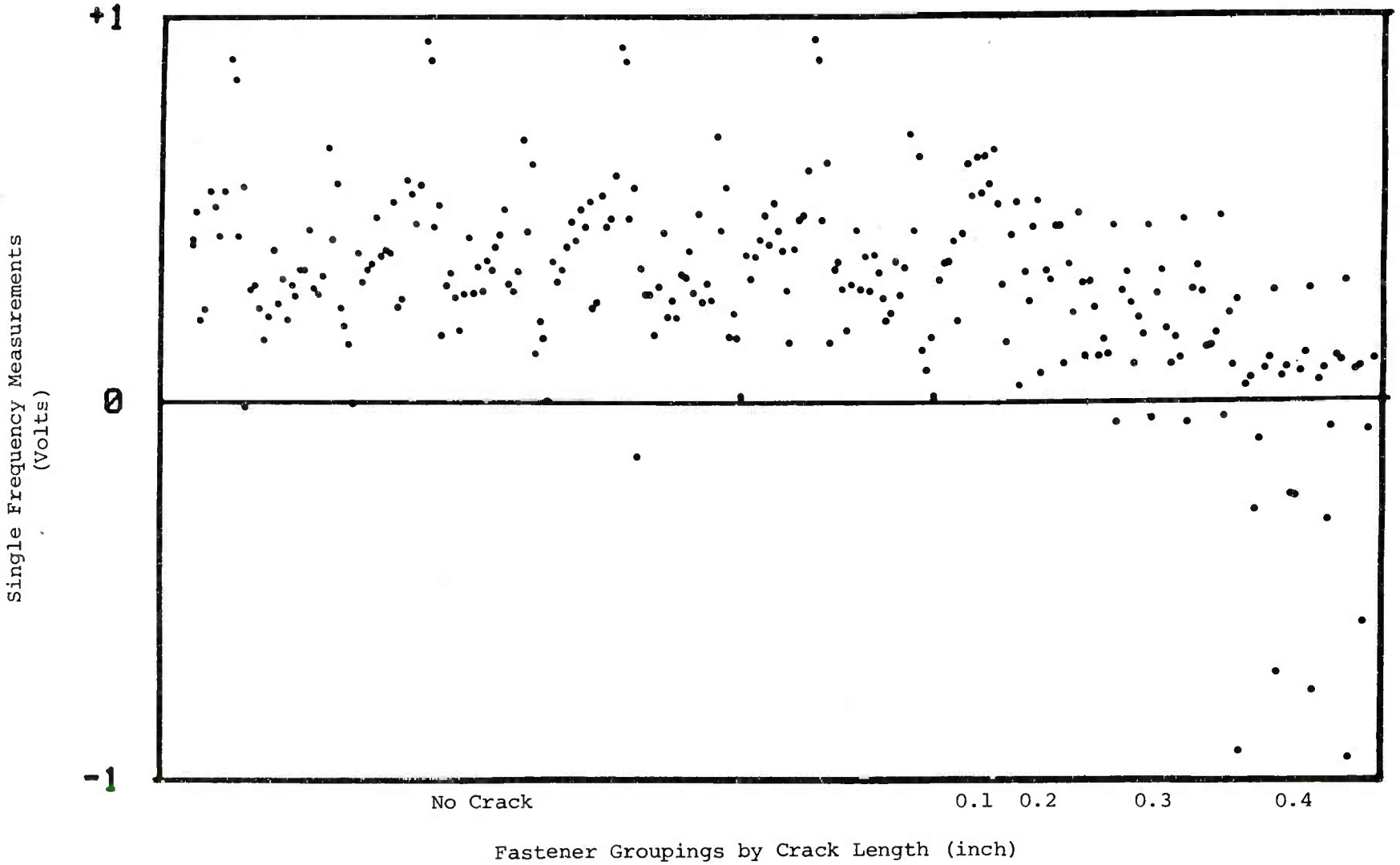

FIGURE D-2. SINGLE FREQUENCY MEASUREMENTS FOR MFEC ANALYSIS ON TITANIUM FASTENERS — 90 HZ, QUADRATURE

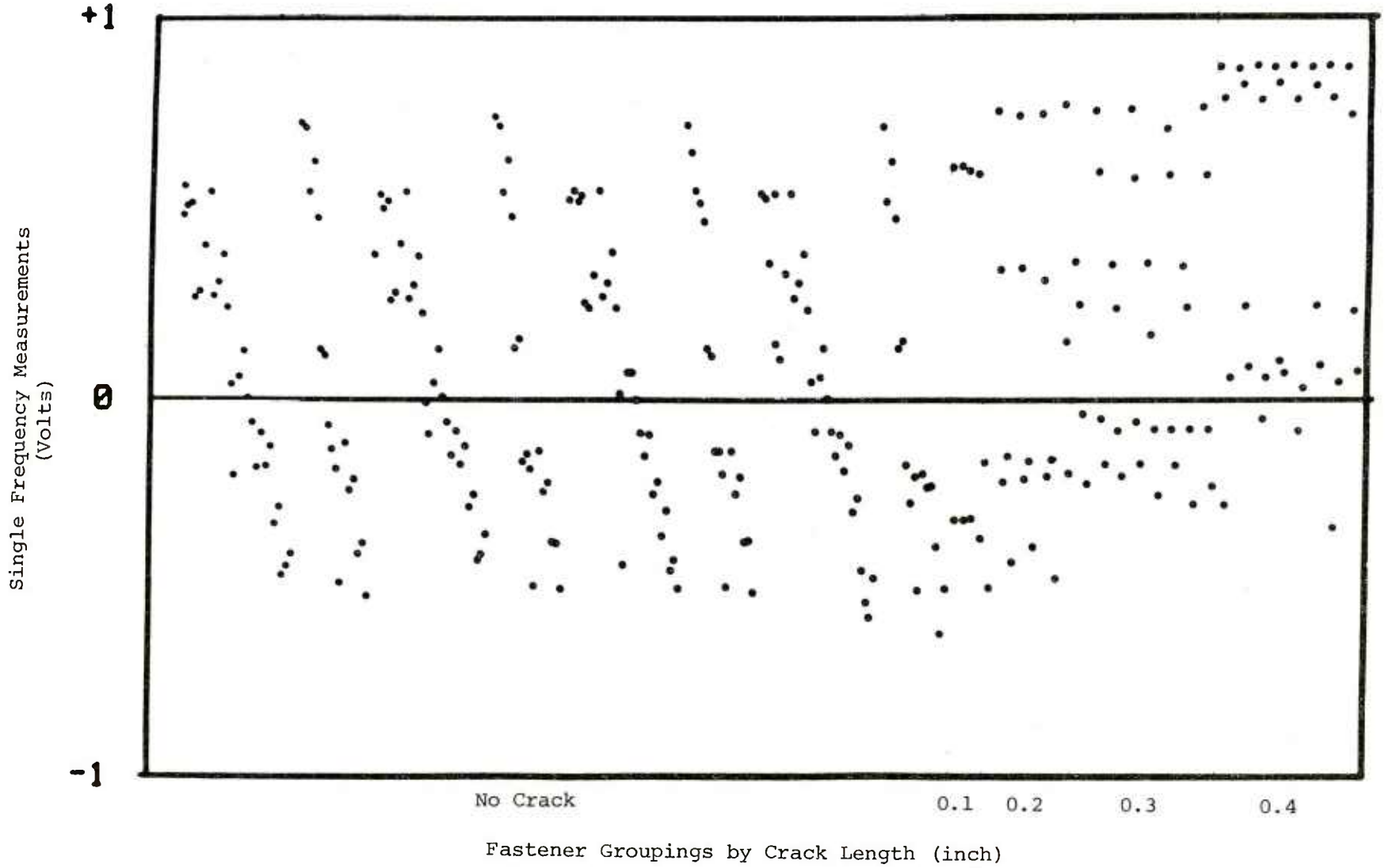

FIGURE D-3. SINGLE FREQUENCY MEASUREMENTS FOR MFEC ANALYSIS ON TITANIUM FASTENERS — 330 HZ, INPHASE

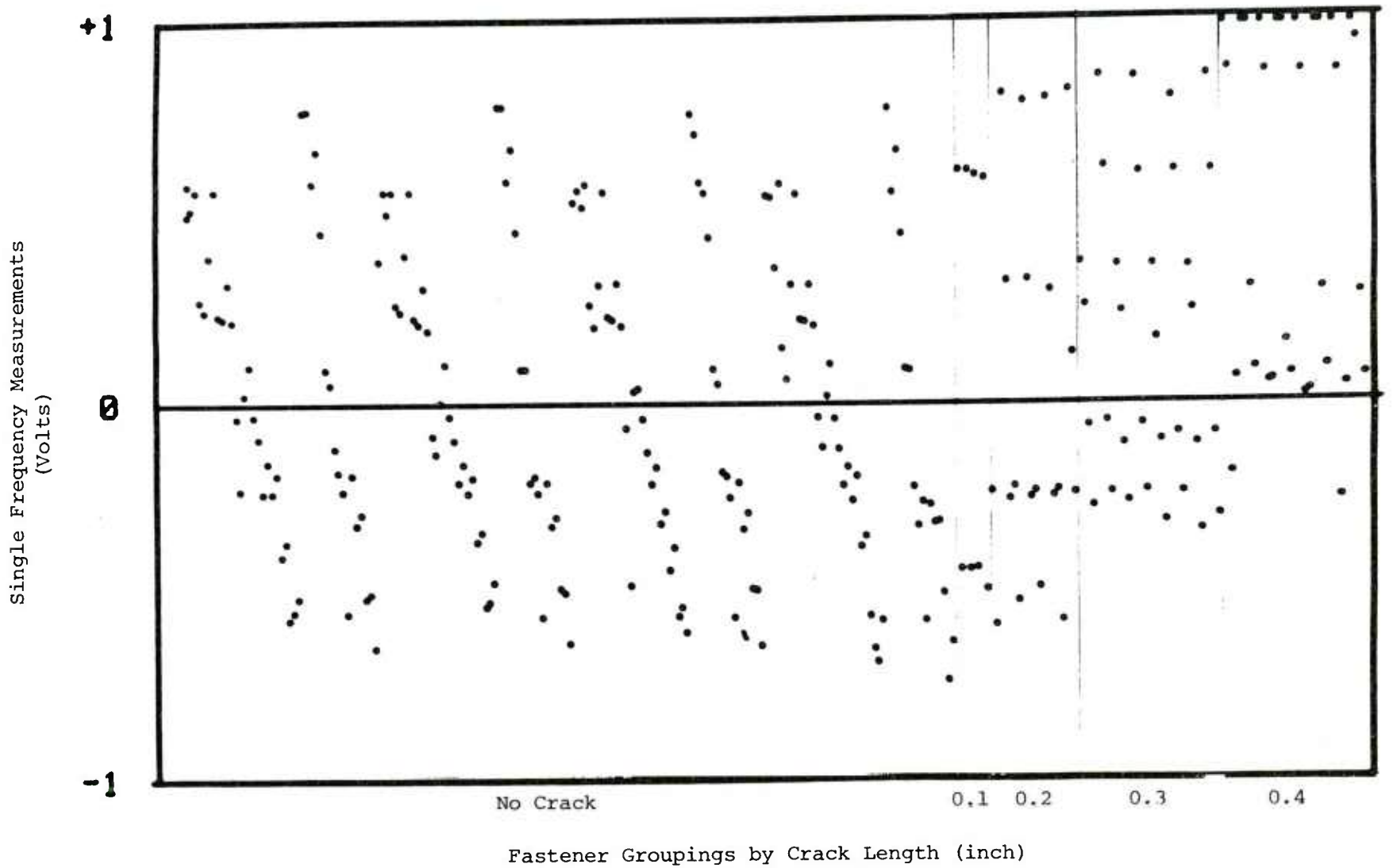

FIGURE D-4. SINGLE FREQUENCY MEASUREMENTS FOR MFEC ANALYSIS ON TITANIUM FASTENERS — 330 HZ, QUADRATURE

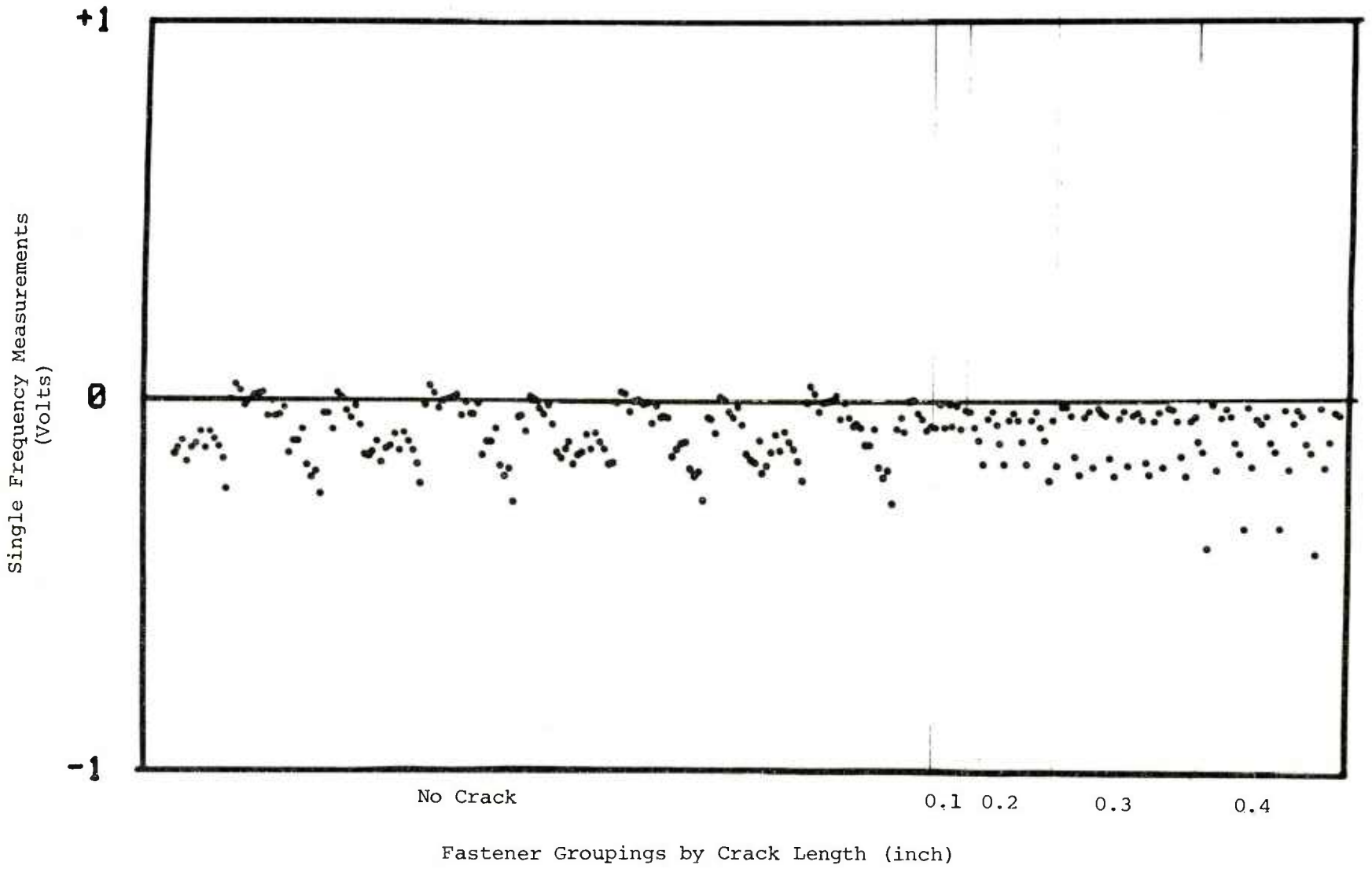

FIGURE D-5. SINGLE FREQUENCY MEASUREMENTS FOR MFEC ANALYSIS ON TITANIUM FASTENERS — 1219 HZ, INPHASE

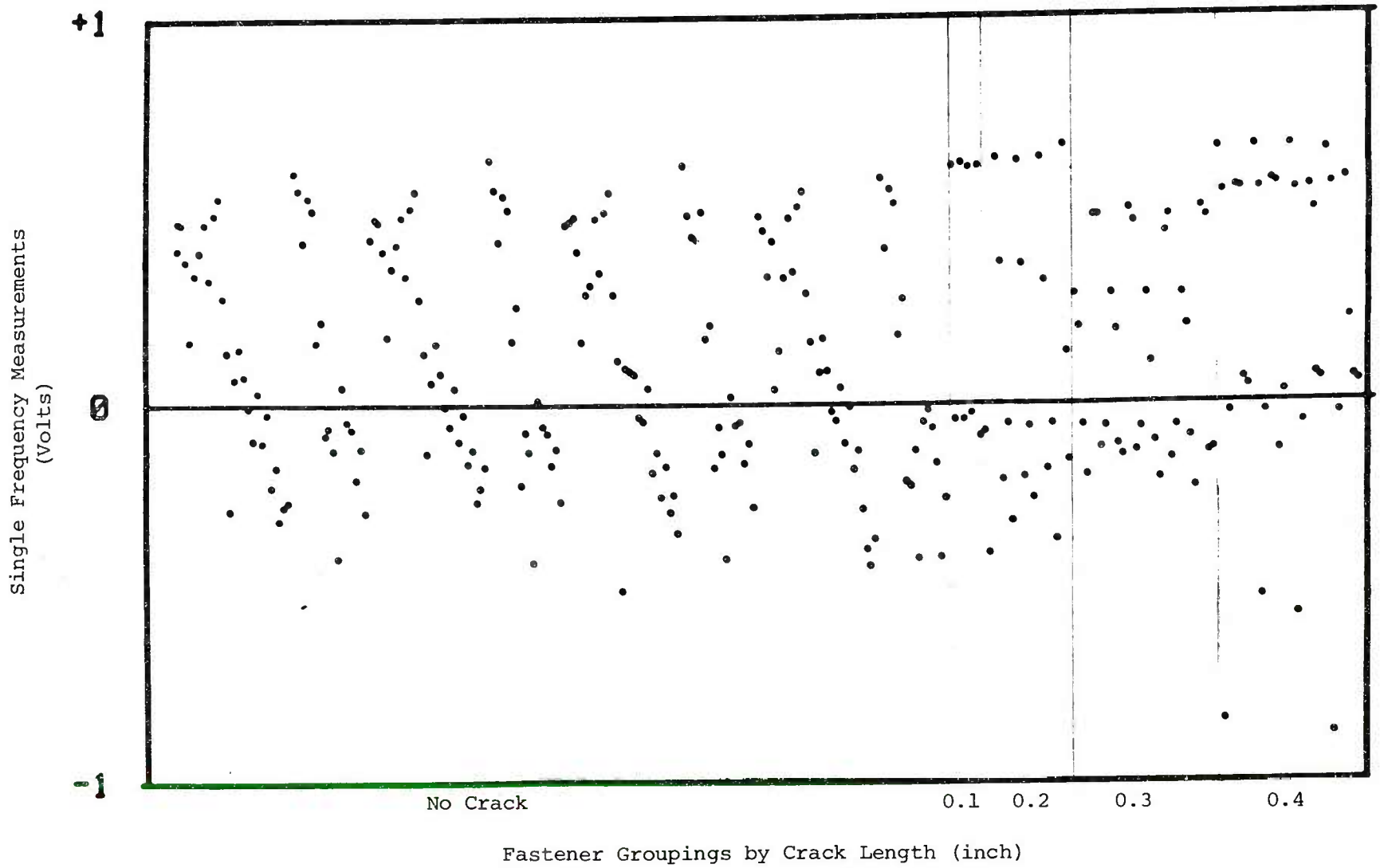

FIGURE D-6. SINGLE FREQUENCY MEASUREMENTS FOR MFEC ANALYSIS ON TITANIUM FASTENERS — 1219 HZ, QUADRATURE

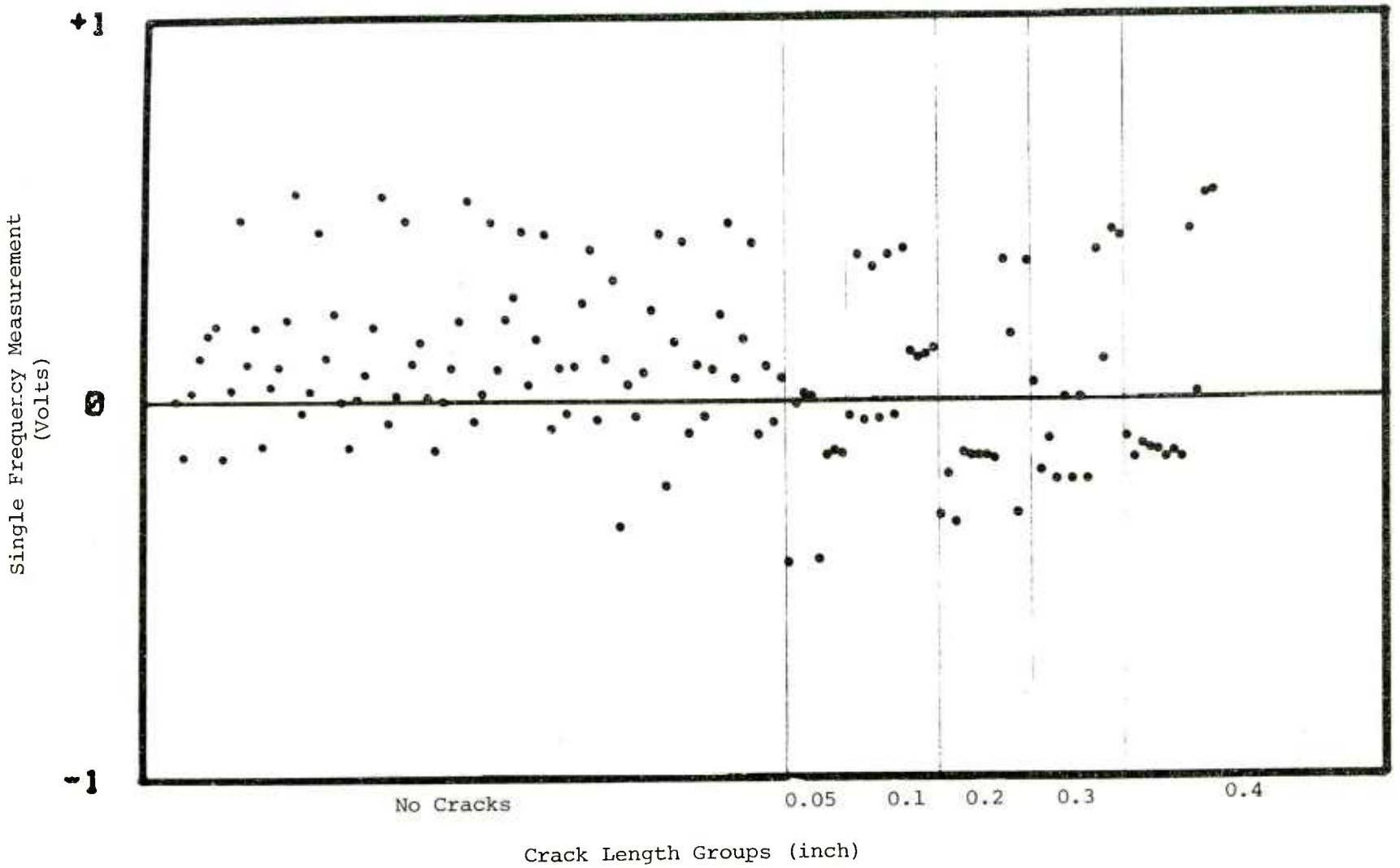

FIGURE D-7. SINGLE FREQUENCY MEASUREMENTS FOR MFEC ANALYSIS ON STEEL FASTENERS — 90 HZ, INPHASE

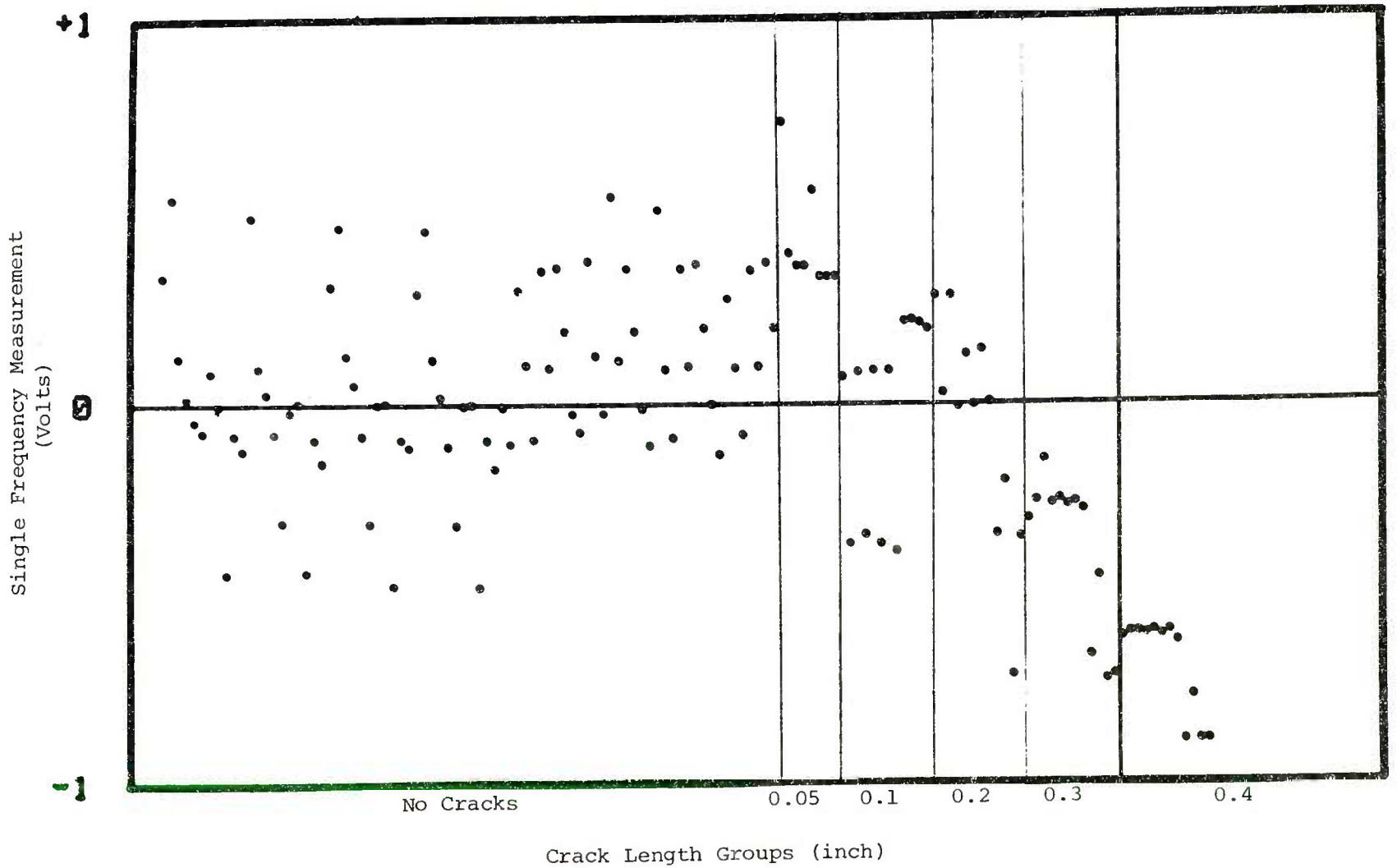

FIGURE D-8. SINGLE FREQUENCY MEASUREMENTS FOR MFEC ANALYSIS ON STEEL FASTENERS - 90 HZ, QUADRATURE

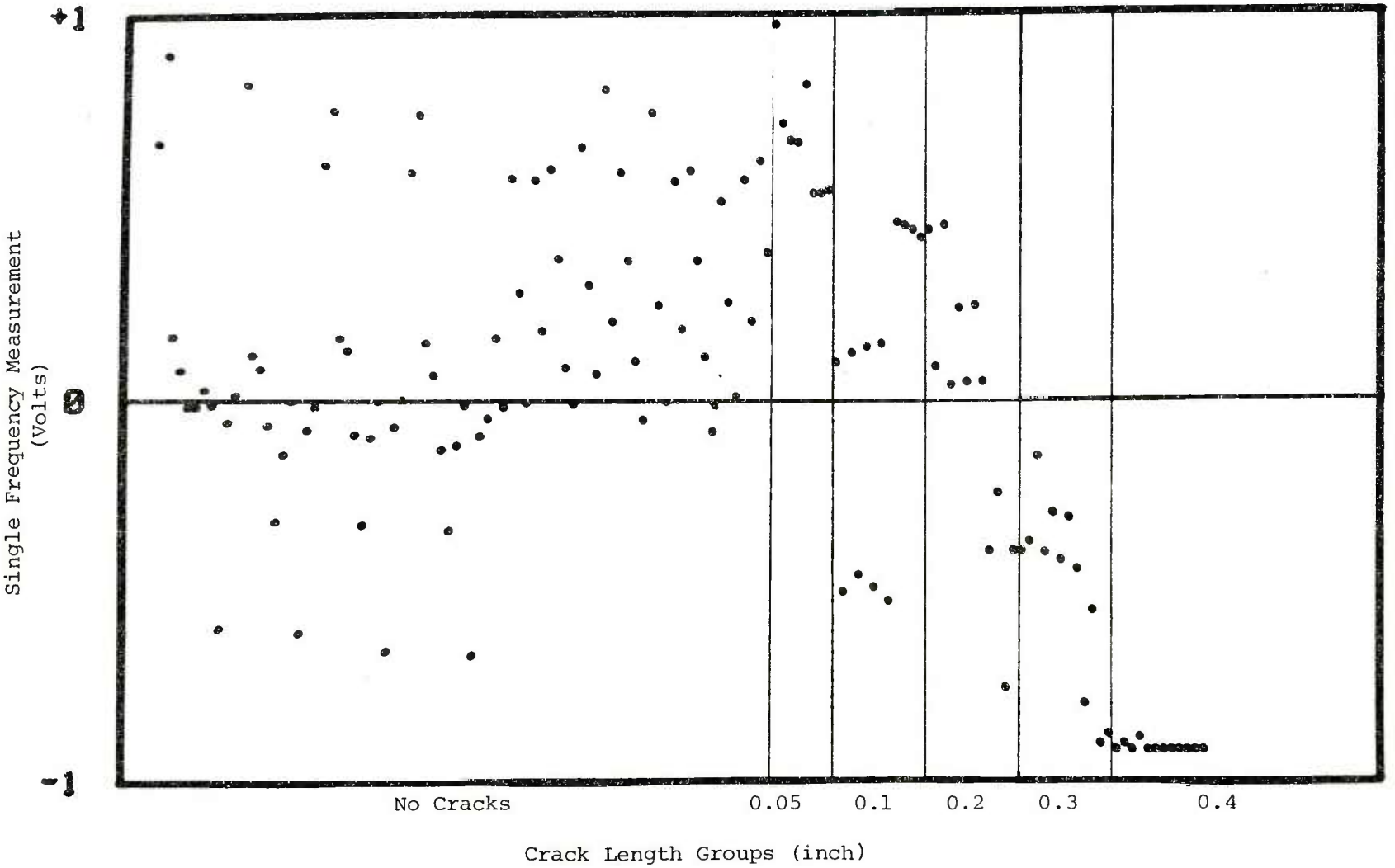

FIGURE D-9. SINGLE FREQUENCY MEASUREMENTS FOR MFEC ANALYSIS ON STEEL FASTENERS - 330 HZ, INPHASE

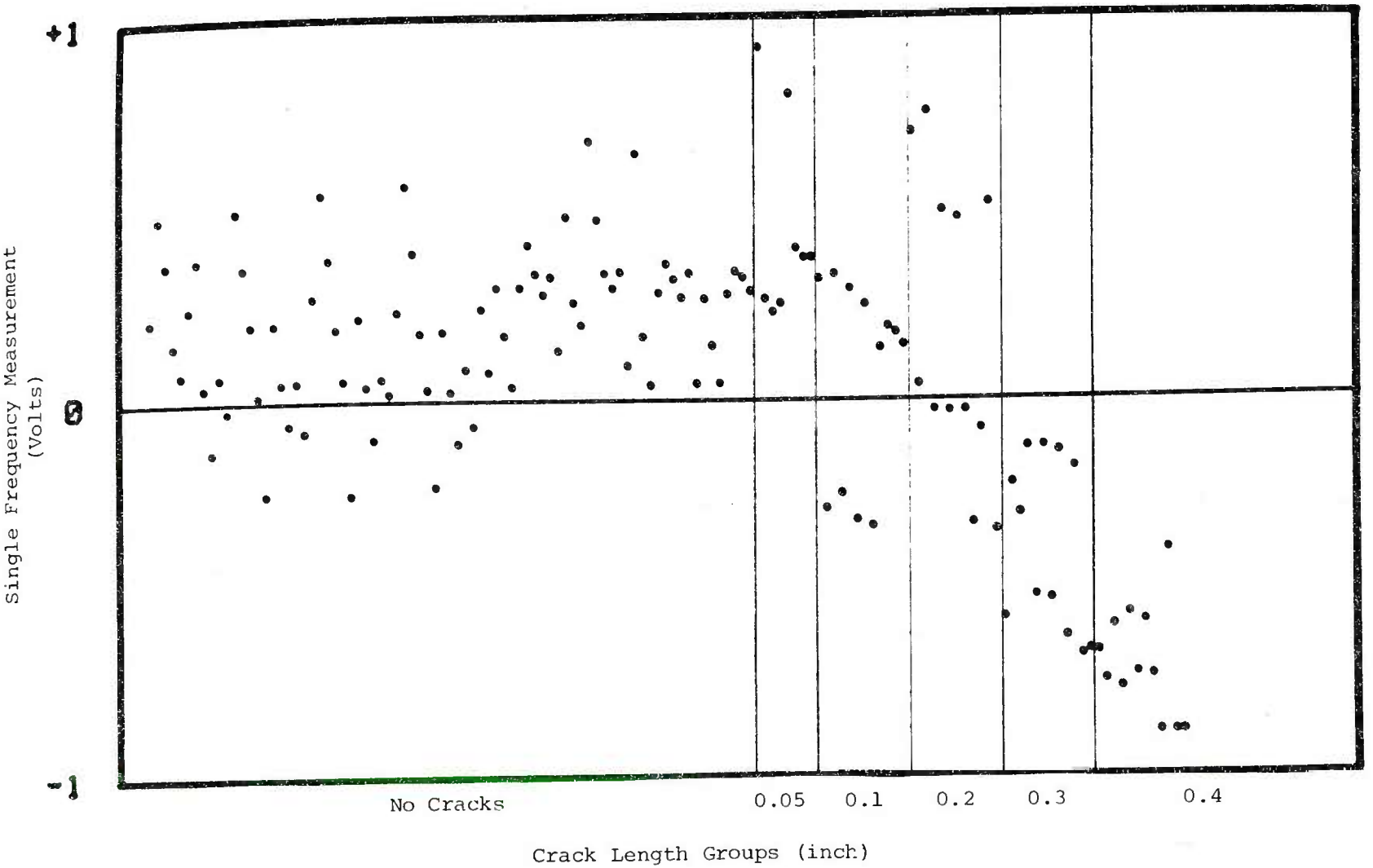

FIGURE D-10. SINGLE FREQUENCY MEASUREMENTS FOR MFEC ANALYSIS ON STEEL FASTENERS - 330 HZ, QUADRATURE

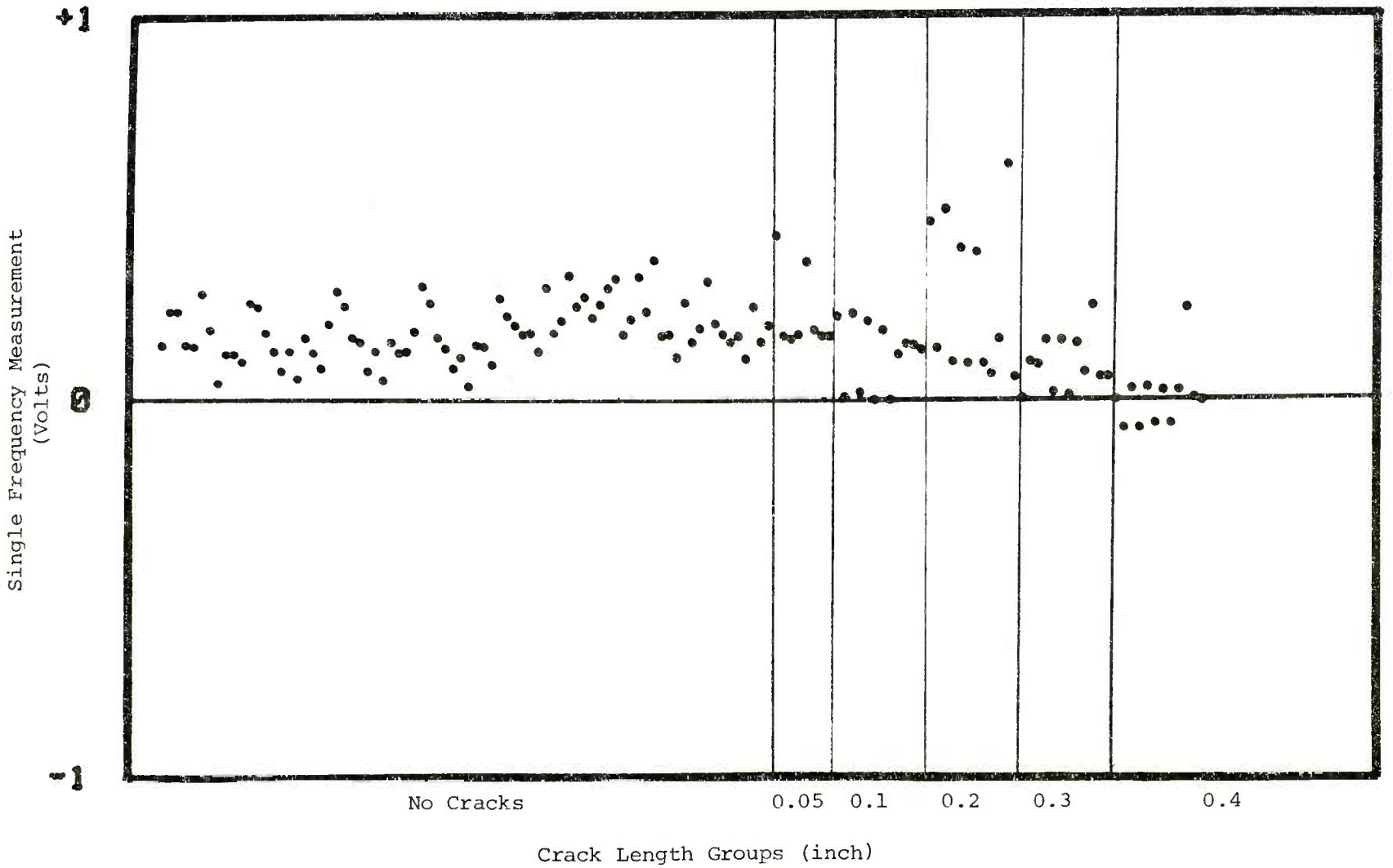

FIGURE D-11. SINGLE FREQUENCY MEASUREMENTS FOR MFEC ANALYSIS ON STEEL FASTENERS - 1219 HZ, INPHASE

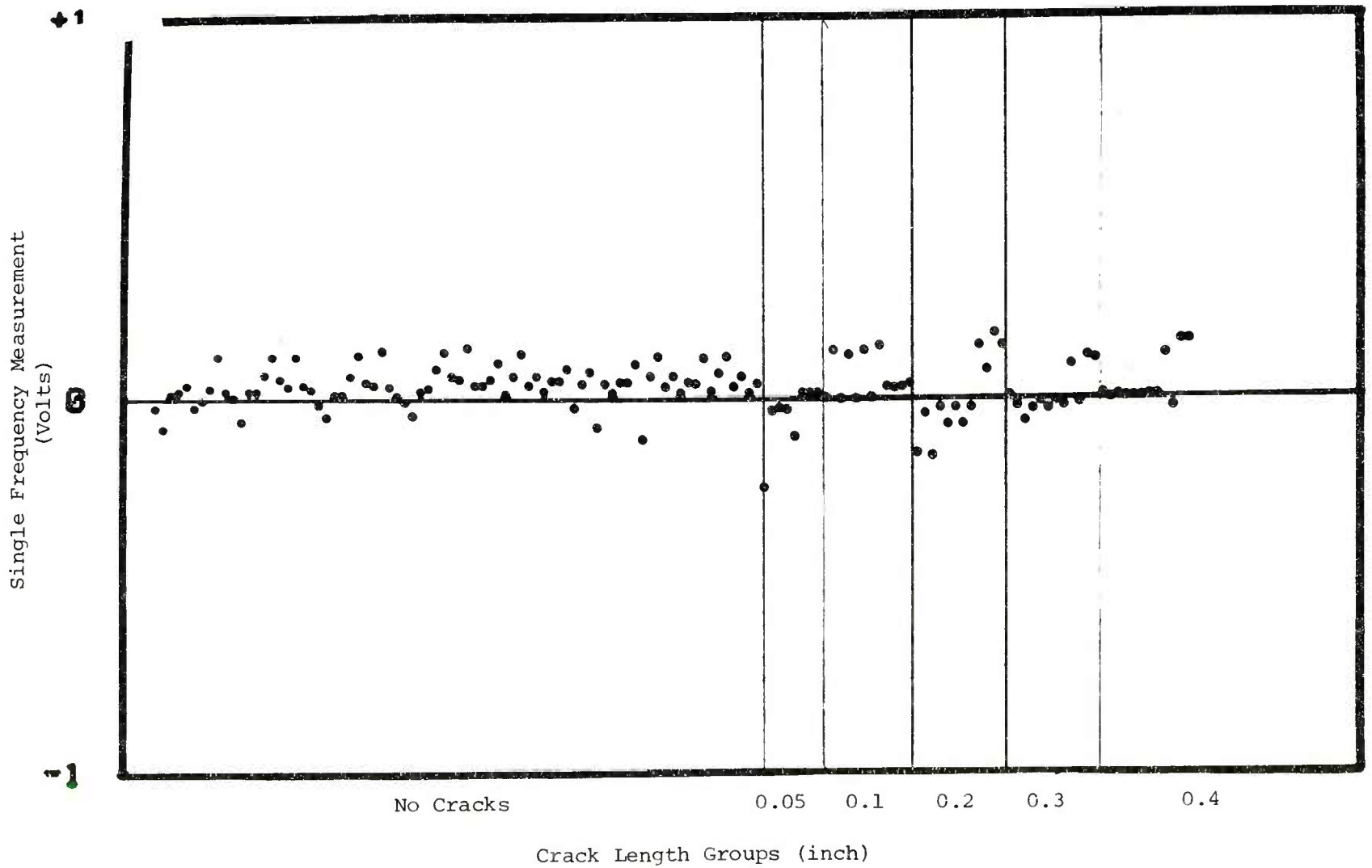

FIGURE D-12. SINGLE FREQUENCY MEASUREMENTS FOR MFEC ANALYSIS ON STEEL FASTENERS - 1219 HZ, QUADRATURE